

Final Report

**Development of an
Advanced Photochemical Model for
Particulate Matter: PMCAMx**

CRC Project A-30

Prepared for:

Coordinating Research Council, Inc.
3650 Mansell Road, Suite 140
Alpharetta, Georgia 30022

Prepared by

ENVIRON International Corporation
101 Rowland Way
Novato, California 94945

Sonoma Technology Inc.
1360 Redwood Way
Petaluma CA, 94954

Carnegie Mellon University
Department of Chemical Engineering
5000 Forbes Avenue
Pittsburgh, PA 15213

January 2003

TABLE OF CONTENTS

| | Page |
|--|-------------|
| EXECUTIVE SUMMARY | ES-1 |
| 1. INTRODUCTION | 1-1 |
| 2. ATMOSPHERIC AEROSOLS | 2-1 |
| Atmospheric Aerosol Properties | 2-1 |
| Atmospheric Aerosol Processes | 2-6 |
| 3. TECHNICAL FORMULATION | 3-1 |
| Aerosol Size Distribution And Chemical Species | 3-1 |
| Gas Phase Chemistry | 3-3 |
| Secondary Organic Aerosol Formation | 3-4 |
| Inorganic Aerosol Chemistry | 3-12 |
| Particle Size Distribution | 3-12 |
| Aqueous Phase Chemistry | 3-14 |
| Deposition | 3-18 |
| Box Model Testing | 3-20 |
| 4. IMPLEMENTATION OF AEROSOL MODULES IN PMCAMx..... | 4-1 |
| 5. PMCAMx TEST APPLICATION FOR LOS ANGELES | |
| Model Inputs | 5-1 |
| PM ₁₀ Technical Enhancement Program..... | 5-2 |
| PMCAMx Performance Evaluation | 5-3 |
| Platform Dependency | 5-18 |
| VSRM Aqueous Chemistry..... | 5-26 |
| Sensitivity Tests | 5-29 |
| REFERENCES..... | R-1 |

APPENDICES

- Appendix A: Gas Phase Chemistry for PMCAMx
Based on the Carbon Bond 4 (CB4)
Chemical Mechanism
- Appendix B: List of Chemical Equilibria
in the ISORROPIA Aerosol
Thermodynamics Module
- Appendix C: List of Chemical Reactions
and Equilibria in the
AQCHEM Aqueous Phase
Chemistry Module

TABLES

| | | |
|-------------|--|------|
| Table 2-1. | Generalize comparison of composition and source for fine and coarse particles. | 2-3 |
| Table 3-1. | Aerosol constituents in PMCAMx. | 3-2 |
| Table 3-2. | Aerosol size sections for PMCAMx version 3.01. | 3-2 |
| Table 3-3. | Example aerosol species names from PMCAMx. | 3-3 |
| Table 3-4. | Gas phase species in the PMCAMx CB4 chemical mechanism. | 3-4 |
| Table 3-5. | Properties of condensable gas precursors (CG1 – CG4) to secondary organic aerosols. | 3-5 |
| Table 3-6. | Aerosol yields and saturation concentrations for the 5-species SOA model ¹ | 3-7 |
| Table 3-7. | Aerosol yields and saturation concentrations for the 4-species SOA model No. 1. | 3-8 |
| Table 3-8. | Aerosol yields and saturation concentrations for the 4-species SOA model No. 2 selected as the basis for PMCAMx. | 3-9 |
| Table 3-9. | Aerosol yields and saturation concentrations for the 3-species SOA model. | 3-10 |
| Table 3-10. | Species considered by ISSORROPIA for gas, liquid and solid phases. | 3-12 |
| Table 3-11. | Species for which differential equations are solved in the VSRM aqueous-phase chemistry. | 3-15 |
| Table 3-12. | Henry's Law constants and other parameters used in the PMCAMx dry-deposition calculation. | 3-19 |
| Table 3-13. | Mass conservation in Test 1 with MADM and SOAP. | 3-21 |
| Table 3-14. | Mass conservation in Test 2 with VSRM and SOAP. | 3-23 |
| Table 5-1 | Aerosol size sections for PMCAMx version 3.01. | 5-2 |
| Table 5-2. | Five-station mean observed and predicted PM concentrations ($\mu\text{g}/\text{m}^3$) for the October 17-19, 1995 PTEP episode. | 5-5 |
| Table 5-3 | CPU Times (hours) for the LA Test Case (65x40 5-km grids with 10 vertical layers) on different workstations. | 5-18 |
| Table 5-4. | CPU time used by each aerosol module on the Linux workstation. | 5-19 |
| Table 5-5a. | Summary of concentration differences between Linux and Sun workstations tests for October 17th, 1995. | 5-20 |

| | | |
|-------------|---|------|
| Table 5-5b. | Summary of concentration differences between Linux and Sun workstations tests for October 18 th , 1995. | 5-21 |
| Table 5-5c. | Summary of concentration differences between Linux and Sun workstations tests for October 19 th , 1995. | 5-22 |
| Table 5-6a. | Summary of concentration differences between Linux and DEC workstations tests for October 17 th , 1995. | 5-23 |
| Table 5-6b. | Summary of concentration differences between Linux and DEC workstations tests for October 18 th , 1995. | 5-24 |
| Table 5-6c. | Summary of concentration differences between Linux and DEC workstations tests for October 19 th , 1995. | 5-25 |
| Table 5-7. | CPU times for aqueous-chemistry module sensitivity tests. | 5-27 |
| Table 5-8. | Summary of concentration differences for aqueous-chemistry module sensitivity tests for October 19 th , 1995. | 5-28 |
| Table 5-9. | PMCAMx emission sensitivity runs and run times on a Linux (Athon MP2000) workstation. | 5-30 |
| Table 5-10. | Summary of changes in PM concentrations due to changing emissions of a single precursor species. | 5-30 |

FIGURES

| | | |
|-------------|---|------|
| Figure 2-1. | Example distribution of aerosol mass with size represented using a sectional approach. | 2-4 |
| Figure 2-2. | Example distribution of aerosol volume with size represented using a modal approach. | 2-5 |
| Figure 2-3. | Example distribution of aerosol number with size represented using a modal approach. | 2-5 |
| Figure 3-1. | Comparison of modeled SOA concentrations using different CG/SOA lumping schemes. | 3-11 |
| Figure 3-2. | Comparison of modeled condensable gas (COG) concentrations using different CG/SOA lumping schemes. | 3-11 |
| Figure 3-3. | Decision algorithm for the VSRM bulk and size-resolved aqueous chemistry models. | 3-17 |
| Figure 3-4. | Time evolution of the aerosol size distribution in Test 1 with MADM and SOAP. | 3-21 |
| Figure 3-5. | Size-resolved aerosol composition at hours 6 and 13 in Test 1 with MADM and SOAP. | 3-22 |
| Figure 3-6. | Time evolution of the aerosol size distribution in Test 2 with VSRM and SOAP. | 3-23 |
| Figure 3-7. | Size-resolved aerosol composition at hours 6 and 13 in Test 2 with VSRM and SOAP. | 3-24 |
| Figure 4-1. | Main calling tree for the aerosol chemistry driver FULLAERO. | 4-4 |
| Figure 4-2. | Calling tree for the aqueous-phase chemistry module (AQCHEM). | 4-5 |
| Figure 4-3. | Calling tree for the calculation of chemical reaction rates by AQFEX within the aqueous-phase chemistry module (AQCHEM). | 4-6 |
| Figure 4-4. | Calling tree for the secondary organic aerosol chemistry module (SOAP_DRV). | 4-7 |

| | | |
|--------------|---|------|
| Figure 4-5. | Calling tree for the equilibrium version of the MADM aerosol size distribution module (EQPART)..... | 4-7 |
| Figure 4-6. | Calling tree for the dynamic version of the MADM aerosol size distribution module (MADM)..... | 4-8 |
| Figure 4-7. | Calling tree for the hybrid version of the MADM aerosol size distribution module (HEQDYN). | 4-9 |
| Figure 5-1. | Modeling domain for the PMCAMx Los Angeles test application. | 5-2 |
| Figure 5-2. | Comparison of 24-hr PM ₁₀ nitrate at PTEP monitoring sites on October 17 th and 18 th , 1995. | 5-7 |
| Figure 5-3. | Comparison of 24-hr PM _{2.5} sulfate at PTEP monitoring sites on October 17 th and 18 th , 1995. | 5-7 |
| Figure 5-4. | Comparison of 24-hr PM _{2.5} organic matter (primary + secondary) at PTEP monitoring sites on October 17 th and 18 th , 1995..... | 5-8 |
| Figure 5-5. | Comparison of 24-hr PM _{2.5} elemental carbon at PTEP monitoring sites on October 17 th and 18 th , 1995. | 5-8 |
| Figure 5-6. | Comparison of 24-hr PM ₁₀ crustal material at PTEP monitoring sites on October 17 th and 18 th , 1995. | 5-9 |
| Figure 5-7. | Comparison of 24-hr PM _{2.5} at Anaheim between PMCAMx, UAM-AERO and UAM-AERO/LT..... | 5-10 |
| Figure 5-8. | Comparison of 24-hr PM _{2.5} at Diamond Bar between PMCAMx, UAM-AERO and UAM-AERO/LT..... | 5-10 |
| Figure 5-9. | Comparison of 24-hr PM _{2.5} at Riverside between PMCAMx, UAM-AERO and UAM-AERO/LT..... | 5-11 |
| Figure 5-10. | Comparison of 24-hr PM _{2.5} at Fontana between PMCAMx, UAM-AERO and UAM-AERO/LT..... | 5-11 |
| Figure 5-11. | Comparison of 24-hr PM _{2.5} at Los Angeles North Main between PMCAMx, UAM-AERO and UAM-AERO/LT..... | 5-12 |
| Figure 5-12. | Comparison of hourly PM _{2.5} ammonium at Riverside between PMCAMx, UAM-AERO and UAM-AERO/LT..... | 5-13 |
| Figure 5-13. | Comparison of hourly PM _{2.5} nitrate at Riverside between PMCAMx, UAM-AERO and UAM-AERO/LT..... | 5-13 |
| Figure 5-14. | Comparison of hourly PM _{2.5} sulfate at Riverside between PMCAMx, UAM-AERO and UAM-AERO/LT | 5-14 |
| Figure 5-15. | Comparison of hourly PM _{2.5} organic matter at Riverside between PMCAMx, UAM-AERO and UAM-AERO/LT. | 5-14 |
| Figure 5-16. | Comparison of hourly PM _{2.5} elemental carbon at Riverside between PMCAMx, UAM-AERO and UAM-AERO/LT. | 5-15 |
| Figure 5-17. | Comparison of hourly PM _{2.5} crustal material at Riverside between PMCAMx, UAM-AERO and UAM-AERO/LT. | 5-15 |
| Figure 5-18. | Daily maximum 24-hour PM ₁₀ concentrations on October 19 th , 1995 for nitrate, sulfate, ammonium, secondary organic aerosol, sodium and chloride. | 5-16 |
| Figure 5-19. | Daily maximum 24-hour concentrations on October 19 th , 1995 for coarse nitrate (PM ₁₀ -PM _{2.5}) and fine nitrate (PM _{2.5})..... | 5-17 |
| Figure 5-20. | Riverside PM ₁₀ on October 19 th at different emission levels. | 5-31 |

Figure 5-21. Change in Riverside PM₁₀ on October 19th with emission level. 5-31
Figure 5-22. LA North Main PM₁₀ on October 19th at different emission levels. 5-32
Figure 5-23. Change in LA North Main PM₁₀ on October 19th with emission level. 5-32

EXECUTIVE SUMMARY

The Comprehensive Air-quality Model with Extensions (CAMx) is a three-dimensional multi-scale photochemical grid model (ENVIRON, 2002) that is publicly available without fees or restrictions on model application. CAMx was developed with all new code during the late 1990s using modern and modular coding practices. This has made the model an ideal platform for the extension to treat a variety of air quality issues including ozone, particulate matter (PM), visibility, acid deposition, and air toxics. The flexible CAMx framework has also made it a convenient and robust host model for the implementation of “probing tool” techniques such as Process Analysis, the Decoupled Direct Method (DDM), and the Ozone Source Apportionment Technology (OSAT). For CRC project A-30, ENVIRON, together with Sonoma Technology, Inc. (STI) and Carnegie Mellon University (CMU), added state-of-the-science algorithms for aerosol modeling to CAMx to create a new particulate matter model called PMCAMx, version 3.01. The source code for the initial version of PMCAMx was delivered to CRC and is being used in follow-on work to further evaluate and refine the model (CRC projects A-40 and A-44). PMCAMx will be made publicly available via the CAMx web page once the model has undergone sufficient testing and evaluation to build confidence in the model.

The development of PMCAMx was based on version 3.01 of CAMx as distributed from <http://www.camx.com>. The extension to treat PM involved the addition of science modules to represent important physical processes for aerosols:

- Size distribution is represented using the Multi-component Aerosol Dynamics Model (MADM), which uses a sectional approach to represent the aerosol particle size distribution (Pilinis et al., 2000). MADM treats the effects of condensation/evaporation, coagulation and nucleation upon the particle size distribution.
- Inorganic aerosol thermodynamics are represented using ISORROPIA (Nenes et al., 1998, 1999) within MADM.
- Secondary organic aerosol thermodynamics are represented using the semi-volatile scheme of Strader et al., (1998).
- Aqueous-phase chemical reactions are modeled using the Variable Size-Resolution Model of Fahey and Pandis (2001), which automatically determines whether water droplets can be represented by a single ‘bulk’ droplet-size mode or whether it is necessary to use fine and coarse droplet-size modes.
- The CAMx deposition algorithms were improved for particle deposition. Dry deposition is represented for the size-resolved particle distribution (ENVIRON, 2002). A new wet-deposition algorithm has been developed but is not yet implemented in PMCAMx.

The main aerosol modules for PMCAMx were provided by CMU. ENVIRON and STI developed the plan for implementing the aerosol modules in CAMx by extending STI's prior experience implementing aerosol modules in the UAM-AERO. The aerosol modules were tested before being implemented in PMCAMx by ENVIRON. The implementation testing resulted in improvements to all of the aerosol modules. The new PMCAMx model was evaluated for a Los Angeles PM episode. The episode selected was October 17-19, 1995 from the PM₁₀ Technical Enhancement Program (PTEP) because this period had previously been modeled using the UAM-AERO and therefore important components of the modeling database were already available and tested. PMCAMx was configured with ten size sections for thirteen chemical constituents of PM so that a total of 130 PM species were simulated. This approach provides a highly detailed chemical and size description of the atmospheric aerosol for both PM₁₀ and PM_{2.5}. Model performance for the Los Angeles October 1995 PTEP episode was evaluated by STI and compared to past performance obtained with the UAM-AERO. After STI concluded that the PMCAMx model performance was reasonable, ENVIRON conducted a series of diagnostic and sensitivity tests to investigate the stability and performance of PMCAMx and test the modeled emissions-air quality relationships.

The application of PMCAMx to Los Angeles for the October 1995 PTEP episode showed that the code was stable over a series of diagnostic and emissions sensitivity tests. This was a challenge because the PM algorithms are complex computer codes developed in a research setting they had not previously been used together in a grid model. The PMCAMx aerosol algorithms appear to be quite robust and form a sound basis for further model development. The PMCAMx results were more sensitive to computer platform than the host CAMx model and future development should seek to improve this. Most of the testing used Linux PC workstations, which are becoming the most-widely used platform for the CAMx modeling community because of their power and cost-effectiveness. Model run times were reasonable, taking about six hours to simulate the three-day episode on a Linux workstation with a 2 GHz class processor. PMCAMx was tested successfully on Linux, Sun and DEC Alpha workstations.

The emissions sensitivity tests looked at the relationships between speciated PM levels and emissions of VOC, ammonia and NO_x at upwind and downwind locations in the Los Angeles basin. The results of the sensitivity tests were consistent with the underlying chemical/physical relationships and showed both linear and non-linear responses depending upon PM species and location. For example, reducing ammonia emissions reduced nitrate, sulfate and ammonium at both upwind and downwind sites. In contrast, reducing NO_x emissions increased ammonium nitrate at the upwind site but decreased ammonium nitrate at the downwind site. These findings illustrate why scientifically credible PM modeling tools will be important to the development of effective PM control strategies in areas such as Los Angeles.

The model performance evaluation found that PMCAMx performance for the Los Angeles episode was reasonable and did not point to any model flaws. The Los Angeles October 1995 PTEP modeling database was limited, especially in the meteorological inputs, and more PMCAMx applications will be needed to learn more about the model performance, sensitivity and stability characteristics. Modeling recent PM episodes will be especially valuable because of the improvements in observations of size/chemically resolved PM and precursor species for model performance evaluation (e.g., EPA's PM supersites data).

Recommendations

The following specific recommendations follow from the work completed in CRC project A-30:

- PMCAMx should be tested for additional episodes under a variety of conditions to further probe the reliability and completeness of the model algorithms. Episodes with extensive ambient data for model performance evaluation and reliable input data will be needed to learn more about PMCAMx model performance.
- PMCAMx should be tested for a nested-grid domain. The grid nesting algorithms have been implemented for PM but not tested, and ENVIRON does not recommend that they be used yet.
- PMCAMx sensitivity tests should investigate optimum model configurations, for example:
 - Aerosol size section schemes – the number of sections and the cut-points needed for specific types of model application.
 - Secondary organic aerosol species – how many volatility groups are warranted for anthropogenic vs. biogenic emissions?
 - Adequacy of current gas-phase chemical mechanisms to support PM modeling.
- Further development of the aqueous-phase chemistry model (VSRM) would be beneficial. For the Los Angeles test case, VSRM consumed about half of the computer time when only approximately 10% of the grid cells were cloudy. Thus, the computational requirements of VSRM may become problematic for a winter episode. Issues in need of attention are efficiency/stability of the numerical integration routines (especially VODE) and removing assumptions that prevent the PMCAMx aerosol size distribution from being a user adjustable parameter. Care is warranted in using the VODE integration package for atmospheric chemistry problems. Also, it may be possible to improve the implementation of VSRM in PMCAMx to make better use of available information, such as remembering liquid-phase concentrations between calls to VSRM (especially when the two-droplet size algorithm is being used) and passing liquid concentrations to the deposition module for use in wet-deposition calculations.
- The PMCAMx host model should be upgraded from CAMx version 3.01 to CAMx version 3.1 (or most current version). When this is done, the SAPRC99 mechanism should be interfaced to the secondary organic aerosols in PMCAMx using the methods described for SAPRC97 in this report.
- Upgrades to the CMU aerosol modules should be implemented and maintained in PMCAMx. For example, CMU enhanced the MADM aerosol size algorithms by using a trajectory-grid approach (CRC project A-39) and this should be maintained in the next version of PMCAMx.
- The wet-deposition module developed by ENVIRON should be added to PMCAMx.

- The secondary organic aerosol module should be integrated with MADM to improve efficiency.
- The PMCAMx “full science” (FS) algorithms should be implemented alongside more efficient “reduced form” (RFM) algorithms in a single model version. This would allow evaluation of FS and RFM approaches in a common platform. There is great interest in RFM algorithms for annual PM and visibility modeling.

1. INTRODUCTION

The objective of CRC project A-30 was to develop a new particulate matter (PM) model based on state-of-the-science algorithms implemented in publicly available computer codes. The Comprehensive Air-quality Model with Extensions (CAMx) is a three-dimensional multi-scale photochemical grid model (ENVIRON, 2002) that is publicly available without fees or restrictions on model application. CAMx was developed with all new code during the late 1990s using modern and modular coding practices. This has made the model an ideal platform for the extension to treat a variety of air quality issues including ozone, particulate matter, visibility, acid deposition, and air toxics. The flexible CAMx framework has also made it a convenient and robust host model for the implementation of “probing tool” techniques such as Process Analysis, the Decoupled Direct Method (DDM), and the Ozone Source Apportionment Technology (OSAT). For CRC project A-30, ENVIRON together with Sonoma Technology Inc. (STI) and Carnegie Mellon University (CMU), added state-of-the-science aerosol modeling algorithms to CAMx to create a new particulate matter model called PMCAMx, version 3.01. The source code for the initial version of PMCAMx was delivered to CRC and is being used in follow-on work to further evaluate and refine the model (CRC projects A-40 and A-44). PMCAMx will be made publicly available via the CAMx web page (<http://www.camx.com>) once the model has undergone sufficient testing and evaluation to build confidence in the model.

The development of PMCAMx was based on version 3.01 of CAMx. The extension to treat PM involved the addition of science modules to represent important physical processes for aerosols:

- Size distribution is represented using the Multi-component Aerosol Dynamics Model (MADM), which uses a sectional approach to represent the aerosol particle size distribution (Pilinis et al., 2000). MADM treats the effects of condensation/evaporation, coagulation and nucleation upon the particle size distribution.
- Inorganic aerosol thermodynamics are represented using ISORROPIA (Nenes et al., 1998, 1999) within MADM.
- Secondary organic aerosol thermodynamics are represented using the semi-volatile scheme of Strader et al., (1998).
- Aqueous-phase chemical reactions are modeled using the Variable Size-Resolution Model of Fahey and Pandis (2001), which automatically determines whether water droplets can be represented by a single ‘bulk’ droplet-size mode or whether it is necessary to use fine and coarse droplet-size modes.
- The CAMx deposition algorithms were improved for particle deposition. Dry deposition is represented for the size-resolved particle distribution (ENVIRON, 2002). A new wet-deposition algorithm has been developed but is not yet implemented in PMCAMx.

This report describes the development and testing of PMCAMx conducted under CRC sponsorship in project A-30. The report is organized as follows:

Section 2 provides a background on the science and modeling approaches for PM as a basis for the following sections.

Section 3 describes the PM modeling algorithms used in PMCAMx.

Section 4 discusses the implementation of the PM modules in the PMCAMx code

Section 5 describes how PMCAMx was tested for a Los Angeles PM episode including the model performance evaluation, diagnostic and sensitivity testing.

The study conclusions and recommendations for further work are presented in the Executive Summary to the report.

2. ATMOSPHERIC AEROSOLS

Atmospheric aerosols are small particles dispersed in the ambient air. Their behavior and impacts in the atmosphere depend upon their physical and chemical characteristics, such as particle size, chemical composition, affinity for water, and physical state (liquid or solid). Atmospheric aerosols, also referred to as particulate matter (PM), have both primary and secondary sources and they originate from natural as well as man-made emissions. Particulate matter is a natural constituent of the atmosphere with concentrations and properties that vary geographically and temporally. This section of the report provides a discussion of physical and chemical characteristics and processes that are important for atmospheric aerosols.

ATMOSPHERIC AEROSOL PROPERTIES

Particle Size and Number Distributions

The lower atmosphere contains large numbers of particles, ranging from hundreds per cm^3 in the most pristine remote areas (e.g., polar areas that are not affected by anthropogenic emissions) to millions per cm^3 in polluted urban areas. These particles span a wide size range, more than 4 orders of magnitude. Mechanical processes (e.g., dust) generate the largest particles, which are up to about 100 micrometers (μm) in diameter. The smallest particles are formed by chemical processes and may be only a few nanometers (nm) in diameter ($1 \text{ nm} = 10^{-3} \mu\text{m}$). The range in particle mass is even greater than the range in size since 1 particle of diameter $10 \mu\text{m}$ has approximately the same mass as 1 million particles of diameter $0.1 \mu\text{m}$. Consequently, larger particles tend to dominate the total mass of atmospheric aerosol whereas small particles tend to dominate the total number of aerosol particles.

Coarse and Fine Particulate

The physical and chemical processes of aerosol formation tend to impose some common features on the particle size distributions observed in the atmosphere. Observed particle mass distributions tend to show several characteristic size peaks, also called modes. The mass distribution for urban aerosols is likely to show three modes:

- A *coarse* mode that is larger than about $3 \mu\text{m}$
- Two *fine* modes that are smaller than about $1 \mu\text{m}$

The smaller fine mode below about $0.1 \mu\text{m}$ is called the nucleation (or Aitken) mode, whereas a mode between about $0.1 \mu\text{m}$ and $1.0 \mu\text{m}$ is called the accumulation mode. Aerosols in rural areas can be described in terms of the same three modes but the total aerosol may be dominated by two of the three modes. The boundaries between these modes are not precise or constant, but since these features are recognizable they have fostered a widely used terminology.

The concept of aerosol modes discussed above is used directly in some atmospheric modeling approaches, such as the modal approach in Models3/CMAQ. In CMAQ, aerosol modes are

represented by log-normal distributions. The discussion above does not imply that atmospheric aerosols actually follow a log-normal (or any other) distribution. Rather, the concept of modes has proven useful in describing atmospheric aerosols, and log-normal distributions have been useful in describing aerosol modes.

The terms coarse and fine particulate have been used to describe EPA's National Ambient Air Quality Standard for particulate matter. EPA's proposed new fine particulate standards, commonly referred to as the fine particulate standards, apply focus on particles that are smaller than 2.5 μm in diameter ($\text{PM}_{2.5}$). EPA's previous particulate standards apply to particles that are smaller than 10 μm in diameter (PM_{10}). Therefore, the term coarse particulate is being applied to particles that are between 2.5 μm and 10 μm in diameter.

Chemical Composition of Primary and Secondary Aerosol

The chemical composition of atmospheric aerosol often reflects the origin of the particles. This fact enables inverse modeling techniques, such as receptor modeling or chemical mass balance (CMB), to be used to estimate source contributions from chemical signatures within atmospheric PM. Chemical signatures are most applicable to primary particulates, meaning particles that are directly emitted to the atmosphere. Since secondary particles are formed by gas to aerosol conversion pathways in the atmosphere, the chemical composition of the aerosol is "disconnected" from the source.

General relationships also exist between the particle source and size for many different types of particles. For example, many types of primary particles formed by mechanical processes tend to be large, whereas secondary particles tend to be small. Thus, generalized relationships can be drawn between size, composition and source in many instances, as shown in Table 2-1.

Table 2-1. Generalize comparison of composition and source for fine and coarse particles.

| | Fine Particles | Coarse Particles |
|-----------------------------|---|---|
| Formation Pathways | Chemical reactions Nucleation Condensation Coagulation Cloud/fog processing | Mechanical disruption Suspension of dusts |
| Composition | Sulfate Nitrate Ammonium Hydrogen ion Elemental carbon (EC) Organic compounds Water Metals (Pb, Cd, V, Ni, Cu, An, Mn, Fe, etc.) | Suspended dust Coal and oil fly ash Crustal element (Si, Al, Ti, Fe) oxides CaCO ₃ , NaCl Pollen, mold, spores Plant, animal debris Tire wear debris |
| Solubility | Largely soluble, hygroscopic | Largely insoluble and non-hygroscopic |
| Sources | Combustion (coal, oil, gasoline, diesel, wood) Gas-to-particle conversion of NO _x , SO ₃ , and VOCs Smelters, mills, etc. | Resuspension of industrial dust and soil Suspension of soil (farming, mining, unpaved roads) Biological sources Construction/demolition Ocean spray |
| Atmospheric Lifetime | Days to weeks | Minutes to days |
| Travel Distance | 100s to 1000s of km | Up to 10s of km |

Source: Pandis and Seinfeld (1998).

Approaches to Describing Aerosol Size Distributions

In general, experimental approaches to measuring atmospheric particles do not directly measure the distribution of particle sizes, rather they provide information that characterizes the size-distribution; e.g., the mass of particles smaller than a given diameter such as 2.5 μm or 10 μm . These experimental methods are the basis of the real world data on aerosol concentrations and compliance with air quality standards. Atmospheric models do not necessarily require a highly detailed representation of the aerosol size distribution to model compliance/non-compliance with regulatory standards; all that is required is an ability to estimate the amount of aerosol in the fine and coarse size ranges defined by regulations. However, since many of the physical and chemical properties of aerosols depend strongly upon the particle size, a detailed representation of the size distribution is required to accurately model the effects of physical and chemical processes on aerosols. Modeling approaches try to balance competing needs for a detailed representation of size distribution, computational burden, and correspondence to experimental metrics used by regulators. Two main modeling approaches are being used to represent particle size, the sectional approach and the modal approach.

Sectional Approach

In the sectional approach, the aerosol size distribution is represented using an array of discrete size sections or bins. An example is shown in Figure 2-1. An individual size section represents all of the particles with size falling between the lower and upper size bounds of the section. This usually means that all of the particles within a section are assumed to have the same physical and chemical properties. A modeling approach that represents 10 chemical constituents (sulfate, nitrate, etc.) in 10 size sections results in 100 species being included in the atmospheric model.

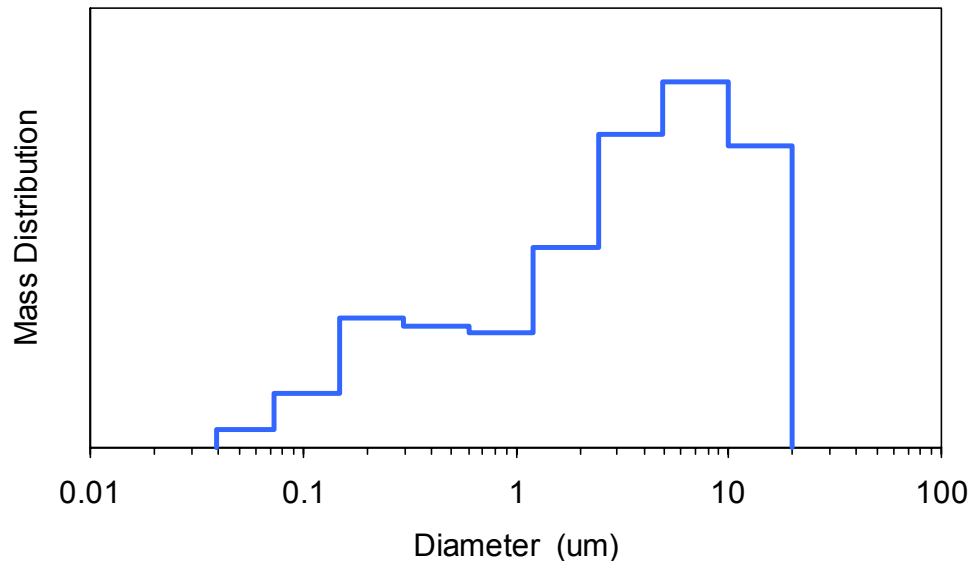


Figure 2-1. Example distribution of aerosol mass with size represented using a sectional approach.

The intervals between size sections can be chosen to match the cut-points used in ambient monitoring (2.5 μm and 10 μm). The example shown in Figure 2-1 uses 9 sections with intervals evenly distributed on a logarithmic scale between a minimum of 0.0391 μm and a maximum of 20 μm . The resulting section intervals are at 0.078, 0.156, 0.313, 0.625, 1.25, 2.5, 5 and 10 μm . The largest section is nominally from 10 to 20 μm , but in fact this section represents all particles larger than 10 μm . Similarly, the smallest section represents all particles smaller than 0.078 μm . Thus, PM_{2.5} is represented by the sum over the 6 smallest sections and PM₁₀ is represented by the sum over the 8 smallest sections.

Modal Approach

A modal approach represents the total aerosol size distribution as the sum of several size modes (discussed above). An example representation of a particle mass distribution using three modes (one coarse and two fine) is shown in Figure 2-2. Each mode is characterized by three parameters:

- Number of particles

- Mean diameter of the log normal size distribution
- Standard deviation of the log normal size distribution

As discussed above, while large particles tend to dominate the mass distribution (against size), small particles tend to dominate the number distribution. Figure 2-3 shows the distribution of aerosol number with size for the particle mass distribution shown in Figure 2-2.

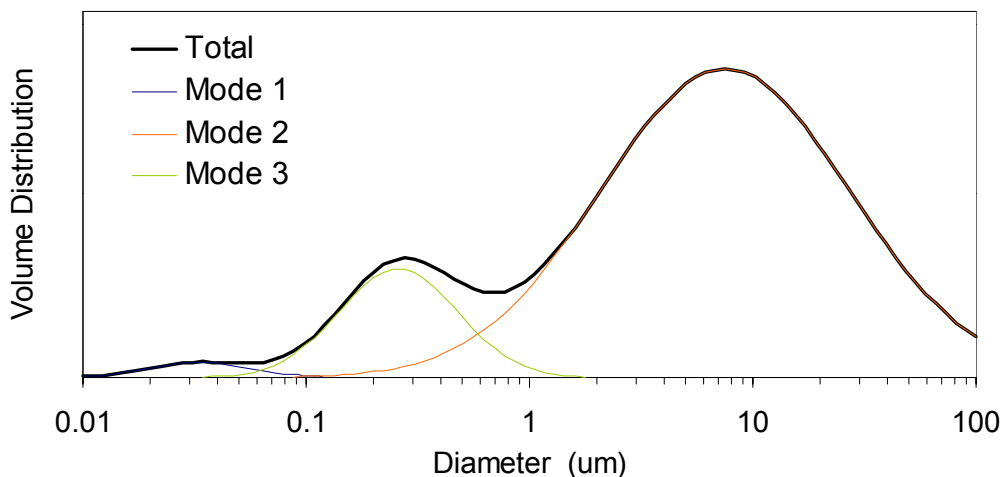


Figure 2-2. Example distribution of aerosol volume with size represented using a modal approach.

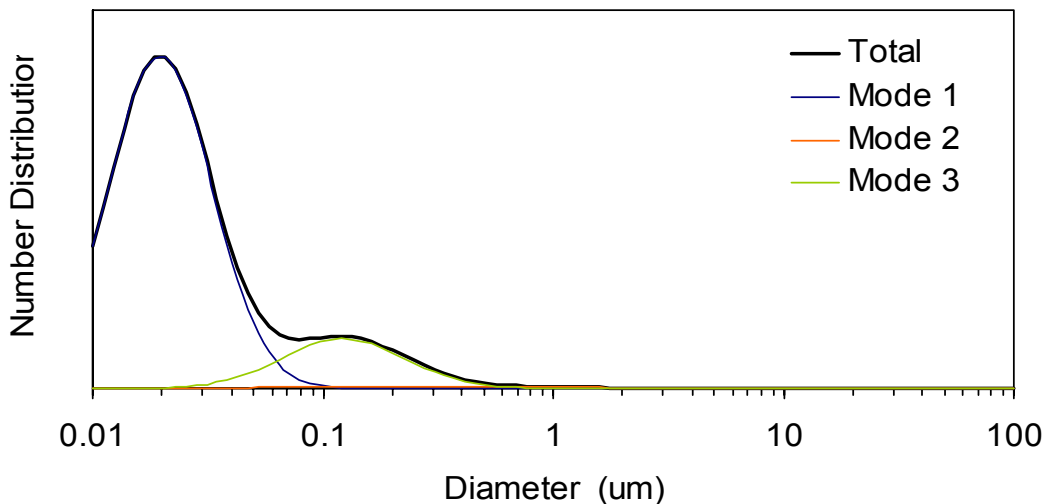


Figure 2-3. Example distribution of aerosol number with size represented using a modal approach.

To use a modal approach in a photochemical model, information must be carried on the size attributes of each mode (3 parameters) plus the chemical composition of each mode (the number of PM components). Thus a modeling approach that represents 10 chemical constituents (sulfate, nitrate, etc.) using 3 size modes might result in 39 species being included in the atmospheric model.

ATMOSPHERIC AEROSOL PROCESSES

Condensation/Evaporation

Condensation is the transfer of mass from the gas phase to the aerosol phase when gas molecules are captured at the surface of an existing particle. Evaporation is the reverse process. The tendency for a gas to condense depends upon its volatility. Some gases (e.g., sulfuric acid vapor) have extremely low volatility such that condensation is essentially irreversible. For example, virtually all sulfuric acid will be found in the aerosol phase. Other gases (e.g., condensable organics, ammonium nitrate) are semi-volatile, meaning that an equilibrium exists with significant fractions of the compound present in both the gas and aerosol phases. Whether this equilibrium favors more the gas or aerosol form depends upon the chemical properties of the compound, the properties of the existing aerosol phase, and the ambient conditions, notably temperature and, in some cases, relative humidity. Thus, a semi-volatile compound may be formed in the gas phase, condense to aerosol phase, and later evaporate back to the gas phase.

Many of the constituents of secondary organic aerosol (SOA) are semi-volatile. The production of condensable organic compounds may peak in the middle of the day when warm temperatures lead to high emissions of organic compounds and active gas-phase photochemistry leads rapid production of condensable organics (e.g., via OH reaction with aromatic hydrocarbons or terpenes). However, warm mid-day temperatures also tend to drive the condensation/evaporation equilibrium for condensable organics in favor of the gas phase. Therefore, the highest organic aerosol concentrations might not occur until later in the day when temperatures are lower and more condensation occurs.

Condensation/evaporation is an important process for several inorganic and organic aerosol constituents. Condensation is the formation pathway for virtually all secondary aerosol mass. Atmospheric models must accurately represent condensation/evaporation processes to predict the amount and size distribution of aerosols.

Nucleation

Nucleation is the process that forms new particles from condensable gases. This is distinct from condensation where gases condense onto existing particles. Nucleation is not an important mechanism for transferring mass from the gas phase to the aerosol phase because most condensable gases will condense onto the surface of existing particles rather than nucleate. Since nucleation forms new particles, it becomes important as a source of particles in very clean air masses where emissions of primary particles are low. Thus, nucleation

should not be an important process in modeling aerosols for either PM or visibility concerns over continental areas.

Nucleation of a single species is termed homomolecular nucleation. For nucleation of a single species to occur, the vapor concentration of the species must be supersaturated. Homonuclear nucleation of sulfuric acid is a source of particles in remote atmospheres. If sufficient particle surface area already exists, condensation will prevent the vapor concentration from reaching supersaturation as required for nucleation. Nucleation with more than one species is termed binary or heteronuclear nucleation and can occur when the concentrations of the combining species are below saturation.

Coagulation

When two particles collide and stick the process is called coagulation. Coagulation tends to change the particle size distribution because it increases the size and reduces the number of particles. Collisions can result from particle motion due to Brownian motion (diffusion), turbulence or sedimentation (settling). The rate of coagulation depends strongly upon the particle concentration and tends to become important in the atmosphere only at very high particle loadings, for example in polluted urban areas. Since such polluted conditions also accelerate other aerosol processes (e.g., emission, condensation/evaporation, and deposition), coagulation never has much influence on atmospheric aerosols.

Deposition

Deposition removes particles from the atmosphere and is an important mechanism for consideration in atmospheric particulate matter models. There are two mechanisms, dry deposition and wet deposition. Dry deposition is the removal of atmospheric particles by contact with the Earth's surface (soil, water, or vegetation). Wet deposition is the removal of atmospheric particles by the atmospheric hydrometeors (fog, cloud, rain, snow, etc.). Other terms used to describe this process include wet scavenging and wet removal. There are two components to wet deposition, rainout and washout. Rainout refers to in-cloud processes that incorporate particles into hydrometeors. Aerosol particles can act as cloud condensation nuclei (CCN), form cloud droplets, and be removed when cloud droplets form raindrops and fall to the ground. Washout refers to below cloud processes where falling hydrometeors capture particles by impaction.

Clouds and Aerosol Activation

Fogs and clouds contribute to both production and removal of aerosols. Aqueous phase chemistry is an important production mechanism for secondary aerosols (especially sulfate) and precipitating clouds are an important aerosol removal mechanism via wet deposition. Clouds can also dramatically affect aerosol size distributions through activation of aerosol as cloud condensation nuclei (CCN). Aerosol activation refers to the growth of a particle into a cloud droplet within a cloud. Activation occurs when the critical saturation ratio for a particle is less than the ambient saturation ratio of water and depends on the number, size distribution,

and composition of the particles. Typically, particles larger than 0.06-0.16 μm in diameter can be activated to grow to cloud droplets. Activation dominates all other in-cloud scavenging mechanisms for aerosols. Upon evaporation of the cloud, the nonvolatile material in the cloud drops is converted to aerosol with a size distribution that is likely different from the aerosol present before cloud formation.

Gas-Aerosol Equilibrium

Semi-volatile species, such as HNO_3 , NH_3 , H_2O , and SOA, partition between the gas and aerosol phases depending on physical (e.g., temperature) and chemical (e.g., gas volatility, particle composition) factors. There are two approaches to modeling this partitioning process:

- Equilibrium, i.e., assuming that the mass-transfer between the gas and aerosol phases has reached equilibrium.
- Dynamic, i.e., explicitly modeling the mass-transfer between the gas and aerosol phases such that it may or may not be at equilibrium.

Currently, most atmospheric PM models make an equilibrium assumption because this is a much simpler and computationally efficient approach to use. The validity of this assumption depends upon whether the time scale for gas/aerosol partitioning to reach equilibrium is short compared to the time scales over which the gas and aerosol concentrations are changing. Water establishes equilibrium very rapidly and can be assumed always to be in equilibrium in the particulate phase. For other semi-volatile species, characteristic times for achieving gas-aerosol equilibrium have been estimated by Wexler and Seinfeld (1990) and Meng and Seinfeld (1996). Equilibration times can be short or long depending upon conditions, and in some circumstances it is likely that the equilibrium assumption is invalid and may over or underestimate PM levels.

3. TECHNICAL FORMULATION

PMCAMx represents particulate matter using a sectional approach that tracks the mass of aerosol constituents in a number of fixed size sections. PMCAMx was developed from version 3.01 of the CAMx air quality model (ENVIRON, 2000) by adding or modifying science modules to represent the following processes:

- Aerosol Size Distributions And Chemical Species
- Gas-Phase Chemistry
- Secondary Organic Aerosol Formation
- Inorganic Aerosol Chemistry
- Particle Size Distribution
- Aqueous Phase Chemistry
- Deposition

This section describes the technical formulation for each of these processes.

AEROSOL SIZE DISTRIBUTION AND CHEMICAL SPECIES

The dynamic behavior of a spatially homogeneous aerosol is described by the so-called aerosol General Dynamic Equation (GDE) (Pilinis and Seinfeld, 1987):

$$\begin{aligned} \frac{dn(m,t)}{dt} = & -\frac{\partial}{\partial m} [I(m,t) \cdot n(m,t)] + \frac{1}{2} \int_0^m K(m,m-m') \cdot n(m',t) \cdot n(m-m',t) dm' \\ & - n(m,t) \int_0^\infty K(m,m') \cdot n(m',t) dm' + E(m,t) + N(m,t) - D(m,t) \end{aligned} \quad (3-1)$$

Where m is the particle mass, $n(m,t)$ is the size distribution function at time t , such that $n(m,t)dm$ is the number concentration of particles having masses in the range $[m, m+dm]$, $K(m,m')$ is the coagulation coefficient for particles with mass m and m' (Friedlander, 1977; Seinfeld, 1986), $I(m,t)$ is the rate of change of particle mass resulting from condensation and evaporation, $E(m,t)$ is the emission rate of particles, $N(m,t)$ is the rate of production by homogeneous nucleation (Seinfeld and Pandis, 1998), and $D(m,t)$ is the rate of removal due to dry deposition. The composition of particles of the same mass m can vary from particle to particle due to external mixing. Due to our lack of understanding of these variations and for mathematical simplicity, PMCAMx assumes that all particles of the same size have the same chemical composition (internal mixture assumption).

PMCAMx tracks thirteen chemical components of aerosols as shown in Table 3-1. These components account for all of the major primary and secondary aerosol constituents. Each component is represented in every size section. In principle, the number of size sections and their size ranges can be defined for each PMCAMx simulation, but with version 3.01 the size

distribution developed for the Los Angeles test case must be used (Table 3-2)¹. This size distribution contains 10 sections defined according to a log-normal distribution and with cut-points at both 2.5 μm and 10 μm . The mass of PM_{2.5} can be calculated by summing over section 1-6 and the mass of PM₁₀ can be calculated by summing over sections 1-8. Thirteen components in ten size sections lead to a total of 130 aerosol species in PMCAMx. Individual aerosol species names specify both the constituent and the size section using a naming convention described below.

Table 3-1. Aerosol constituents in PMCAMx.

| PMCAMx | | | | Molecular |
|--------|---------------------------------|---------|-----------|------------------|
| Name | Description | Primary | Secondary | Weight |
| SOA1 | Secondary organic aerosol 1 | | X | n/a ¹ |
| SOA2 | Secondary organic aerosol 2 | | X | n/a |
| SOA3 | Secondary organic aerosol 3 | | X | n/a |
| SOA4 | Secondary organic aerosol 4 | | X | n/a |
| POC | Primary organic carbon (matter) | X | | n/a |
| PEC | Primary elemental carbon | X | | n/a |
| CRST | Crustal material (dust) | X | | n/a |
| PH2O | Water in aerosol phase | | X | 18 |
| PCL | Chloride ion | X | | 36.5 |
| NA | Sodium ion | X | | 23 |
| PNH4 | Ammonium ion | | X | 18 |
| PNO3 | Nitrate ion | | X | 62 |
| PSO4 | Sulfate ion | X | X | 96 |

1. Molecular weight is not applicable for these species. Nominal values are used on the PMCAMx chemistry parameters file shown in Appendix A.

Table 3-2. Aerosol size sections for PMCAMx version 3.01.

| Section | Lower Cut-point (μm) | Upper Cut-point (μm) |
|---------|--------------------------------------|--------------------------------------|
| 1 | 0.039063 | 0.078125 |
| 2 | 0.078125 | 0.15625 |
| 3 | 0.15625 | 0.3125 |
| 4 | 0.3125 | 0.625 |
| 5 | 0.625 | 1.25 |
| 6 | 1.25 | 2.5 |
| 7 | 2.5 | 5 |
| 8 | 5 | 10 |
| 9 | 10 | 20 |
| 10 | 20 | 40 |

¹ The restriction to using the size distribution shown in Table 3-2 arises in the aqueous phase chemistry module and will be lifted in later versions of PMCAMx.

PMCAMx Species Names

The aerosol species simulated by PMCAMx are named according to chemical constituent (see Table 3-1) and size section (see Table 3-2). The naming convention is “constituent_section” and some examples are given in Table 3.

Table 3-3. Example aerosol species names from PMCAMx.

| Species Name | Constituent | Size Section |
|--------------|-------------|--------------|
| PSO4_7 | Sulfate | 7 |
| PNH4_4 | Ammonium | 4 |

GAS PHASE CHEMISTRY

The PMCAMx gas-phase chemistry was modified to simulate the formation of secondary aerosol precursors. The changes were as follows:

- Track production of condensable gases (CG1 – CG4) formed in the oxidation of VOCs that are secondary organic aerosol (SOA) precursors. The selection and properties of these four SOA precursors are described in more detail in the discussion of the SOA module.
- Add a new olefin species called OLE2 to the CB4 mechanism to distinguish high SOA-yield biogenic olefins (monoterpenes) from low SOA-yield anthropogenic olefins.
- Track ammonia as a precursor to ammonium aerosols.
- Track SO₂ and gaseous sulfuric acid as precursors to sulfate aerosols.
- Track HCl as a precursor to and vaporization product of sea salt (sodium chloride) aerosols.

These changes were implemented in the most current version of the CB4 mechanism in CAMx, called mechanism 3, which already includes updated isoprene chemistry and radical-radical termination reactions. Similar modifications will be made for the SAPRC99 mechanism introduced in CAMx version 3.1. The enhanced CB4 mechanism is called mechanism 8 in PMCAMx and is implemented for the CMC fast chemistry solver. The complete list of gas-phase species for CB4 chemical mechanism 8 is shown in Table 3-4, and a listing of the mechanism is provided in Appendix A.

Table 3-4. Gas phase species in the PMCAMx CB4 chemical mechanism.

| PMCAMx Name | Description | Aerosol Precursor |
|----------------|-----------------------------------|----------------------|
| NO | Nitric oxide | |
| NO2 | Nitrogen dioxide | |
| O3 | Ozone | |
| PAN | Peroxyacyl nitrates | |
| NXOY | Nitrogen in NO3 and N2O5 | |
| OLE | CB4 olefins (anthropogenic) | X |
| PAR | CB4 paraffin | X |
| TOL | CB4 toluene | X |
| XYL | CB4 xylene | X |
| FORM | Formaldehyde | |
| ALD2 | CB4 higher aldehyde | |
| ETH | Ethene | |
| CRES | CB4 Cresol | X |
| MGLY | CB4 Methylglyoxal | |
| OPEN | CB4 aromatic ring opening product | |
| PNA | Peroxyacetic acid | |
| CO | Carbon monoxide | |
| HONO | Nitrous acid | |
| H2O2 | Hydrogen peroxide | |
| HNO3 | Nitric acid | X |
| ISOP | Isoprene | |
| MEOH | Methanol | |
| ETOH | Ethanol | |
| ISPD | Isoprene product | |
| NTR | Organic nitrates | |
| OLE2 | CB4 olefins (biogenic) | X |
| CG1 | Condensable gas precursor to SOA1 | X |
| CG2 | Condensable gas precursor to SOA2 | X |
| CG3 | Condensable gas precursor to SOA3 | X |
| CG4 | Condensable gas precursor to SOA4 | X |
| NH3 | Ammonia | X |
| HCL | Hydrogen chloride | X |
| SO2 | Sulfur dioxide | |
| SULF | Gas phase sulfuric acid | X |

SECONDARY ORGANIC AEROSOL FORMATION

The partitioning of the condensable organic gases between the gas and aerosol phases is simulated using the methods developed by Strader et al. (1998). The secondary organic aerosol (SOA) module was designed to accommodate varying levels of chemical detail in the condensable organic components. In PMCAMx, the SOA module is implemented with four classes of semi-volatile organics that have different volatility properties (defined by saturation concentration and heat of vaporization as shown in Table 3-5). The four condensable gases

are called CG-1 – CG4 and the corresponding secondary organic aerosols are called SOA1 – SOA4, as shown in Tables 3-1 and 3-5. The SOA module calculates the equilibrium distribution between the gas and aerosol phase for each CG/SOA pair (i.e., the amount in the gas and aerosol phases). Secondary organic material may condense to the aerosol phase or evaporate to the gas phase depending upon the CG/SOA equilibrium distribution. Evaporation and condensation change the aerosol size distribution, which uses the same algorithms as for the inorganic aerosol that is described below.

The volatility properties of the condensable gases (CG1 – CG4) are shown in Table 3-5 along with the aerosol yields ($\mu\text{g m}^{-3}$ of aerosol precursor per ppm of gas reacted) from different VOC precursors. The CG species are the only gas species in CAMx that are not in ppm units; they are in $\mu\text{g m}^{-3}$ units because the aerosol yields are conventionally defined this way. However, carrying the CGs in $\mu\text{g m}^{-3}$ when all other gases are in ppm is confusing, and will be changed in the future. The yields of the condensable gases (CG1 – CG4) are included in the listing of the gas-phase chemical mechanism shown in Appendix A.

Table 3-5. Properties of condensable gas precursors (CG1 – CG4) to secondary organic aerosols.

| CB4 VOC Precursor | Condensable Gas Species | Aerosol Yield ($\mu\text{g m}^{-3} \text{ ppm}^{-1}$) | Saturation Concentration ($\mu\text{g m}^{-3}$ at 281.5 K) | Heat of vaporization ΔH_{vap} (J mole^{-1}) | Molecular Weight (g mole^{-1}) |
|-------------------|-------------------------|---|---|---|---|
| PAR | CG3 | 14.5 ^A | 0.007 | 0 | 150 |
| OLE | CG3 | 14.6 | 0.007 | 0 | 150 |
| TOL | CG1 | 430 | 0.023 | 156,250 | 150 |
| TOL | CG2 | 836 | 0.674 | 156,250 | 150 |
| XYL | CG1 | 268 | 0.023 | 156,250 | 150 |
| XYL | CG2 | 1178 | 0.674 | 156,250 | 150 |
| CRES | CG3 | 221 | 0.007 | 0 | 150 |
| OLE2 | CG4 | 999 | 0.008 | 0 | 180 |

A. The yield of CG3 from PAR is 53.6 in PMCAMx version 3.01, but it should be 14.5 and this will be changed in future versions.

Selection of the Condensable Gases and Secondary Organic Aerosol Scheme

The physical/chemical properties of condensable gases and secondary organic aerosols depend upon the chemical reaction in which they are formed. A lumping scheme is needed to efficiently represent the distinct properties of organic aerosols using a reasonable number of model species. Each CG/SOA combination included in a 10-section model adds one gas phase species and ten aerosol species. A lumping scheme was developed for PMCAMx that uses 4 CG/SOA combinations.

Strader et al. (1998) recommended a six SOA species scheme, where three species (SOA1, SOA2, and SOA3) were associated with aromatic precursors; one species (SOA4) was associated with higher alkanes, anthropogenic alkenes, benzaldehyde, cresol, phenols, and nitro-phenols; and two species (SOA5-SOA6) were associated with biogenic alkenes. However, there were insufficient data to distinguish the properties of SOA5 and SOA6 so the starting point was effectively a 5-species SOA model.

Table 3-6 presents the parameters of the 5-species SOA model. Tables 3-7, 3-8, and 3-9 present the parameters for three more condensed models. All of the schemes treat the anthropogenic and biogenic SOAs separately, and distinguish the high saturation concentration products of aromatic precursors separately from other products. One 4-species SOA model (No. 1) assumes the properties (i.e., saturation concentration, enthalpy of vaporization, and reference temperature) of the original CG4/SOA4 species are the same as those for CG1/SOA1. This approach essentially assigns a slightly higher saturation concentration and a strong temperature dependency to the original SOA4 species. Another 4-species SOA model (No. 2) assumes that the properties of the two aromatic products with high saturation concentrations are the same ($SOA_{23_{new}} = SOA_{2_{old}} + . SOA_{3_{old}}$). This is a fairly minor change since the saturation concentration of the lumped species (SOA23) is within $\pm 18\%$ or $\pm 0.1 \mu\text{g}/\text{m}^3$ of the individual compounds. A third condensed SOA model has only 3 species and incorporates the lumping assumptions of both 4-species models.

These four models were compared in photochemical box model simulations with fast VOC oxidation and the SAPRC97 chemical mechanism. The simulations were carried out at ambient temperatures varying from 273 to 313 K. Figures 3-1 and 3-2 summarize the results for afternoon concentrations of total SOA and total condensable gas (CG) from the simulations. All of the models produce similar results for temperatures from 273 K to 298 K (i.e., for conditions where the aerosol phase is favored over the gas phase). Above the 298 K temperature, the results from the 3-species model and 4-species model No. 1 diverge from those for the 5-species model and 4-species model No. 2. Note, these two pairs of schemes give similar results over the whole temperature range (273 K to 313 K). However, above 298 K, the 5-species model and 4-species model No. 2 partitions more of the organic material into the aerosol phase than the 3-species model and 4-species model No. 1. At the highest temperature (313 K), the 5-species model estimates 12.4 $\mu\text{g}/\text{m}^3$ of the 45 $\mu\text{g}/\text{m}^3$ of organic material is SOA whereas the 3-species models only estimates 2.3 $\mu\text{g}/\text{m}^3$ is SOA. The reason for this difference is almost entirely due to the assumed temperature dependency of the original CG4/SOA4 in the condensed lumping schemes. Under these conditions, differences in saturation concentrations are much less important. It should be noted that this particular test problem produces lots of condensable material and, therefore, is not sensitive to small differences in saturation concentrations.

PMCAMx CG/SOA Species

Based on these results, the 4-species SOA model No.2 was selected for PMCAMx. The aerosol yields and saturation concentrations for this model are shown in Table 3-8 in terms of SAPRC97 lumped VOC species. These species were mapped to CB4 species to obtain the PMCAMx parameters shown in Table 3-5 (above). The mapping is direct for the CG products of reactions with aromatics:

- CB4 species TOL corresponds to SAPRC97 species ARO1
- CB4 species XYL corresponds to SAPRC97 species ARO2
- CB4 species CRES corresponds to SAPRC97 species CRES.

Simple assumptions were made for other species:

- CB4 species PAR was assumed to correspond to 0.6 ALK1 and 0.4 ALK2

- CB4 species OLE2 was assumed to correspond to 1.33 OLE3.

The assumption for PAR comes down to estimating the relative contributions of lighter (ALK1) and heavier (ALK2) alkanes (and related species lumped with alkanes) and accounting for the numbers of carbon atoms in the alkane species². The assumption for OLE2 depends upon the way biogenic olefins (i.e., monoterpenes in current biogenic emission inventories) are treated by SAPRC and CB4. SAPRC97 treats each monoterpene as OLE3. CB4 splits monoterpenes to variable mixtures of OLE, ALD2 and PAR. (In PMCAMx the OLE from biogenics is called OLE2 to distinguish it from anthropogenic olefins such as propene). The CB4 split factors for terpenes to OLE2 vary by species from 0.5 for α -pinene, to 1 for β -pinene and limonene to 2 for β -phellandrene. An average split factor for OLE2 of 0.75 was assumed so that the CB4 OLE2 aerosol yield was 1.33 times the SAPRC97 OLE3 aerosol yield.

Table 3-6. Aerosol yields and saturation concentrations for the 5-species SOA model¹.

| Gas-Phase Precursor | Condensable Gas Species | Aerosol Species | Aerosol Yield ($\mu\text{g m}^{-3} \text{ppm}^{-1}$) | Saturation Concentration ² | ΔH_{vap} (J mole^{-1}) |
|---------------------|-------------------------|-----------------|--|---------------------------------------|--|
| ALK1 | CG4 | SOA4 | 1.9 | 0.007 | 0 |
| ALK2 | CG4 | SOA4 | 131 | 0.007 | 0 |
| ARO1 | CG1 | SOA1 | 430 | 0.023 | 156,250 |
| | CG2 | SOA2 | 836 | 0.572 | 156,250 |
| ARO2 | CG1 | SOA1 | 268 | 0.023 | 156,250 |
| | CG3 | SOA3 | 1178 | 0.776 | 156,250 |
| OLE1 | CG4 | SOA4 | 9.2 | 0.007 | 0 |
| OLE2 | CG4 | SOA4 | 19 | 0.007 | 0 |
| OLE3 | CG5 | SOA5 | 749 | 0.008 | 0 |
| BALD | CG4 | SOA4 | 5 | 0.007 | 0 |
| PHEN | CG4 | SOA4 | 192 | 0.007 | 0 |
| CRES | CG4 | SOA4 | 221 | 0.007 | 0 |
| NPHE | CG4 | SOA4 | 285 | 0.007 | 0 |

1) From Strader et al., 1998

2) In $\mu\text{g m}^{-3}$ at 281.5 K

² The yield of CG3 from PAR in PMCAMx v3.01 is $53.6 \mu\text{g m}^{-3}$ but this should be $14.5 \mu\text{g m}^{-3}$ accounting for the fact that each OH + PAR reaction removes 3.7 carbons.

Table 3-7. Aerosol yields and saturation concentrations for the 4-species SOA model No. 1.

| Gas-Phase Precursor | Condensable Gas Species | Aerosol Species | Aerosol Yield ($\mu\text{gm}^{-3}\text{ppm}^{-1}$) | Saturation Concentration ² | $\Delta\text{H}_{\text{vap}}$ (J mole^{-1}) |
|---------------------|-------------------------|-----------------|--|---------------------------------------|--|
| ALK1 | CG1 | SOA1 | 1.9 | 0.023 | 156,250 |
| ALK2 | CG1 | SOA1 | 131 | 0.023 | 156,250 |
| ARO1 | CG1 | SOA1 | 430 | 0.023 | 156,250 |
| | CG2 | SOA2 | 836 | 0.572 | 156,250 |
| ARO2 | CG1 | SOA1 | 268 | 0.023 | 156,250 |
| | CG3 | SOA3 | 1178 | 0.776 | 156,250 |
| OLE1 | CG1 | SOA1 | 9.2 | 0.023 | 156,250 |
| OLE2 | CG1 | SOA1 | 19 | 0.023 | 156,250 |
| OLE3 | CG5 | SOA5 | 749 | 0.008 | 0 |
| BALD | CG1 | SOA1 | 5 | 0.023 | 156,250 |
| PHEN | CG1 | SOA1 | 192 | 0.023 | 156,250 |
| CRES | CG1 | SOA1 | 221 | 0.023 | 156,250 |
| NPHE | CG1 | SOA1 | 285 | 0.023 | 156,250 |

- 1) This 4-species SOA model assumes the saturation concentration of condensable organics from alkanes, anthropogenic alkenes, benzaldehyde, cresols, phenols, and nitro-phenols is the same as that for the low saturation concentration condensable aromatic products of toluene and xylene.
- 2) In $\mu\text{g m}^{-3}$ at 281.5 K

Table 3-8. Aerosol yields and saturation concentrations for the 4-species SOA model No. 2 selected as the basis for PMCAMx.

| Gas-Phase Precursor | Condensable Gas Species | Aerosol Species | Aerosol Yield ($\mu\text{g m}^{-3} \text{ ppm}^{-1}$) | Saturation Concentration ² | ΔH_{vap} (J mole^{-1}) |
|---------------------|-------------------------|-----------------|---|---------------------------------------|--|
| ALK1 | CG4 | SOA4 | 1.9 | 0.007 | 0 |
| ALK2 | CG4 | SOA4 | 131 | 0.007 | 0 |
| ARO1 | CG1 | SOA1 | 430 | 0.023 | 156,250 |
| | CG23 | SOA23 | 836 | 0.674 | 156,250 |
| ARO2 | CG1 | SOA1 | 268 | 0.023 | 156,250 |
| | CG23 | SOA23 | 1178 | 0.674 | 156,250 |
| OLE1 | CG4 | SOA4 | 9.2 | 0.007 | 0 |
| OLE2 | CG4 | SOA4 | 19 | 0.007 | 0 |
| OLE3 | CG5 | SOA5 | 749 | 0.008 | 0 |
| BALD | CG4 | SOA4 | 5 | 0.007 | 0 |
| PHEN | CG4 | SOA4 | 192 | 0.007 | 0 |
| CRES | CG4 | SOA4 | 221 | 0.007 | 0 |
| NPHE | CG4 | SOA4 | 285 | 0.007 | 0 |

1. This 4-species SOA model assumes the saturation concentration of condensable organics from ARO1 and ARO2 are the same.
2. In $\mu\text{g m}^{-3}$ at 281.5 K

Table 3-9. Aerosol yields and saturation concentrations for the 3-species SOA model.

| Gas-Phase Precursor | Condensable Gas Species | Aerosol Species | Aerosol Yield ($\mu\text{gm}^{-3}\text{ppm}^{-1}$) | Saturation Concentration ² | $\Delta\text{H}_{\text{vap}}$ (J mole^{-1}) |
|---------------------|-------------------------|-----------------|--|---------------------------------------|--|
| ALK1 | CG1 | SOA1 | 1.9 | 0.023 | 156,250 |
| ALK2 | CG1 | SOA1 | 131 | 0.023 | 156,250 |
| ARO1 | CG1 | SOA1 | 430 | 0.023 | 156,250 |
| | CG23 | SOA23 | 836 | 0.674 | 156,250 |
| ARO2 | CG1 | SOA1 | 268 | 0.023 | 156,250 |
| | CG23 | SOA23 | 1178 | 0.674 | 156,250 |
| OLE1 | CG1 | SOA1 | 9.2 | 0.023 | 156,250 |
| OLE2 | CG1 | SOA1 | 19 | 0.023 | 156,250 |
| OLE3 | CG5 | SOA5 | 749 | 0.008 | 0 |
| BALD | CG1 | SOA1 | 5 | 0.023 | 156,250 |
| PHEN | CG1 | SOA1 | 192 | 0.023 | 156,250 |
| CRES | CG1 | SOA1 | 221 | 0.023 | 156,250 |
| NPHE | CG1 | SOA1 | 285 | 0.023 | 156,250 |

1. This 3 species SOA model incorporates the assumptions of both 4-species SOA models.

2. In $\mu\text{g m}^{-3}$ at 281.5 K.

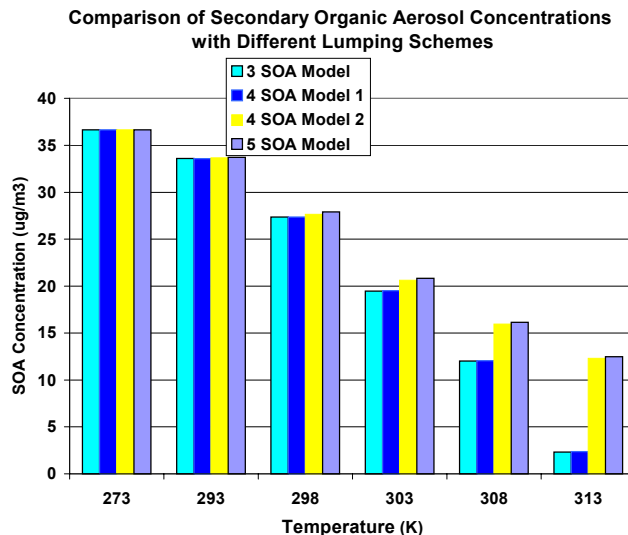


Figure 3-1. Comparison of modeled SOA concentrations using different CG/SOA lumping schemes.

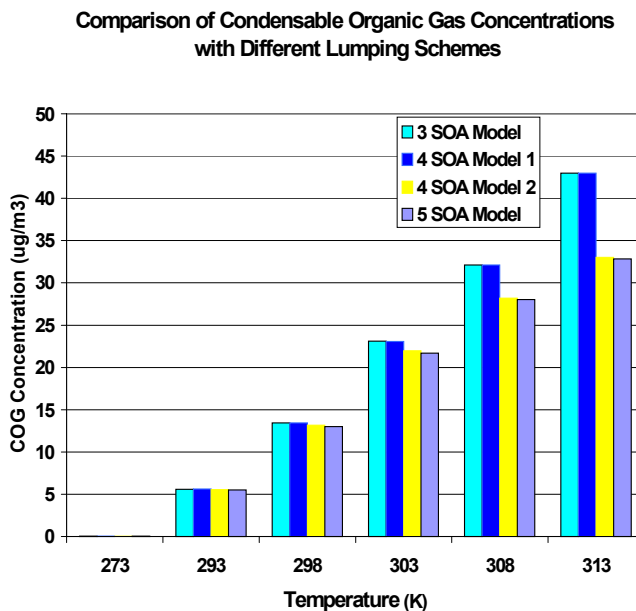


Figure 3-2. Comparison of modeled condensable gas (COG) concentrations using different CG/SOA lumping schemes.

INORGANIC AEROSOL CHEMISTRY

The chemical composition of the inorganic aerosol phase is calculated using the ISSORROPIA model (Nenes et al., 1998; 1999). ISSORROPIA was selected over alternative algorithms (e.g., SCAPE, SEQUILIB, MARS) because it provides good performance for accuracy, speed and stability (Ansari and Pandis, 1999). Solid, liquid and gas phase chemistry is modeled for the sulfate, nitrate, ammonium, and chloride aerosol system using the internally mixed assumption. The chemical species that are possible in each phase are listed in Table 3-10.

Table 3-10. Species considered by ISSORROPIA for gas, liquid and solid phases.

| Phase | Possible Species |
|--------|--|
| Gas | NH ₃ , HNO ₃ , HCl, H ₂ O |
| Liquid | H ⁺ , NH ₄ ⁺ , Na ⁺ , NO ₃ ⁻ , Cl ⁻ , SO ₄ ²⁻ , HSO ₄ ⁻ , H ₂ O |
| Solid | NH ₄ HSO ₄ , NH ₄ NO ₃ , (NH ₄) ₂ SO ₄ , NaCl, NH ₄ Cl, NaNO ₃ , NaHSO ₄ , Na ₂ SO ₄ , (NH ₄) ₃ H(SO ₄) ₂ |

ISSORROPIA can solve the composition of the aerosol system in either partitioning mode or equilibrium concentration mode. The latter feature is essential for compatibility with the hybrid and dynamic mass-transfer options for size-distribution, described below. In the partitioning mode, ISSORROPIA calculates the aerosol and gas-phase concentrations of semi-volatile components from known gas/aerosol total concentrations. In the equilibrium concentration mode, the ISSORROPIA calculates the equilibrium vapor pressure of the semi-volatile components from the known aerosol composition.

PARTICLE SIZE DISTRIBUTION

The size distribution of aerosols is solved using the algorithms described by Pilinis et al. (2000) for the Multicomponent Aerosol Dynamics Model (MADM). The aerosol size distribution can be modified by the following physical processes that are represented in PMCAMx:

- Condensation/evaporation of inorganic and organic aerosol constituents
- Coagulation
- Nucleation of sulfuric acid
- Aqueous-phase chemistry
- Deposition

Coagulation is modeled assuming Brownian diffusion and the formulas of Fuchs (Seinfeld, 1986, Table 10.1). To improve the accuracy of the coagulation calculation, the PMCAMx size distribution is over-resolved to finer distribution, coagulation is modeled, and the modified size distribution is placed back onto the PMCAMx size sections. In PMCAMx version 3.01 the coagulation size distribution is three times finer than the PMCAMx size distribution. The degree of over-resolution is determined by a model parameter that may need to be changed if PMCAMx is used with different size sections in the future.

Nucleation is modeled based on the parameterization of Russell et al. (1994) and the work of Jaecker-Voirol and Mirabel (1989). The nucleation rate depends upon the gaseous sulfuric acid concentration, which in PMCAMx is from the gas-phase $\text{OH} + \text{SO}_2$ reaction. This approach is appropriate for estimating the effect of nucleation on the particle mass distribution but not the number distribution. The inclusion of a nucleation process should ensure some particle population in the finest size sections to provide a surface area onto which condensation can occur.

The impacts of aqueous-phase chemistry and deposition on the particle size distribution are described in the respective sections on these processes, below.

MADM simulates the complete atmospheric aerosol size/composition distribution by solving the condensation-evaporation equation (equation 3.1). MADM includes three methods for solving the particle size distribution called the equilibrium, hybrid and dynamic methods. The equilibrium algorithm of Pandis et al. (1993) has been used in the UAM-AERO model (Lurmann et al., 1997). The SOA and ISORROPIA modules calculate the equilibrium partitioning between the gas and aerosol phases assuming that mass transfer reaches equilibrium, and MADM calculates the resulting particle size distribution. The accuracy of the equilibrium assumption depends upon the time scale for mass transfer to reach equilibrium. Small particles reach equilibrium rapidly because of their high surface area to volume ratio, whereas large particles take longer to reach equilibrium. The fully dynamic algorithm of Pilinis et al. (2000) avoids the equilibrium assumption by explicitly integrating the mass-transfer rate equations between gases and particles. For small particles, the mass transfer rates can be very high relative to the particle mass making the dynamic equations difficult to solve. The hybrid algorithm of Pilinis et al. (2000) attempts to find an optimum balance between the equilibrium and dynamic assumptions by using the equilibrium method for sub-micron aerosols and performing dynamic calculations for the coarse aerosols.

The equilibrium algorithm is the fastest and most stable approach but may introduce errors under certain conditions (Wexler and Seinfeld, 1990). Meng and Seinfeld (1996) suggested that while the sub-micron aerosol may reach equilibrium in a few minutes, it may take hours or days for the coarse particles to attain this state. Laboratory measurements of Dassios and Pandis (1999) showed that the mass transport of ammonium nitrate is significantly faster than the above theoretical studies had assumed, and that the time scale for equilibration of the accumulation mode probably is less than 20 minutes.

PMCAMx version 3.01 always uses the equilibrium assumption within MADM to solve the particle size distribution. The hybrid and dynamic options are retained within the MADM code and may be activated in future versions of PMCAMx once we have more experience with the model and based on the results of ongoing improvements in algorithm efficiency by the developers of MADM.

AQUEOUS PHASE CHEMISTRY

Aqueous-phase chemistry is important for modeling the production of sulfate from the oxidation of sulfur dioxide in cloud and/or fog water droplets (Seigneur and Saxena, 1988). The rate of sulfate production is a non-linear function of aqueous concentrations, such as the cloud water pH, and the concentration conditions in cloud droplets depends upon the size of the water droplets. For simplicity and/or efficiency, many aqueous-phase chemistry algorithms assume that all the cloud droplets are the same size, which may be called a “bulk approximation” because it leads to the simplifying assumption that the concentrations in all cloud droplets can be represented by bulk average values. The bulk approximation is fast but tends to under-predict sulfate production if the coarse aerosol mode is alkaline and the accumulation mode is acidic (Gurciullo and Pandis, 1997). In these cases, improved accuracy can be obtained by using a more computationally demanding size-resolved algorithm that explicitly represents cloud droplets of several different sizes (Gurciullo and Pandis, 1997; Fahey and Pandis, 2001). The aqueous-phase chemistry in PMCAMx uses either bulk or size-resolved droplet models depending upon ambient conditions.

Variable Size-Resolution Model

In PMCAMx, aqueous-phase chemistry is simulated using the method described using the Variable Size-Resolution Model (VSRM) of Fahey and Pandis (2001). The VSRM allows both bulk and size-resolved (two sections) aqueous-phase chemistry. Selection of either the bulk algorithm or the two-section algorithm is made automatically using heuristic rules (Fahey and Pandis, 2001) every time the aqueous-phase chemistry module is called, i.e., for each grid cell at each timestep. Both algorithms simulate the dissolution of gaseous and aerosol material into cloud water droplets, partitioning of species between the aqueous and gas phases, and chemical reactions within the aqueous phase. The aqueous-phase chemistry module also modifies the size distribution of the inorganic aerosol constituents.

The VSRM simulates the aqueous-phase chemistry and exchange of species between the gaseous and aqueous phases occurring within a cloud. Cloud droplets are assumed to form instantaneously upon aerosol particles with diameters exceeding a critical size, or activation diameter, while those with sizes less than the activation diameter remain as interstitial aerosol for the duration of the cloud event. Inputs to the model include the initial aerosol size/composition distribution, initial gas-phase concentrations, temperature, cloud liquid water content, length of cloud event, droplet diameters, aerosol activation diameter, and alkaline dust fraction. After initial aqueous-phase concentrations are determined, the model solves the following differential equations for each droplet group and species:

$$\frac{dp_i}{dt} = \sum_j \left(-k_{mt,i,j} w_{Lj} p_i + \frac{1}{H_{i,j}} k_{mt,i,j} C_{i,j,aq} w_{Lj} \right) \quad (3-2)$$

$$\frac{dC_{i,j,aq}}{dt} = \frac{k_{mt,i,j}}{RT} p_i - \frac{k_{mt,i,j}}{H_{i,j} RT} C_{i,j,aq} - Q_{i,j} R_{i,j,aq} \quad (3-3)$$

Where:

- p_i is the bulk partial pressure of vapor gas i in the cloud
- $k_{mt,i,j}$ is the mass transfer coefficient of gas i to droplets of size j
- $w_{L,j}$ is the cloud liquid water content of droplet group j
- $H_{i,j}$ is the effective Henry's Law coefficient for gas i
- R is the gas constant
- T is temperature
- $C_{i,j,aq}$ is the aqueous-phase concentration of i at the surface of the droplets of size j
- $Q_{i,j}$ is a mass transfer correction factor for species i in droplet group j
- $R_{i,j,aq}$ is the net consumption rate of species, i , in the aqueous phase (Seinfeld and Pandis, 1998, 634-635).

Chemical Mechanism

The aqueous-phase chemical mechanism is based on Pandis and Seinfeld (1989), with the only differences being the addition of Ca^{2+} to the list of aqueous-phase species and H_2SO_4 to the gas phase. The mechanism treats 50 aqueous-phase and 21 gas-phase species. It also includes 17 aqueous-phase ionic equilibria, 21 gas-phase/aqueous-phase reversible reactions, and 109 aqueous-phase chemical reactions. As only a fraction of the species are treated dynamically, 13 differential equations are solved in the bulk version of the model, 21 in the two-section droplet size-resolved version, and 54 in a six-section version that dynamically treats the mass transfer of nitric acid. These dynamic species are listed in Table 3-11. It is assumed that the dissolution time scale for the strong acids is small and they are completely dissolved at the beginning of the simulation. They are distributed based on the amount of liquid water and droplet size in each aerosol section. The validity of this assumption has been tested by comparing the results of the VSRM to a six-section model that allows for the dynamic transfer of HNO_3 (Fahey and Pandis, 2001). An activation diameter of $0.7 \mu m$ (at 80% RH) is assumed (Strader et al., 1998; Pandis et al., 1990). For the two-section model, the droplet sections are split at $2.5 \mu m$. The alkalinity of the mineral aerosol component depends upon "alkaline dust fraction," and it is assumed that 10% of the mass of crustal material is calcium carbonate. For the metal-catalyzed oxidation of SO_2 the iron and manganese also are scaled to the crustal material assuming mass fractions of 3×10^{-5} and 1×10^{-5} , respectively.

Table 3-11. Species for which differential equations are solved in the VSRM aqueous-phase chemistry.

| Dynamic Species |
|---------------------------------------|
| Total Formaldehyde |
| Total Formic Acid |
| SO_2 (g) |
| H_2O_2 (g) |
| NH_3 (g) |
| S(IV) (aq) for each droplet group |
| H_2O_2 (aq) for each droplet group |
| Nitrate (aq) for each droplet group |
| Chloride (aq) for each droplet group |
| Ammonium (aq) for each droplet group |
| Sulfate (aq) for each droplet group |
| HSO_5^- (aq) for each droplet group |
| HMSA (aq) for each droplet group |

Selection of the Bulk or Size-Resolved Droplet Models

Differences between bulk and size-resolved model predictions can be linked to the pH differences across the droplet size spectrum and the pH-dependent reactions forming S(VI). There are many circumstances under which the difference in sulfate production between bulk and size-resolved droplet models is small (Fahey and Pandis, 2001). The VSRM uses the more efficient bulk method when the error is expected to be small and the more expensive two-section size-resolved method when necessary. In general, longer cloud processing time and higher alkaline dust lead to smaller differences between the bulk and size-resolved models. A set of heuristic rules can determine whether the bulk or size-resolved calculations are used. The “decisions” are based on six input conditions: liquid water content, aerosol alkaline dust content, and the initial gas-phase concentrations of SO₂, H₂O₂, NH₃, and HNO₃. These variables were chosen because aqueous-phase sulfate production is particularly sensitive to changes in these variables (Pandis and Seinfeld, 1989). The decision algorithm is shown in Figure 3-3.

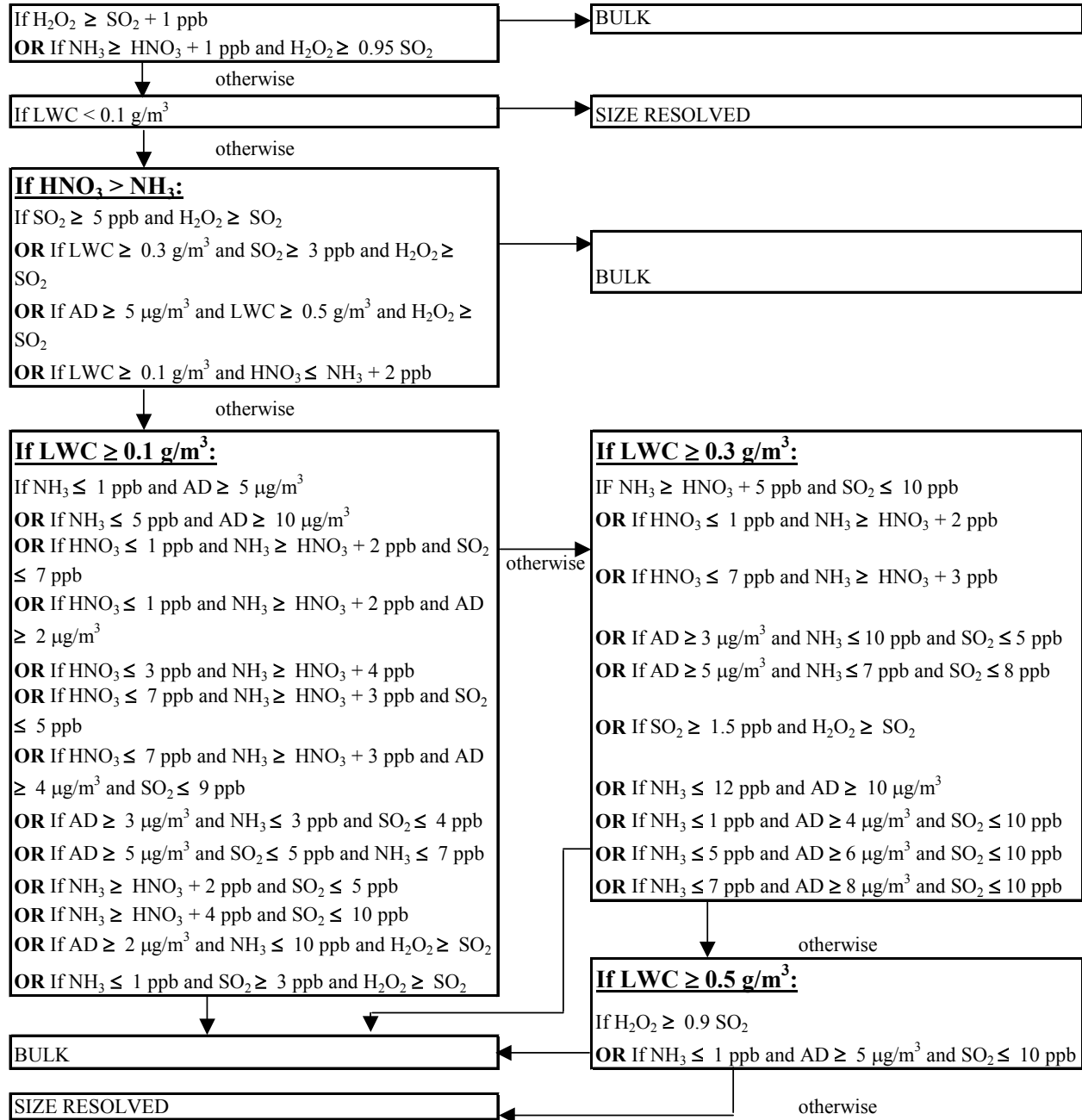


Figure 3-3. Decision algorithm for the VSRM bulk and size-resolved aqueous chemistry models.

Numerical Methods

The ordinary differential equations describing the time-evolution of the aqueous-phase concentrations are stiff and must be solved using an appropriately stable and accurate numerical integration method. The VSRM uses the VODE and LSODE numerical integration packages, both of which are based on Gear's method. These are general purpose stiff ODE solvers available from the NETLIB numerical library (<http://www.netlib.org>). Past studies (Sandu et al., 1997; Strader et al., 1998) found VODE (Brown et al., 1989) to be accurate and faster than the more widely used LSODE (Hindmarsh, 1983). However, when the VSRM was tested prior to implementation in PMCAMx mass conservation problems were found for the sulfur species in some cases. Tests showed that LSODE did not have mass conservation problems for the same tests suggesting that the problem was related to VODE. LSODE and VODE used the same aero tolerance parameters in these tests, and the mass balance errors with VODE were not correctable by tightening the error tolerances. These tests also confirmed that VODE was faster than LSODE at the same error tolerance settings. To balance efficiency and accuracy, the VSRM was modified to use the VODE algorithm, then check the sulfur balance and repeat the calculation using LSODE if the sulfur balance error exceeds 0.1%. Box model tests suggested that this strategy would be more efficient than always using LSODE.

DEPOSITION

Removal of particles and gases by dry deposition processes are modeled as a lower boundary condition in the solution of the vertical diffusion process in PMCAMx. This means that the removal of pollutants from each column of grid cells is governed both by the deposition velocity at the surface layer and the diffusive coupling of layers moving up the column from the surface.

Dry deposition of gases is modeled based on an improved version of the Wesely (1989) resistance model which is described in Section 2 of the CAMx User's Guide (ENVIRON, 2002). Deposition velocities are derived from models that account for the reactivity, solubility, and diffusivity of gases, local meteorological conditions, and surface characteristics. The parameters governing the dry deposition rates of the gas-phase species are shown in Table 3-12.

Dry deposition of particles occurs via diffusion, impaction, and/or gravitational settling. Particle size is the dominant variable controlling these processes. The resistance approach of Slinn and Slinn (1980), as implemented in UAM-AERO (Kumar et al., 1996), has been implemented in CAMx. These algorithms are described in Section 2 of the CAMx User's Guide (ENVIRON, 2002).

Wet deposition is an important removal process for particles. Particles act as cloud condensation nuclei; the cloud droplets grow and collect into sufficiently large sizes to fall as precipitation. A fraction of particles that are subsequently entrained into the cloud, and that exist within sub-cloud layers, are scavenged by liquid precipitation via impaction. The rates of nucleation and impaction depend upon cloud type (e.g., prolonged stratiform vs. vigorous convective development), rainfall rate, and particle size distribution.

Wet deposition is currently treated in PMCAMx using a simple scavenging coefficient approach based on Maul (1980) as implemented in CALPUFF. In this approach the fraction of pollutant mass removed from a given cell per time step is an exponential function of a species-dependent scavenging coefficient. For gases, the scavenging coefficient is dependent upon temperature-dependent Henry's Law solubility and rainfall rate. The algorithm is implemented for gases and is considered adequate for ozone chemistry.

An improved wet deposition algorithm has been developed for gases and particles that is suitable for aerosol modeling. This algorithm is currently undergoing testing and evaluation in PMCAMx. However, it was not available at the time the test runs were made for this report. The improved wet deposition algorithm will be implemented and evaluated in 2002. Until then, PMCAMx will over-estimate aerosol concentrations during periods of rain due to the neglect of particle wet deposition.

Table 3-12. Henry's Law constants and other parameters used in the PMCAMx dry-deposition calculation.

| Species | H ₂₉₈ (M/atm) | H Temperature Dependence (K) | Diffusivity Ratio ¹ | Reactivity Parameter ² |
|--------------------------------|-----------------------------|---------------------------------|-----------------------------------|--------------------------------------|
| NO | 0.0019 | -1480 | 1.29 | 0 |
| NO ₂ | 0.01 | -2516 | 1.6 | 0.1 |
| PAN | 3.6 | -5910 | 2.59 | 0.1 |
| HONO | 59 | -4781 | 1.62 | 0.1 |
| HNO ₃ | 200000 | -8707 | 1.87 | 0 |
| NTR | 9400 | -8706 | 2.72 | 0 |
| N ₂ O ₅ | 32000 | -8706 | 2.45 | 0.1 |
| O ₃ | 0.011 | -2415 | 1.63 | 1 |
| CO | 1 x 10 ⁻¹⁰ | 0 | 1.25 | 0 |
| PAR | 0.001 | 0 | 2 | 0 |
| ETH | 0.01 | 0 | 1.25 | 0 |
| OLE | 0.005 | 0 | 1.8 | 0 |
| TOL | 1.2 | 0 | 2.26 | 0 |
| XYL | 1.4 | 0 | 2.43 | 0 |
| MEOH | 220 | -4932 | 1.33 | 0 |
| ETOH | 220 | -4932 | 1.6 | 0 |
| ISOP | 0.01 | 0 | 1.94 | 0 |
| HCHO | 6300 | -6492 | 1.29 | 0 |
| ALD2 | 6300 | -6492 | 1.56 | 0 |
| MGLY | 2700 | -6492 | 2 | 0 |
| CRES | 2700 | -6492 | 2.45 | 0 |
| OPEN | 2700 | -6492 | 2.47 | 0 |
| ISPD | 6300 | -6492 | 1.97 | 0 |
| H ₂ O ₂ | 74000 | -6643 | 1.37 | 1 |
| NH ₃ | 20000 | -3400 | 0.97 | 0 |
| HCL | 100000 | 0 | 1.42 | 0 |
| SO ₂ | 100000 | -3156 | 1.89 | 0 |
| H ₂ SO ₄ | 1000000 | 0 | 2.33 | 0 |

1. Diffusivity Ratio = (M.Wt.)^{0.5}/(Water M.Wt.)^{0.5}

2. Wesely's reactivity parameter describes whether gases react with leaf tissues.

BOX MODEL TESTING

The aerosol modules were tested in a photochemical box model prior to implementation in PMCAMx to:

- Develop the interface between the modules and PMCAMx.
- Test the modules under closely controlled conditions.
- Test the modules on different computer platforms to identify what compiler options are needed.

This testing resulted in several rounds of revisions to the MADM aerosol, VSRM aqueous, and SOAP secondary organic aerosol modules. Some example test results are shown below.

Test 1. MADM with SOAP and Gas-Phase Chemistry

In this test the MADM and SOAP modules were run with active gas-phase chemistry from 6 am to 4 pm. The size distribution is represented using 10 size sections from 0.01 to 10 μm , with section 1 being the smallest. Figure 3-4 shows the evolution of the particle size distribution through the tests, and Figure 3-5 shows the size-resolved particle composition at the start and near the end of the test. The gas-phase chemistry forms condensable species (nitrate, sulfate and organics) and these condense onto the initial particle distribution to form a fine mode centered on sections 3 and 4. The mass conservation for key species families in the test is good, as shown in Table 3-13.

Test 2. VSRM with SOAP and Gas-Phase Chemistry

In this test the VSRM and SOAP modules were run with active gas-phase chemistry from 6 am to 4 pm. The size distribution is represented using 10 size sections from 0.01 to 10 μm , with section 1 being the smallest. Figure 3-6 shows the evolution of the particle size distribution through the tests, and Figure 3-7 shows the size-resolved particle composition at the start and near the end of the test. Particulate species are formed in both the gas and aqueous-phase chemistry modules leading to growth in the mass of particles in all sections. The aqueous sulfate production dominates the changes in the size distribution and forms fine and coarse particles predominantly in sections 4 through 9. The mass conservation for key species families in the test is fair for most species but poor for chloride, as shown in Table 3-14. This test resulted in correction of a chloride balance error in the VSRM and development of strategies to control mass-balance errors by monitoring the S-balance.

Table 3-13. Mass conservation in Test 1 with MADM and SOAP.

| | Mass Balance (%) |
|-------------------|------------------|
| Oxidized Nitrogen | 100.84 |
| Reduced Nitrogen | 103.37 |
| Sulfur | 99.94 |
| Chlorine | 99.86 |
| Sodium | 100.00 |

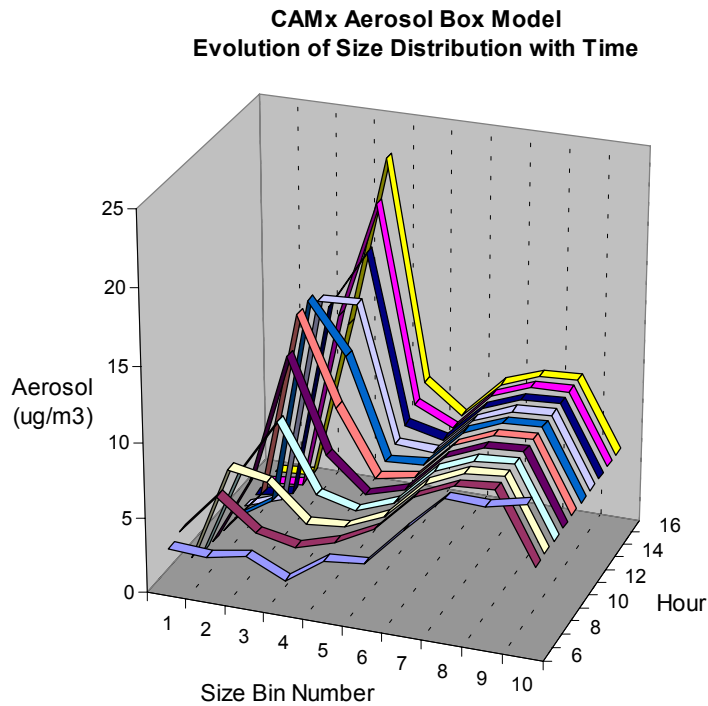


Figure 3-4. Time evolution of the aerosol size distribution in Test 1 with MADM and SOAP.

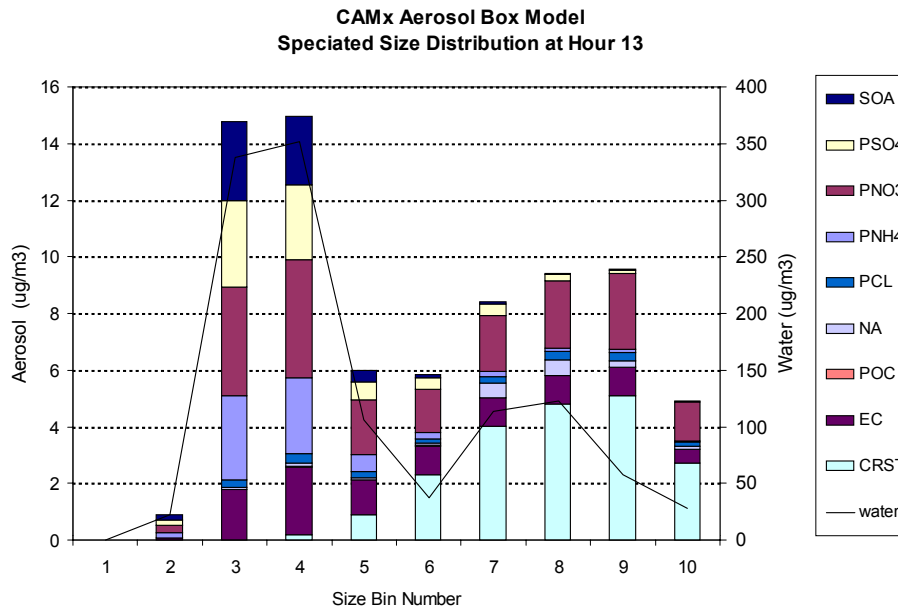
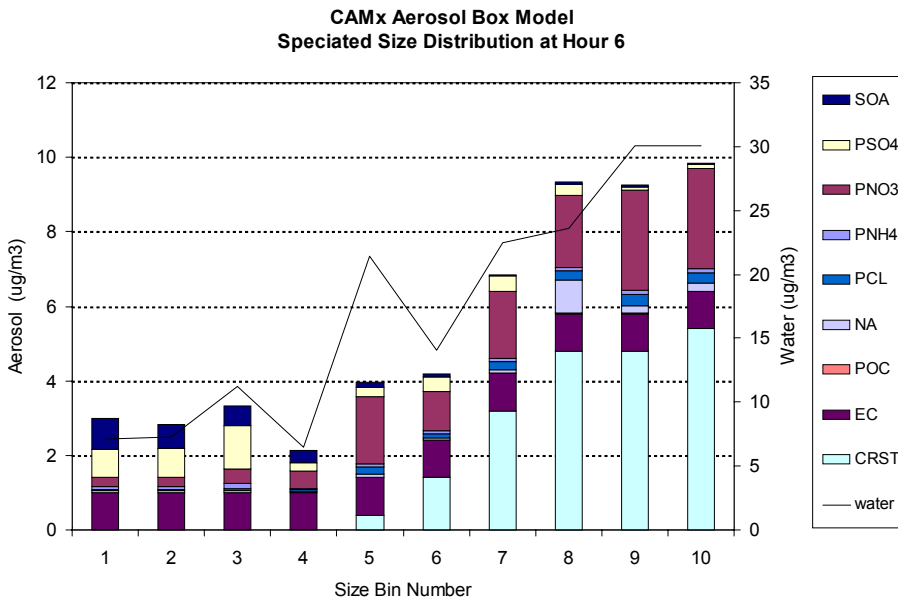


Figure 3-5. Size-resolved aerosol composition at hours 6 and 13 in Test 1 with MADM and SOAP.

Table 3-14. Mass conservation in Test 2 with VSRM and SOAP.

| | Mass Balance (%) |
|-------------------|-------------------------|
| Oxidized Nitrogen | 104.46 |
| Reduced Nitrogen | 103.54 |
| Sulfur | 106.29 |
| Chlorine | 81.93 |
| Sodium | 100.00 |

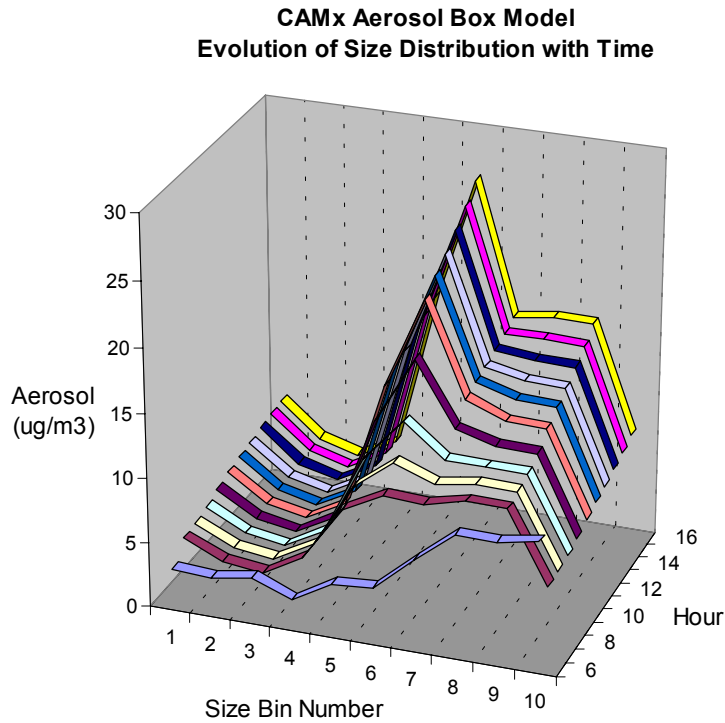


Figure 3-6. Time evolution of the aerosol size distribution in Test 2 with VSRM and SOAP.

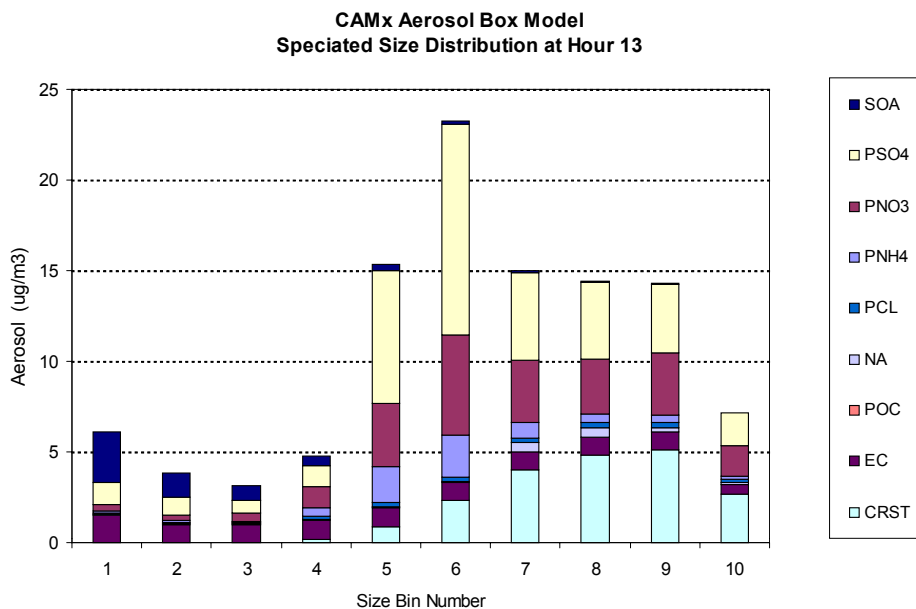
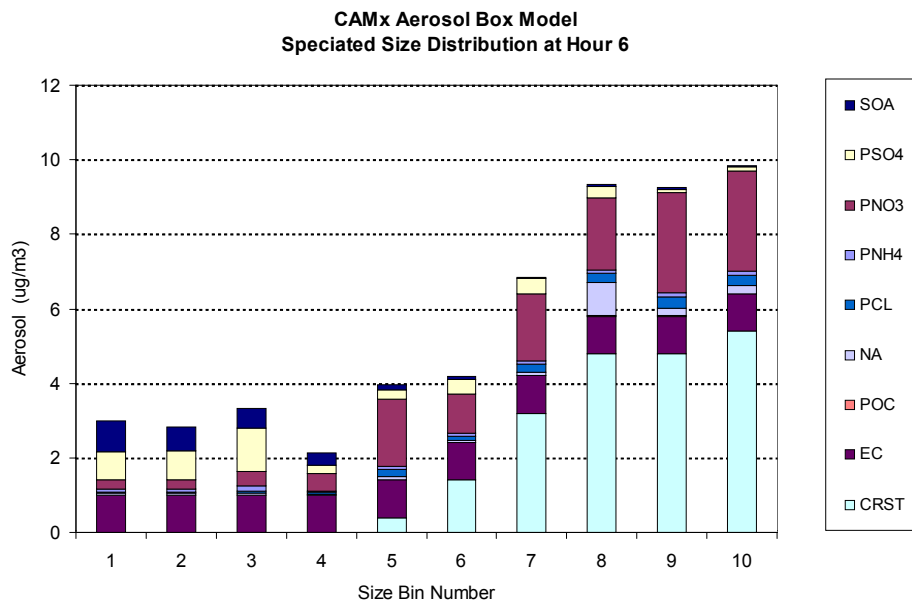


Figure 3-7. Size-resolved aerosol composition at hours 6 and 13 in Test 2 with VSRM and SOAP.

4. IMPLEMENTATION OF AEROSOL MODULES IN PMCAMx

This section describes how the aerosol modules are implemented in PMCAMx. Many aspects of the implementation were straightforward because CAMx version 3.01 already included a simplified approach to aerosol modeling so that many of the data-structures needed for aerosols already existed in CAMx. The emissions, advection, diffusion and grid nesting algorithms treat gas and aerosol species the same way and were essentially unchanged between CAMx and PMCAMx. Significant changes were required to the chemistry algorithms and these are described below.

Chemical Species

The chemistry parameters file determines the chemical species in each PMCAMx simulation. The chemistry parameters file is read by the READCHM subroutine and the species are ordered so that gases come first followed by aerosols. The total number of species (nspec) is equal to the number of gases (ngas) plus the number of aerosols (naero). When necessary, PMCAMx distinguishes between gases and aerosols by knowing that the gases are stored in arrays as species 1 to ngas and the aerosols are species (ngas + 1) to nspec.

The aerosol modules do not necessarily follow the same species order conventions as PMCAMx and so it is necessary to synchronize some information between PMCAMx and the aerosol modules. This is done by the AEROSSET subroutine, which is called from READCHM at model startup.

“FULLAERO” Chemistry Driver

The main driver for the aerosol chemistry in PMCAMx is the subroutine FULLAERO. FULLAERO is called for each grid cell immediately after gas-phase chemistry has been performed in that grid cell. FULLAERO will either perform inorganic aerosol chemistry (AEROCHEM) or aqueous chemistry (AQCHEM) depending upon whether the grid cell contains a cloud/fog or not. The rationale is that if a grid cell is cloudy (foggy), the aerosol has been activated and is contained in water droplets, and the aqueous chemistry determines how the aerosol evolves. Neither the aqueous chemistry nor the inorganic aerosol chemistry module update the secondary organic aerosol. (AEROCHEM could modify the organic aerosol based on the assumption that condensable organic gases are involatile, but this option is not used in PMCAMx.) The secondary organic aerosol chemistry module (SOAP_DRV) updates the organics after the aqueous or inorganic aerosol chemistry has been performed.

The main calling tree for FULLAERO is shown in Figure 4-1. AEROCHEM updates the inorganic aerosol chemistry and size distribution using the MADM module as described in Section 3. MADM has three options, equilibrium, dynamic or hybrid, but in the current version 3.01 of PMCAMx the equilibrium option is always used, as discussed in Section 3. The main aerosol chemistry modules shown in Figure 4-1 are:

- FULLAERO – The main driver for the aerosol chemistry in PMCAMx that controls all of the aerosol and aqueous phase chemical processes.
- AQCHEM – The driver for the aqueous phase chemistry module.
- MADM – The driver for the dynamic version of the MADM inorganic aerosol composition and size distribution module.
- EQPART – The driver for the equilibrium version of the MADM inorganic aerosol composition and size distribution module.
- HEQDYN – The driver for the hybrid version of the MADM inorganic aerosol composition and size distribution module.
- SOAP_DRV – The driver for the secondary organic aerosol equilibrium and size distribution module.

The calling trees for these modules are shown in Figures 4-2 through 4-7. These calling trees have been simplified by removing repetitive calls to the same subroutine, and by collapsing the extensive structures of several standard numerical solvers (discussed below) and the ISORROPIA module.

Aerosol Update Time Interval

PMCAMx performs chemistry at each model time step. This time step varies throughout the simulation and by grid because it is determined by the stable time step for horizontal advection (Courant number) combined with the user input maximum time step. Time steps tend to decrease with smaller grid spacing and decrease with higher wind speeds and typically range from a few minutes to 20 minutes.

Because PMCAMx is configured to use the equilibrium version of the MADM module, the assumption is made that condensable gases and aerosols reach equilibrium every time aerosol chemistry is performed. As discussed in section 3, it is believed that in the atmosphere this equilibrium is established on timescales of about 15 minutes or less. Therefore it may not be necessary to equilibrate the condensable gases and aerosols more frequently than every 15 minutes. Aerosol chemistry requires a lot of CPU time relative to other model processes so there is an efficiency advantage in limiting how often the aerosol chemistry is performed.

The time interval between calls to the aerosol chemistry is a model input parameter on the chemistry parameters file. A value of 15 minutes is suggested. This means that aerosol chemistry is performed at each time step on or after 15-minute intervals. When the aerosol chemistry is performed, the MADM and SOAP modules re-equilibrate the inorganic and organic aerosols with the condensable gases, and the aqueous chemistry is performed for the elapsed time since the last call to the aerosol chemistry modules. If the dynamic or hybrid versions of MADM are used with PMCAMx in the future they will operate for the elapsed time since the last call to the aerosol chemistry modules, as for aqueous chemistry.

The aerosol modules may be called at different times in a nested-grid because they usually use smaller time steps. Note that the aerosol modules are always called at the end of an hour. For example, if a minimum 15 minute aerosol integration time step is specified and the coarse grid is using a 12 minute advection time step then the aerosol modules will be called at 24, 36, 48, and 60 minutes past the hour with integration time steps of, respectively, 24,12,12, and 12

minutes. If the fine nested grid has an advection integration time step of 6 minutes, then the aerosol modules will be called at 18, 30, 48, and 60 minutes past the hour with integration time steps of 18, 12, 18, and 12 minutes, respectively.

Nested Grids

Nested grids take different time steps because fine grids sub-divide the time step of their parent as needed to maintain stability in the horizontal advection. This means that the aerosol update time must be considered separately for each grid. We have not yet run PMCAMx with nested grids and so these algorithms are un-tested. Therefore, we do not recommend running PMCAMx version 3.01 with nested grids.

If grid nesting is needed, 1-way nesting can be used. This entails running PMCAMx independently for each grid from coarsest to finest and passing information from coarser to finer grids via boundary conditions. The limitation of 1-way nesting is that information does not propagate from fine grids to coarse grids, which compromises the accuracy of coarse grid results downwind of fine grids.

Input Files

Aerosols must be included in the emissions and initial/boundary condition files. PMCAMx identifies the species on these files by name so the species can be in any order. However, if nested grids are used, the emissions files for each grid must have the same species in the same order. It is not necessary to include all species being modeled on all of these input files. If a species is omitted from the emissions it means that the emissions for that species are zero. If a species is omitted from the initial or boundary conditions it means that initial/boundary condition will be set to the lower bound value for that species, which is specified in the chemistry parameters file.

Numerical Packages

The PMCAMx aerosol modules use several standardized numerical packages:

- LSODE – Livermore Solver for Ordinary Differential Equations, a Gear-type ODE solver developed by Lawrence Livermore National Laboratory (Hindmarsh, 1983).
- VODE – Variable-coefficient Ordinary Differential Equation solver, a Gear-type ODE solver developed by Lawrence Livermore National Laboratory (Brown et al., 1989).
- HYBRD – Find a zero of a system of n nonlinear functions in n variables using a modification of the Powell hybrid method. (Argonne National Laboratory, MINPACK Project, March 1980).

PMCAMx requires both single and double precision versions of LSODE, which means that subroutine names must differ in the two versions. The single and double precision versions were based on the standard distributions of LSODE from NETLIB (<http://www.netlib.org>) by adding a leading “S” and “D” to subroutine names in the single and double precision versions, e.g., SLSODE and DLSODE. This is the same naming convention used in other math libraries distributed by NETLIB.

Code Organization

The PMCAMx source code is organized into several directories to facilitate understanding and maintaining the code:

- /AERO – Contains the subroutines that are specific to the aerosol modules.
- /Inc – Contains the aerosol module “include files” as well as the other PMCAMx “include files.” The “include files” contain parameters and common variables that are used in several subroutines to ensure that the declarations are consistent wherever they are used.

PM Module Error Handling

The PM modules contain several error traps that print out diagnostic messages before they terminate model execution. However, because the PM modules were developed outside of PMCAMx, they were not designed to provide all of the diagnostic information that would be needed to debug an error in a grid model simulation. For example, the PM modules do not know what grid cell they are operating on. To alleviate this problem a general-purpose error handling routine called AERO_ERR was developed for use with the PM modules. If a fatal error occurs in one of the PM modules, rather than terminating the model run with a FORTRAN stop statement, the AERO_ERR subroutine is called. AERO_ERR can determine which grid cell caused the error and report the concentrations and conditions for the grid cell just before the error. AERO_ERR reports this information and then stops the model.

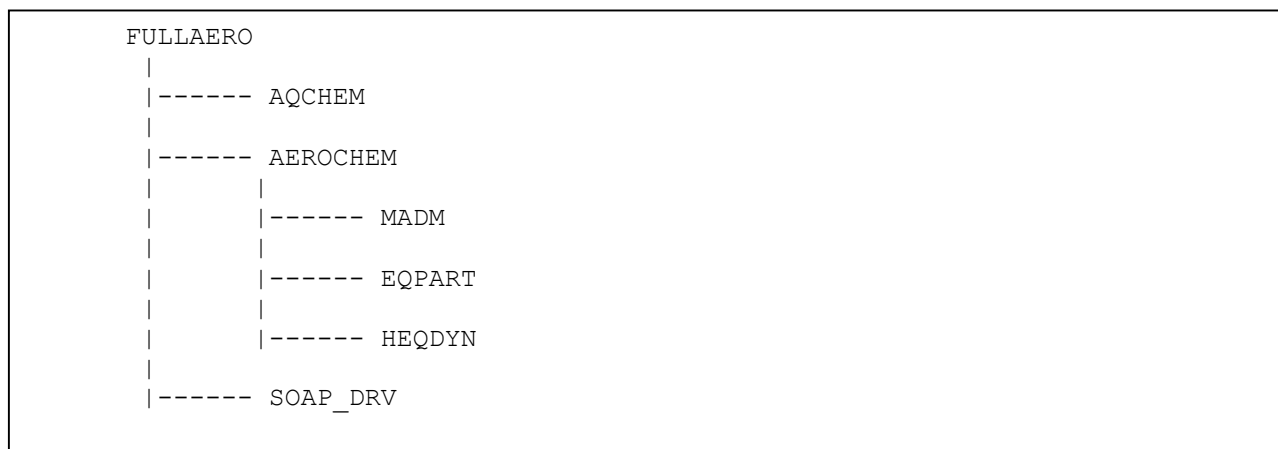


Figure 4-1. Main calling tree for the aerosol chemistry driver FULLAERO.

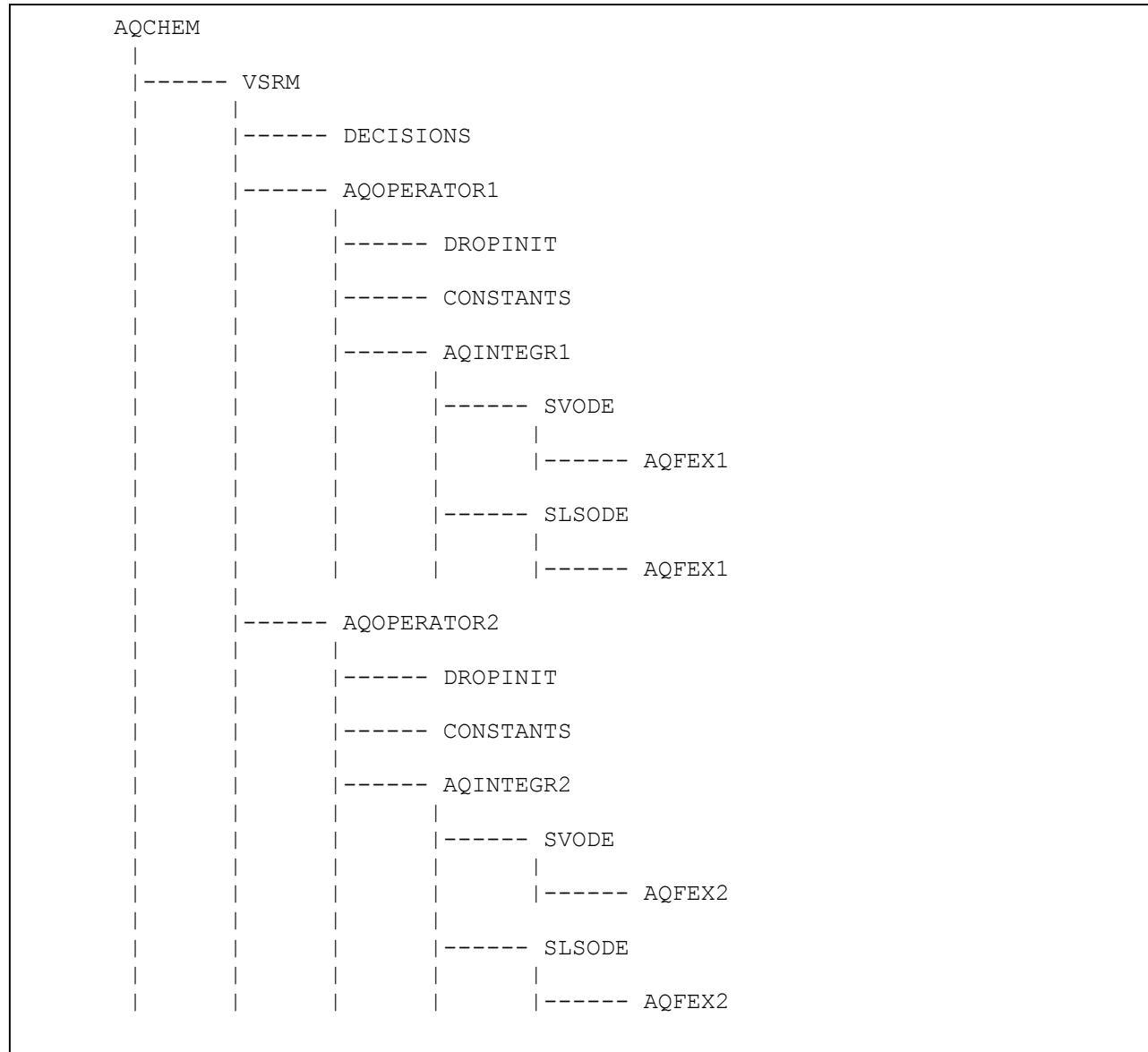


Figure 4-2. Calling tree for the aqueous-phase chemistry module (AQCHEM).

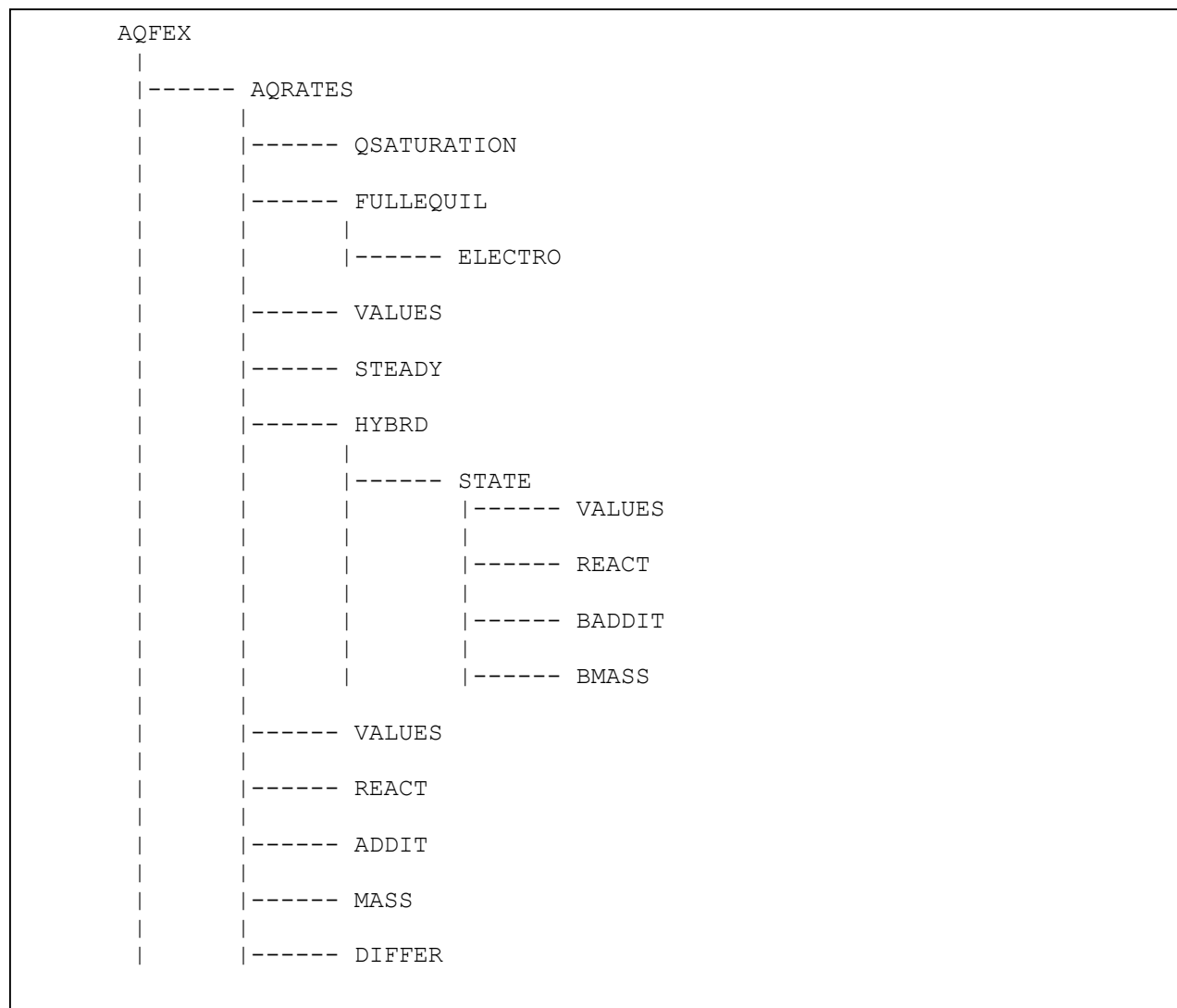


Figure 4-3. Calling tree for the calculation of chemical reaction rates by AQFEX within the aqueous-phase chemistry module (AQCHEM).

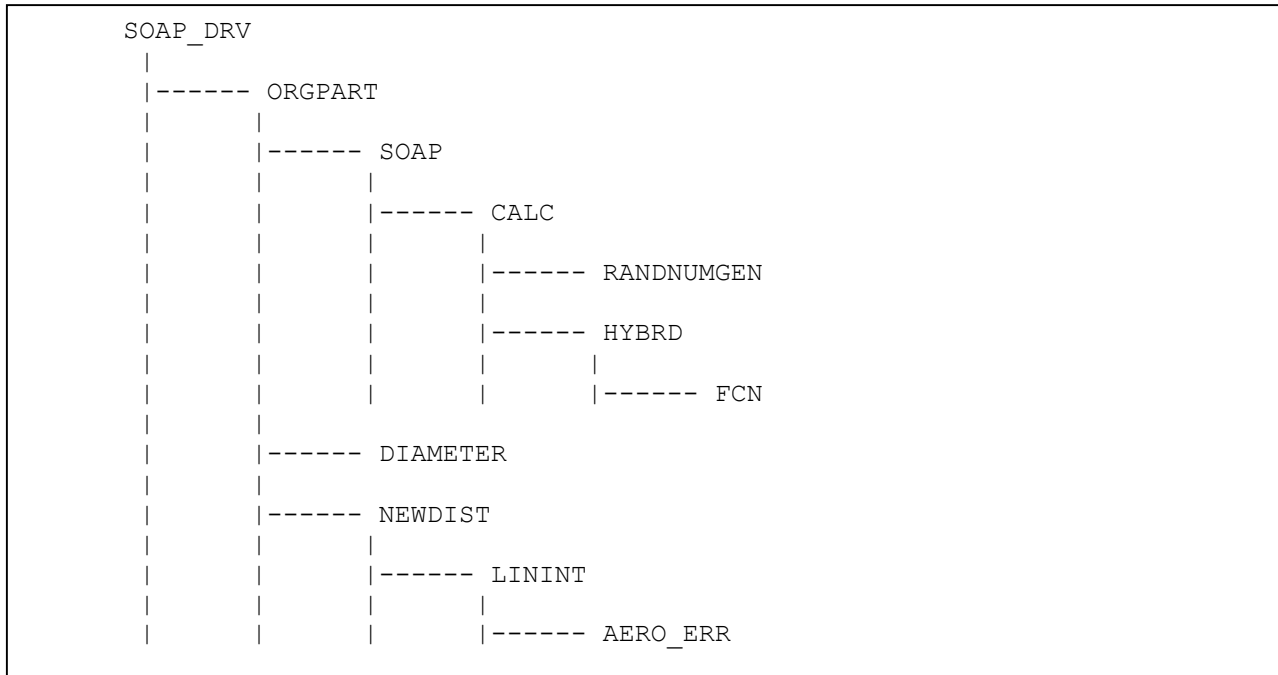


Figure 4-4. Calling tree for the secondary organic aerosol chemistry module (SOAP_DRV).

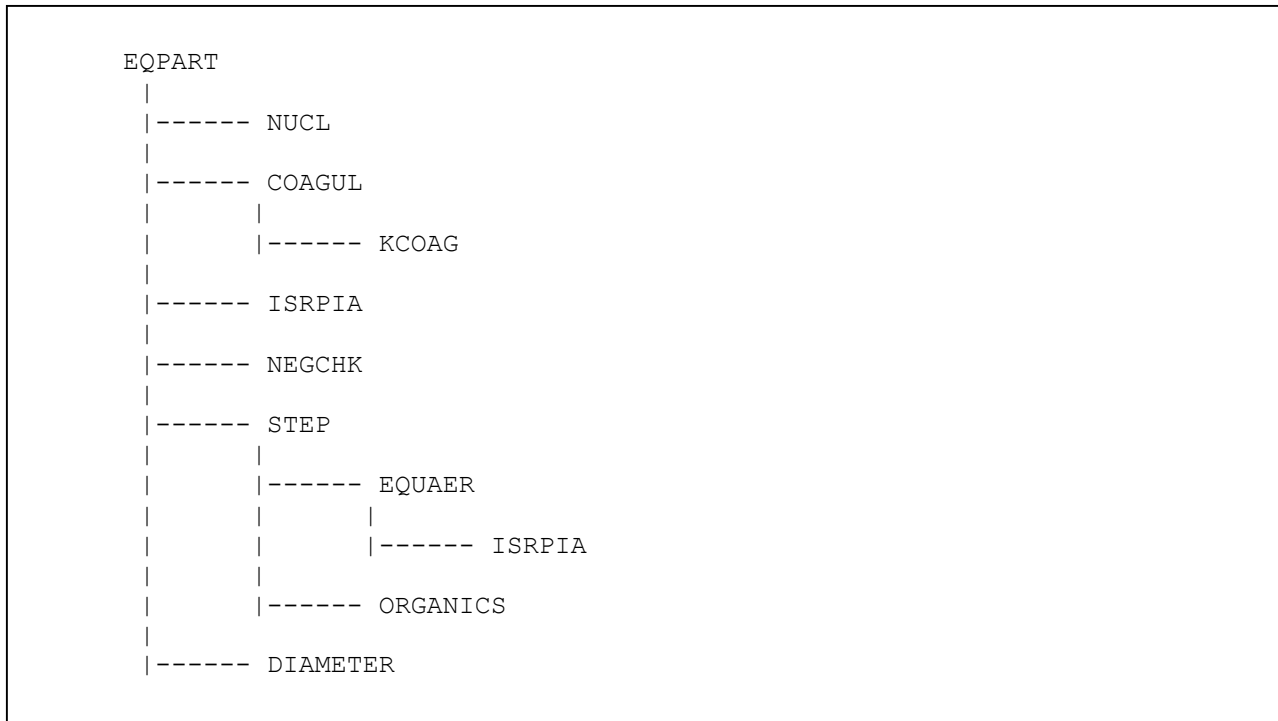


Figure 4-5. Calling tree for the equilibrium version of the MADM aerosol size distribution module (EQPART).

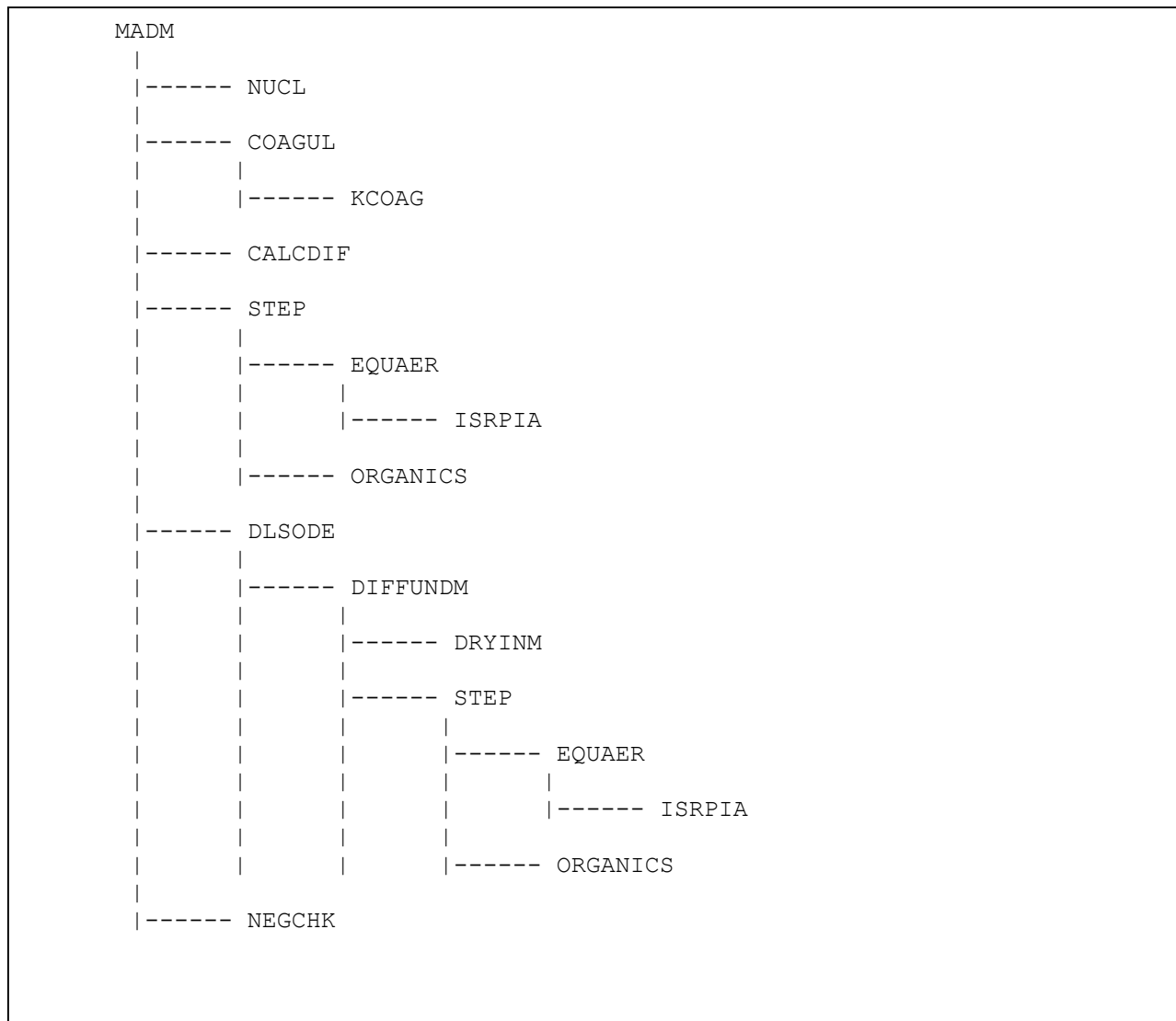


Figure 4-6. Calling tree for the dynamic version of the MADM aerosol size distribution module (MADM).

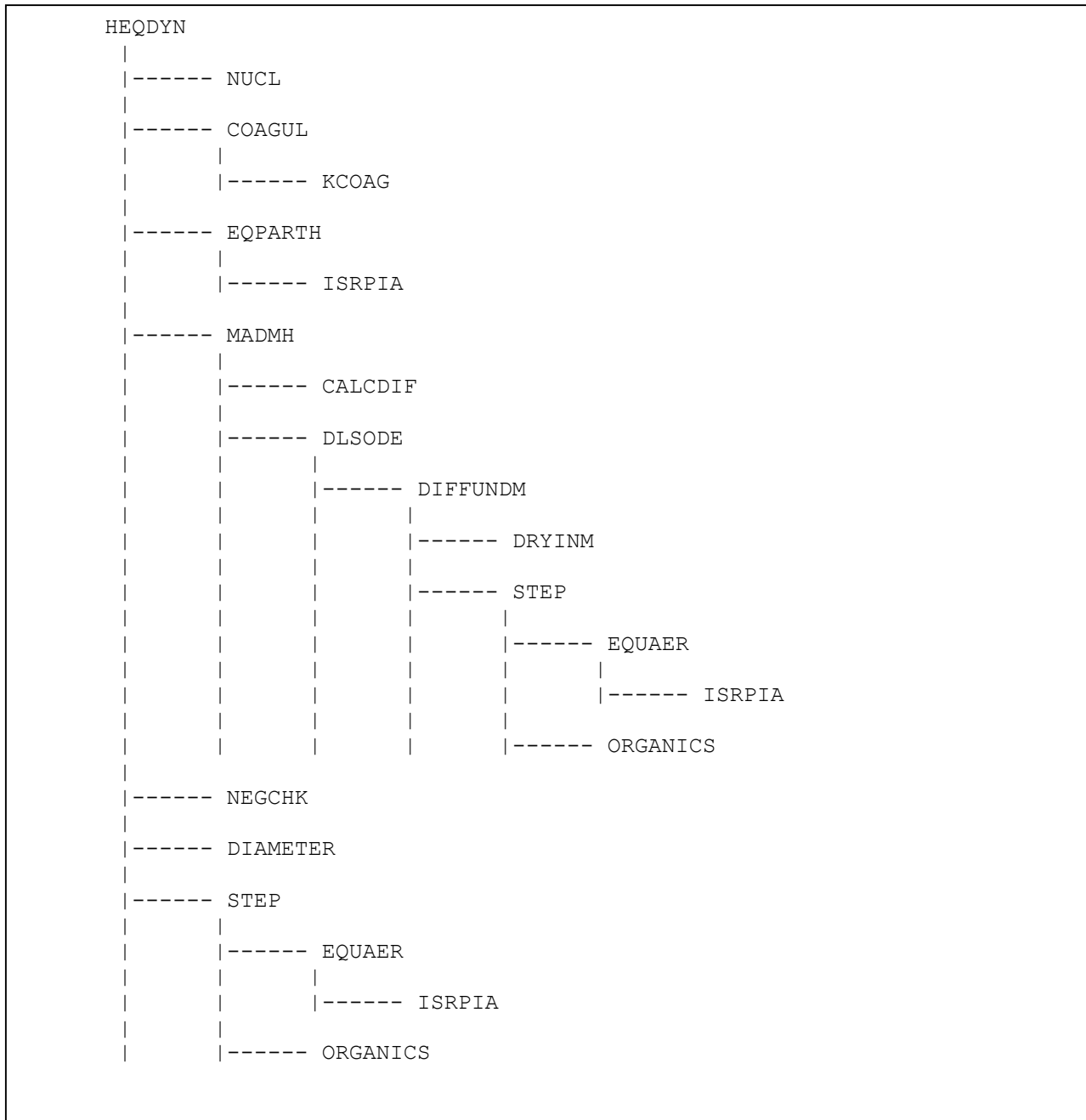


Figure 4-7. Calling tree for the hybrid version of the MADM aerosol size distribution module (HEQDYN).

5. PMCAMx TEST APPLICATION FOR LOS ANGELES

PMCAMx was tested for an October 17-19, 1995 episode in the Los Angeles area. This episode has the advantage of having been modeled previously with the UAM-AERO and UAMAERO-LT. The model inputs for PMCAMx were developed using methods similar to the UAM-AERO application, i.e., diagnostic wind modeling rather than prognostic meteorological modeling. The objective was to develop a reasonable test case for an episode that had been previously modeled, however we do not generally recommend using diagnostic wind models to drive PMCAMx (or CAMx for that matter). PMCAMx performance was evaluated against the ambient data collected in the PM₁₀ Technical Enhancement Program (PTEP) and compared to the previous model performance with the UAM-AERO models. The model inputs were developed by ENVIRON, whereas the model performance evaluation was conducted independently by STI. PMCAMx results were compared across three different computer systems to investigate any platform dependencies. Sensitivity studies were conducted to investigate the performance of the aqueous-phase chemistry module. Emissions sensitivity studies were conducted to characterize responses to reductions in ammonium, NO_x and VOC emissions.

MODEL INPUTS

PMCAMx was set up on the Los Angeles modeling domain shown in Figure 5-1. This is the modeling domain used for the UAM-AERO by the South Coast Air Quality Management District with 65 by 40, 5-km grid cells defined in UTM coordinates. The PMCAMx vertical layer structure was chosen to have the same model top as UAM-AERO but with finer vertical resolution. PMCAMx was configured with 10 layers with layer tops at 20, 50, 100, 250, 500, 750, 1000, 1500, 2000 and 2300 meters.

Meteorological input data for PMCAMx were prepared using diagnostic methods and the observed meteorological data, similar to the UAM-AERO application. The UAM-AERO meteorological data were prepared using the UAM Diagnostic Wind Model (DWM) but this model is unsuitable for PMCAMx because it does not treat parameters other than winds (Douglas et al., 1990). Therefore, the CALMET model (Scire et al., 1990) was used to prepare met inputs for PMCAMx. CALMET was supplied all of the met inputs except for the cloud (fog) file. UAM-AERO has a fog file that shows the 2-D spatial extent of fog at each hour (Kumar and Lurmann, 1996) whereas PMCAMx requires a 3-D cloud file (ENVIRON, 2002). The UAM-AERO fog file was converted to a PMCAMx cloud file by assuming that the fog layer was 250 meters deep with a liquid water content of 1 g/m³.

Emissions and initial/boundary conditions for PMCAMx also were developed from the UAM-AERO files. The UAM-AERO files included data for 8 sections and PMCAMx was configured so that sections 1-8 corresponded to the 8 UAM-AERO size sections. The PMCAMx size sections are shown in Table 5-1.

Table 5-1. Aerosol size sections for PMCAMx version 3.01.

| Section | Lower Cut-point (μm) | Upper Cut-point (μm) |
|---------|--------------------------------------|--------------------------------------|
| 1 | 0.039063 | 0.078125 |
| 2 | 0.078125 | 0.15625 |
| 3 | 0.15625 | 0.3125 |
| 4 | 0.3125 | 0.625 |
| 5 | 0.625 | 1.25 |
| 6 | 1.25 | 2.5 |
| 7 | 2.5 | 5 |
| 8 | 5 | 10 |
| 9 | 10 | 20 |
| 10 | 20 | 40 |

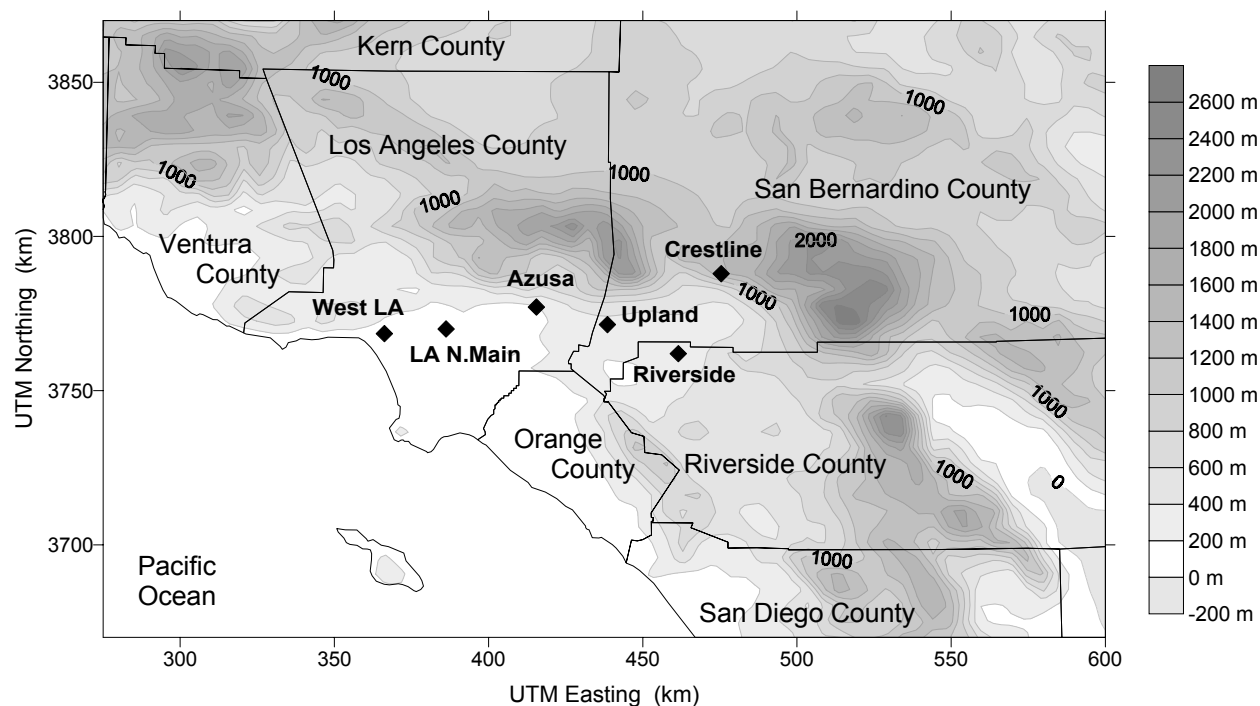


Figure 5-1. Modeling domain for the PMCAMx Los Angeles test application.

PM₁₀ TECHNICAL ENHANCEMENT PROGRAM

The PTEP Monitoring Data (PTEP) monitoring data and the episode conditions for the October 17-19, 1995 period are described in the 1997 AQMP (SCAQMD, 1997). Enhanced monitoring was performed at six sites in the LA area, namely, Downtown Los Angeles, Anaheim, Diamond Bar, Rubidoux, Fontana; and San Nicolas Island. Daily sampling was conducted during the October 17-19th, 1995 episode period. Additional description of the monitoring program are given in Kim, et al., (1996) and CARB (1998).

The October 17-19th, 1995 period was a typical fall PM episode in the Los Angeles area with stagnant winds, extensive fog near the coast and inland, cool nighttime temperatures and high

moisture availability. Ozone levels were lower than during summer stagnation periods and the federal ozone standard was exceeded only on October 19th. PM₁₀ concentrations were very high with a maximum level of 218 $\mu\text{g}/\text{m}^3$ at the Rubidoux monitoring site in Riverside.

PMCAMx PERFORMANCE EVALUATION

The first element in the review of the initial PMCAMx test simulation involved examining the spatial tile maps of hourly concentrations using the PAVE software. The spatial maps shows results that were comparable to those from other model simulation for the important chemical species. There are some primary species for which unusually high concentrations are estimated in the Long Beach area. Long Beach is a coastal area with high emission rates and some of the model estimates are probably unrealistically high for this area. The second element of the review involved examining the minimum and maximum concentrations on the grid on an hourly basis. The minimum and maximum estimated concentrations were plausible.

In the third step, we compared the estimated concentrations of NO, NO₂, and ozone with the observed values at the PTEP stations (Anaheim, downtown Los Angeles, Diamond Bar, Fontana, and Riverside-Rubidoux). The NO and NO₂ estimates do not agree particularly well with the observations at the three sites that have data, but this is not uncommon for urban-scale model applications for Los Angeles. The ozone performance is more consistent across stations. The estimated ozone concentrations are 40% to 70% lower than the observed values at the five stations. The underestimation of ozone concentrations suggests a bias in the general level of photochemical reactivity in the simulation. The simulated photo-oxidation rates of NO_x, SO₂, and VOCs are probably underestimated, which is likely to reduce the estimated concentrations of secondary aerosols (nitrate, sulfate, and secondary organic).

The fourth step involved comparing the estimated and measured daily chemical components of PM at the PTEP stations. These results are displayed in Figures 5-2 through 5-6 and Table 5-1. The specific components considered are nitrate, sulfate, ammonium, elemental carbon, organic material, and crustal material in PM_{2.5}, PM_{2.5-10}, and PM₁₀. The bias, normalized bias, error, and normalized error are computed for cases where the observed concentrations exceed the following thresholds: 2 $\mu\text{g}/\text{m}^3$ for nitrate and crustal material, 1 $\mu\text{g}/\text{m}^3$ for ammonium, sulfate, and organic material, and 0.5 $\mu\text{g}/\text{m}^3$ for elemental carbon. The five-station mean statistics are shown in Table 5-2. The results show a mixture of positive and negative bias for nitrate, sulfate, ammonium, and organic material. They also show consistent underestimation of elemental carbon concentrations and a tendency to underestimate crustal material. Note, the crustal observations are suspect because they are calculated by subtracting the other measured chemical components from the measured mass, which is uncertain because of mass measurement artifacts and volatilization losses. Also, note that the performance statistics are included for the first day of the simulation for completeness rather than as an indication of model performance. These performance statistics are not sufficient to meaningfully evaluate the model performance. There are too few days simulated, too few stations with data, and too little high time-resolution PM data to evaluate the model comprehensively.

The fifth step in the process was to compare the PMCAMx model estimates with those from other models for this same episode. The UAM-AERO and UAMAERO-LT models had been

run for the same episode with the same emissions but slightly different meteorological inputs. Figures 5-7 through 5-11 show comparisons of daily $PM_{2.5}$ component estimates from the three different models at the five PTEP stations. Figures 5-12 through 5-17 show the comparison of the hourly concentration estimates from the three models at Riverside for $PM_{2.5}$ ammonium, nitrate, sulfate, organic material, elemental carbon, and crustal material. The model results are quite different at times. Notable differences are evident in all of the species, but especially sulfate and organic material. PMCAMx uses more advanced modules to simulate sulfate formation in fogs and secondary organic aerosol formation, so it is not surprising that some of the larger differences in concentrations and concentration profiles are evident for these species. Differences in the meteorological inputs as well as model formulations are expected to account for significant differences in the results.

The spatial distributions of daily maximum 24-hour PM_{10} concentrations on October 19th, 1995 are shown in Figure 5-18 for nitrate, sulfate, ammonium, secondary organic aerosol, sodium and chloride. High nitrate, ammonium and sulfate levels are formed inland, especially in San Bernardino and Riverside counties, which agrees with the observed distributions for this and other fall PM episodes in the Los Angeles area. High sulfate also is formed near the coast in the Long Beach area and is associated with SO_2 emissions from shipping and port operations in the ports of Long Beach and Los Angeles. The secondary organic aerosol (SOA) levels are much lower than the nitrate-sulfate-ammonium levels with the highest SOA levels occurring well inland. The higher inland SOA levels are mainly due to SOA species types 1-3, which are associated with anthropogenic emissions (aromatics and alkanes). The SOA formation occurred far downwind because of the time required for VOCs to react and form SOA under the atmospheric reactivity conditions of this fall episode.

Sodium and chloride (i.e. sea salt) are highest over the ocean and did not penetrate far inland. The removal process for sodium is deposition, whereas chloride is lost to deposition and also acidification of the aerosol by sulfuric or nitric acids which liberate gaseous hydrochloric acid. Sodium is important to the formation of coarse nitrate because sodium nitrate aerosol is hygroscopic and can grow into the coarse size range (2.5 to 10 μm) by taking up water. Daily maximum 24-hour coarse nitrate (PM_{10} - $PM_{2.5}$) and fine nitrate ($PM_{2.5}$) concentrations on October 19th, 1995 are shown in Figure 5-19. The coarse nitrate is distributed closer to the ocean than fine nitrate consistent with interaction between sodium and nitrate leading to the formation of coarse nitrate in PMCAMx. Although PMCAMx coarse nitrate estimates are less than the fine nitrate, it is still significant component of the total nitrate, especially in the western portion of the basin. This raises questions regarding the appropriateness of some measurement approaches that only measure nitrate in the fine mode (e.g. IMPROVE) and some modeling approaches that assume nitrate is all in the fine mode (e.g., the CMAQ model approach).

In reviewing the PMCAMx simulation results, we looked for evidence that might suggest the model was seriously flawed or broken. Anomalously high or low concentrations, chemically unrealistic relationships between species, or unphysical spatial or diurnal patterns might suggest a serious flaw. Despite the high primary concentrations in Long Beach noted above, our overall review of the model outputs did not detect any serious flaws.

Table 5-2. Five-station mean observed and predicted PM concentrations ($\mu\text{g}/\text{m}^3$) for the October 17-19, 1995 PTEP episode.

| Date | Species /Size | Observed ($\mu\text{g}/\text{m}^3$) | PMCAMx ($\mu\text{g}/\text{m}^3$) | Bias ($\mu\text{g}/\text{m}^3$) | Normalized Bias (%) | Error ($\mu\text{g}/\text{m}^3$) | Normalized Error (%) |
|---|---------------|--|--|--------------------------------------|------------------------|---------------------------------------|-------------------------|
| Nitrate | | | | | | | |
| Oct 17 | NO3 PM2.5 | 12.68 | 11.94 | -0.74 | 11 | 4.21 | 37 |
| Oct 17 | NO3 PM2.5-10 | 10.03 | 0.71 | -9.32 | -93 | 9.32 | 93 |
| Oct 17 | NO3 PM10 | 22.71 | 12.65 | -10.06 | -42 | 10.06 | 42 |
| Oct 18 | NO3 PM2.5 | 24.94 | 30.39 | 5.45 | 30 | 5.45 | 30 |
| Oct 18 | NO3 PM2.5-10 | 7.44 | 2.34 | -5.10 | -54 | 5.33 | 64 |
| Oct 18 | NO3 PM10 | 32.38 | 32.74 | 0.36 | 4 | 4.96 | 17 |
| Oct 19 | NO3 PM2.5 | 34.93 | 32.77 | -2.16 | -4 | 7.65 | 21 |
| Oct 19 | NO3 PM2.5-10 | 6.53 | 2.92 | -5.44 | -69 | 5.44 | 69 |
| Oct 19 | NO3 PM10 | 41.46 | 35.68 | -5.78 | -15 | 5.78 | 15 |
| Ammonium | | | | | | | |
| Oct 17 | NH4 PM2.5 | 5.71 | 5.57 | -0.14 | 6 | 1.21 | 21 |
| Oct 17 | NH4 PM2.5-10 | 1.00 | 0.57 | -1.43 | -78 | 1.43 | 78 |
| Oct 17 | NH4 PM10 | 6.71 | 6.14 | NA | NA | NA | NA |
| Oct 18 | NH4 PM2.5 | 11.28 | 11.12 | -0.16 | 1 | 1.59 | 15 |
| Oct 18 | NH4 PM2.5-10 | 1.67 | 0.58 | -1.67 | -89 | 1.67 | 89 |
| Oct 18 | NH4 PM10 | 12.61 | 11.69 | NA | NA | NA | NA |
| Oct 19 | NH4 PM2.5 | 15.89 | 12.42 | -3.47 | -20 | 3.79 | 22 |
| Oct 19 | NH4 PM2.5-10 | 1.47 | 0.57 | -1.18 | -53 | 1.18 | 53 |
| Oct 19 | NH4 PM10 | 17.36 | 12.99 | -4.38 | -24 | 4.50 | 25 |
| Sulfate | | | | | | | |
| Oct 17 | SO4 PM2.5 | 3.66 | 5.62 | 1.96 | 53 | 1.96 | 53 |
| Oct 17 | SO4 PM2.5-10 | 0.82 | 1.39 | 0.71 | 61 | 0.71 | 61 |
| Oct 17 | SO4 PM10 | 4.48 | 7.01 | 2.53 | 56 | 2.53 | 56 |
| Oct 18 | SO4 PM2.5 | 7.84 | 6.05 | -1.78 | -17 | 2.48 | 29 |
| Oct 18 | SO4 PM2.5-10 | 1.39 | 1.21 | -0.19 | -8 | 0.41 | 22 |
| Oct 18 | SO4 PM10 | 9.23 | 7.27 | -1.96 | -17 | 2.79 | 28 |
| Oct 19 | SO4 PM2.5 | 11.45 | 7.68 | -3.76 | -29 | 4.43 | 37 |
| Oct 19 | SO4 PM2.5-10 | 2.20 | 1.40 | -1.08 | -37 | 1.08 | 37 |
| Oct 19 | SO4 PM10 | 13.21 | 9.09 | -4.12 | -30 | 4.65 | 34 |
| Organic Matter (Primary + Secondary) | | | | | | | |
| Oct 17 | OM PM2.5 | 5.72 | 8.11 | 2.40 | 49 | 2.40 | 49 |
| Oct 17 | OM PM2.5-10 | 3.55 | 2.32 | -1.95 | -32 | 1.98 | 34 |
| Oct 17 | OM PM10 | 9.27 | 10.43 | 1.16 | 29 | 3.54 | 47 |
| Oct 18 | OM PM2.5 | 6.82 | 8.88 | 2.06 | 36 | 2.06 | 36 |
| Oct 18 | OM PM2.5-10 | 5.35 | 2.31 | -3.90 | -41 | 4.32 | 58 |
| Oct 18 | OM PM10 | 12.16 | 11.19 | -0.97 | 0 | 3.03 | 25 |
| Oct 19 | OM PM2.5 | 8.51 | 9.42 | 0.91 | 14 | 1.80 | 22 |
| Oct 19 | OM PM2.5-10 | 3.94 | 2.27 | -1.59 | -29 | 1.93 | 49 |

| Date | Species /Size | Observed ($\mu\text{g}/\text{m}^3$) | PMCAMx ($\mu\text{g}/\text{m}^3$) | Bias ($\mu\text{g}/\text{m}^3$) | Normalized Bias (%) | Error ($\mu\text{g}/\text{m}^3$) | Normalized Error (%) |
|-------------------------|----------------------|---|---|---|--------------------------------|--|---------------------------------|
| Oct 19 | OM PM10 | 11.67 | 11.69 | 0.02 | 3 | 1.76 | 16 |
| Elemental Carbon | | | | | | | |
| Oct 17 | EC PM2.5 | 5.04 | 2.58 | -2.46 | -47 | 2.46 | 47 |
| Oct 17 | EC PM2.5-10 | 0.24 | 0.15 | NA | NA | NA | NA |
| Oct 17 | EC PM10 | 5.28 | 2.73 | -2.54 | -47 | 2.54 | 47 |
| Oct 18 | EC PM2.5 | 5.31 | 2.91 | -2.41 | -40 | 2.41 | 40 |
| Oct 18 | EC PM2.5-10 | 0.43 | 0.16 | NA | NA | NA | NA |
| Oct 18 | EC PM10 | 5.74 | 3.07 | -2.67 | -41 | 2.67 | 41 |
| Oct 19 | EC PM2.5 | 5.40 | 2.98 | -2.42 | -43 | 2.42 | 43 |
| Oct 19 | EC PM2.5-10 | 0.61 | 0.16 | NA | NA | NA | NA |
| Oct 19 | EC PM10 | 6.01 | 3.14 | -2.87 | -45 | 2.87 | 45 |
| Crustal Material | | | | | | | |
| Oct 17 | CRUS PM2.5 | 1.92 | 10.37 | 7.80 | 253 | 7.80 | 253 |
| Oct 17 | CRUS PM2.5-10 | 23.11 | 8.08 | -19.54 | -46 | 19.66 | 48 |
| Oct 17 | CRUS PM10 | 25.02 | 18.46 | -6.57 | 6 | 18.50 | 63 |
| Oct 18 | CRUS PM2.5 | 13.14 | 10.76 | -4.79 | 77 | 13.55 | 117 |
| Oct 18 | CRUS PM2.5-10 | 12.62 | 8.41 | -11.79 | -44 | 12.37 | 50 |
| Oct 18 | CRUS PM10 | 25.76 | 19.16 | -6.60 | 48 | 16.43 | 98 |
| Oct 19 | CRUS PM2.5 | 9.20 | 11.80 | 1.65 | 223 | 12.23 | 254 |
| Oct 19 | CRUS PM2.5-10 | 27.08 | 8.28 | -18.79 | -52 | 19.15 | 58 |
| Oct 19 | CRUS PM10 | 36.27 | 20.09 | -16.18 | 4 | 21.36 | 53 |

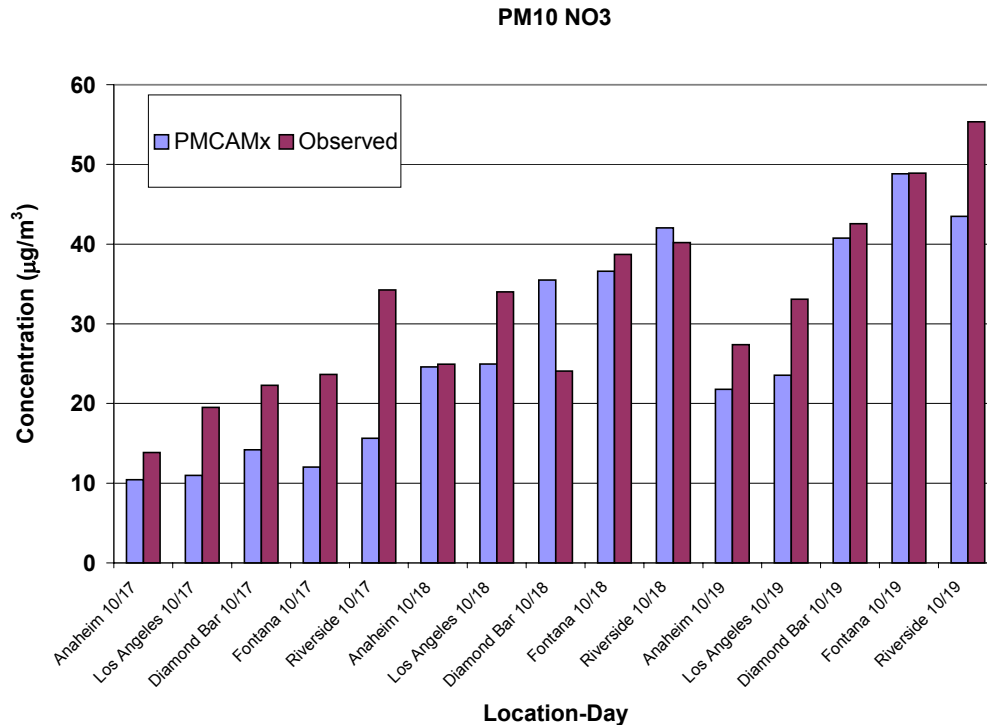


Figure 5-2. Comparison of 24-hr PM₁₀ nitrate at PTEP monitoring sites on October 17th and 18th, 1995.

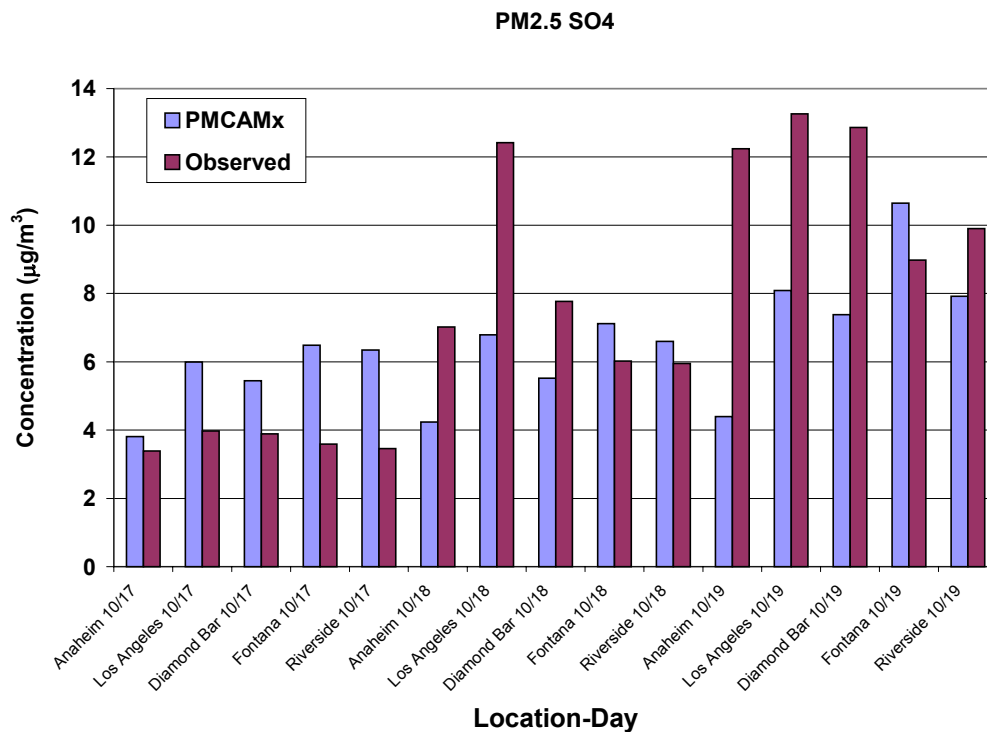


Figure 5-3. Comparison of 24-hr PM_{2.5} sulfate at PTEP monitoring sites on October 17th and 18th, 1995.

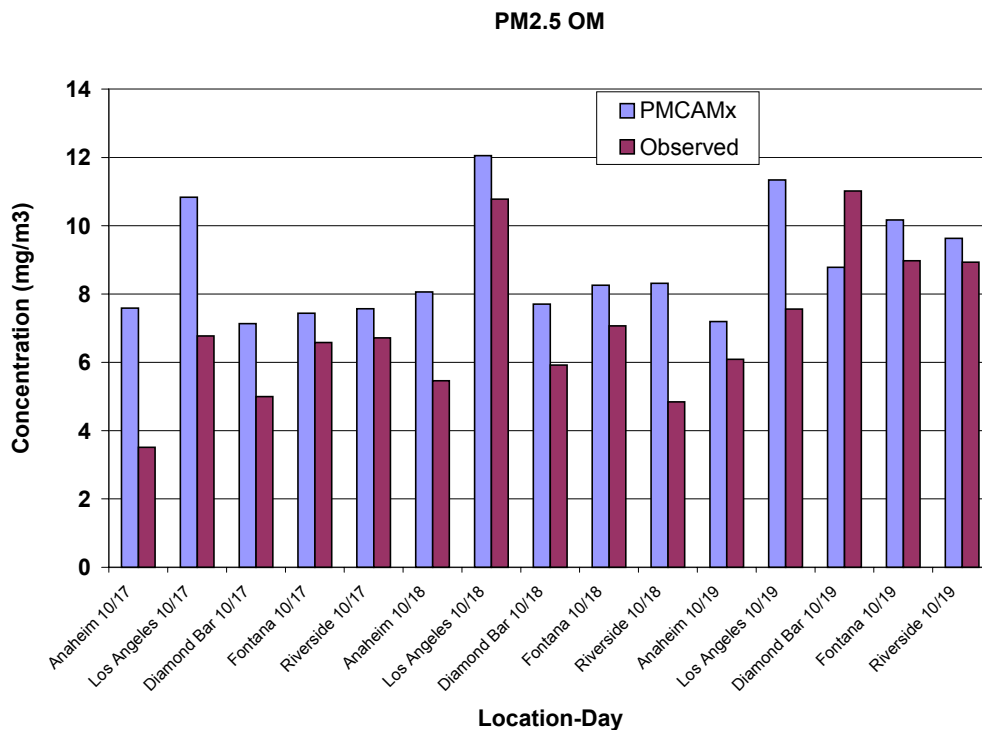


Figure 5-4. Comparison of 24-hr PM_{2.5} organic matter (primary + secondary) at PTEP monitoring sites on October 17th and 18th, 1995.

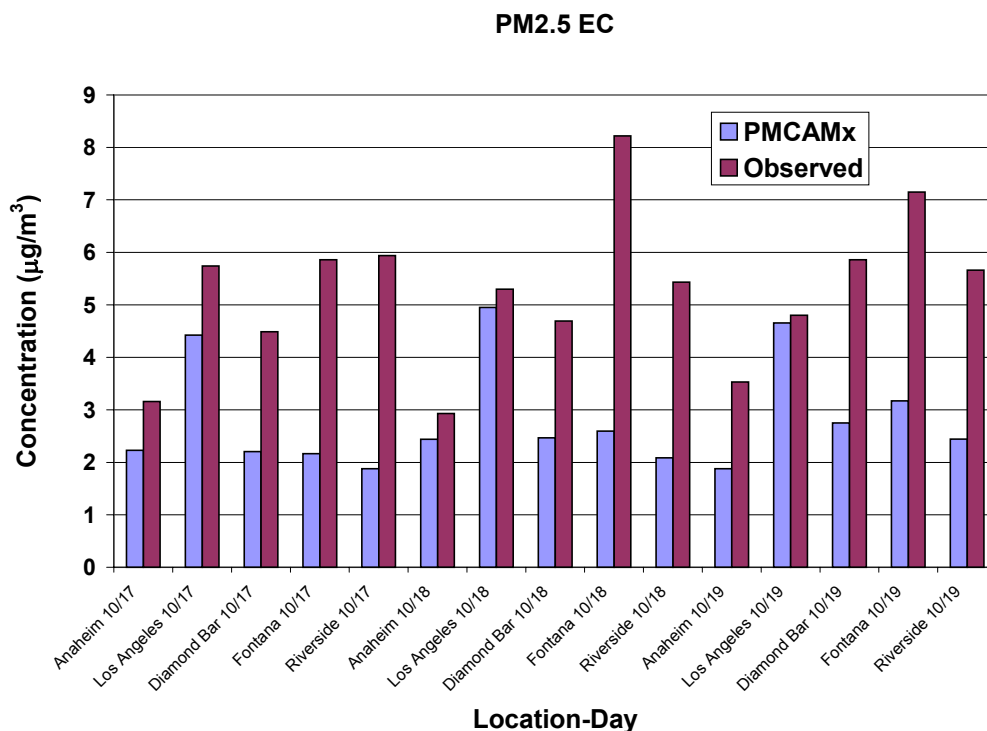


Figure 5-5. Comparison of 24-hr PM_{2.5} elemental carbon at PTEP monitoring sites on October 17th and 18th, 1995.

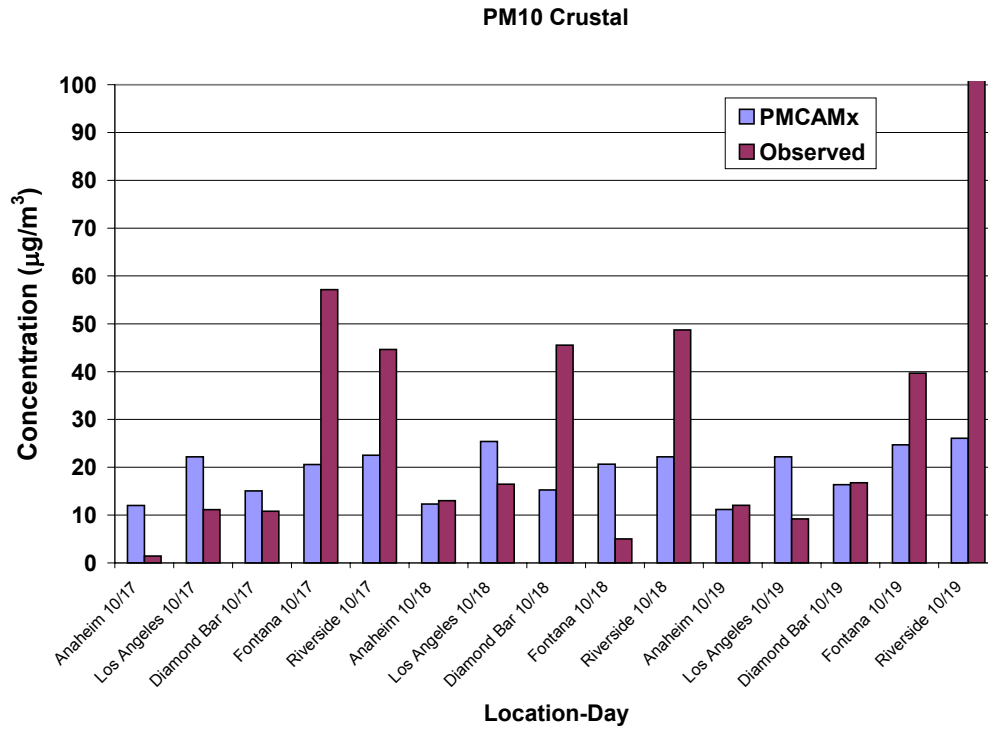


Figure 5-6. Comparison of 24-hr PM₁₀ crustal material at PTEP monitoring sites on October 17th and 18th, 1995.

**24-hr PM_{2.5} Predictions for Anaheim
Comparison of PMCAMx with Other Models**

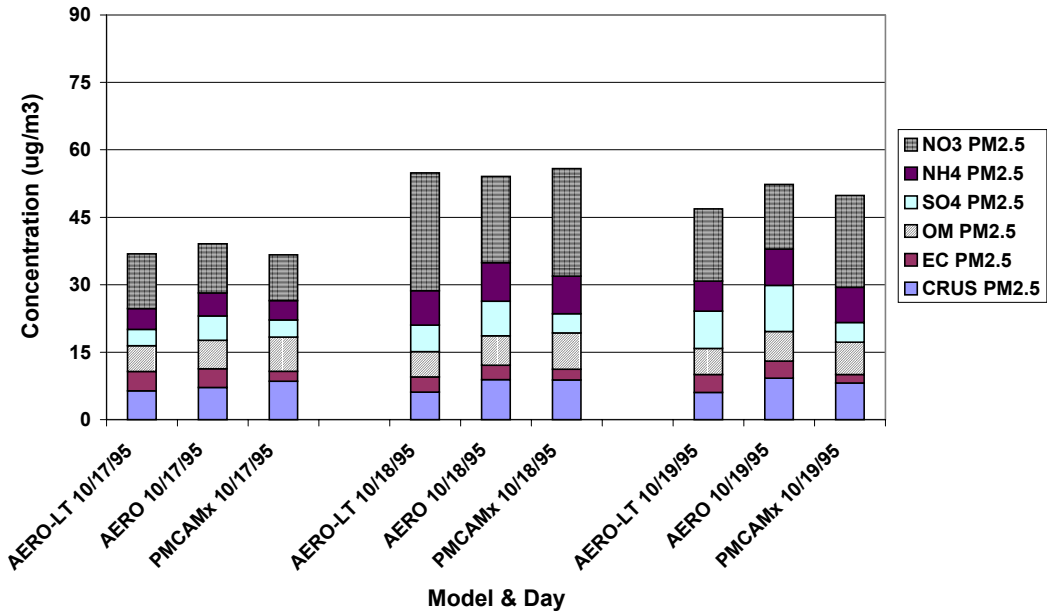


Figure 5-7. Comparison of 24-hr PM_{2.5} at Anaheim between PMCAMx, UAM-AERO and UAMAERO-LT.

**24-hr PM_{2.5} Predictions for Diamond Bar
Comparison of PMCAMx to Other Models**

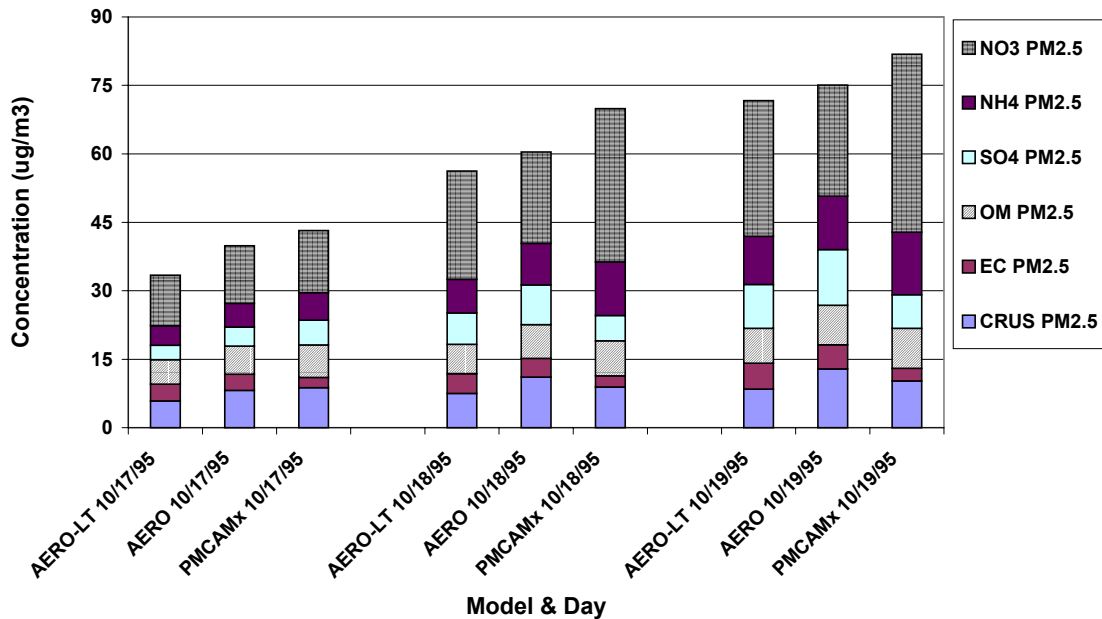


Figure 5-8. Comparison of 24-hr PM_{2.5} at Diamond Bar between PMCAMx, UAM-AERO and UAMAERO-LT.

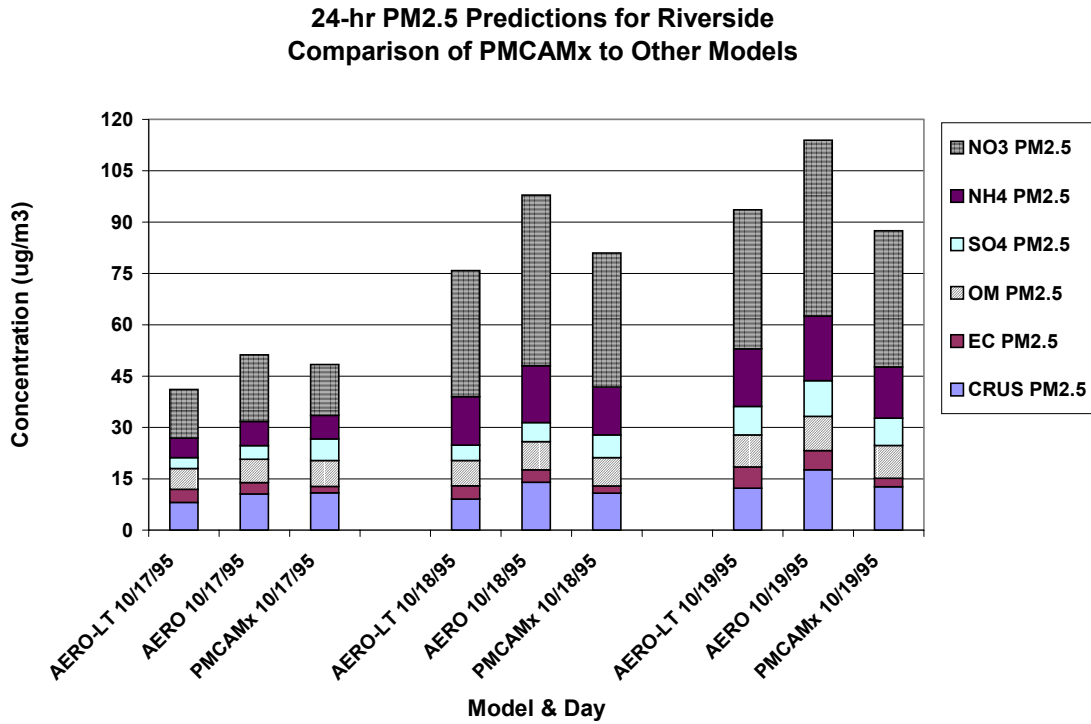


Figure 5-9. Comparison of 24-hr PM_{2.5} at Riverside between PMCAM_x, UAM-AERO and UAMAERO-LT.

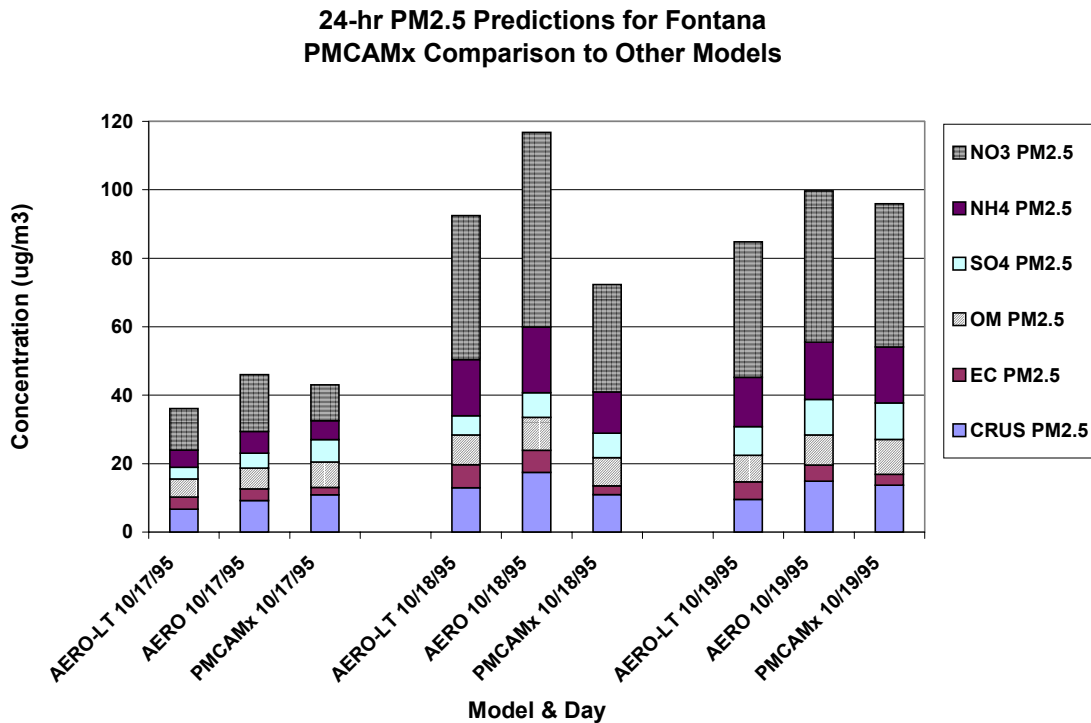


Figure 5-10. Comparison of 24-hr PM_{2.5} at Fontana between PMCAM_x, UAM-AERO and UAMAERO-LT.

**24-hr PM_{2.5} Predictions for Los Angeles
Comparison of PMCAMx to Other Models**

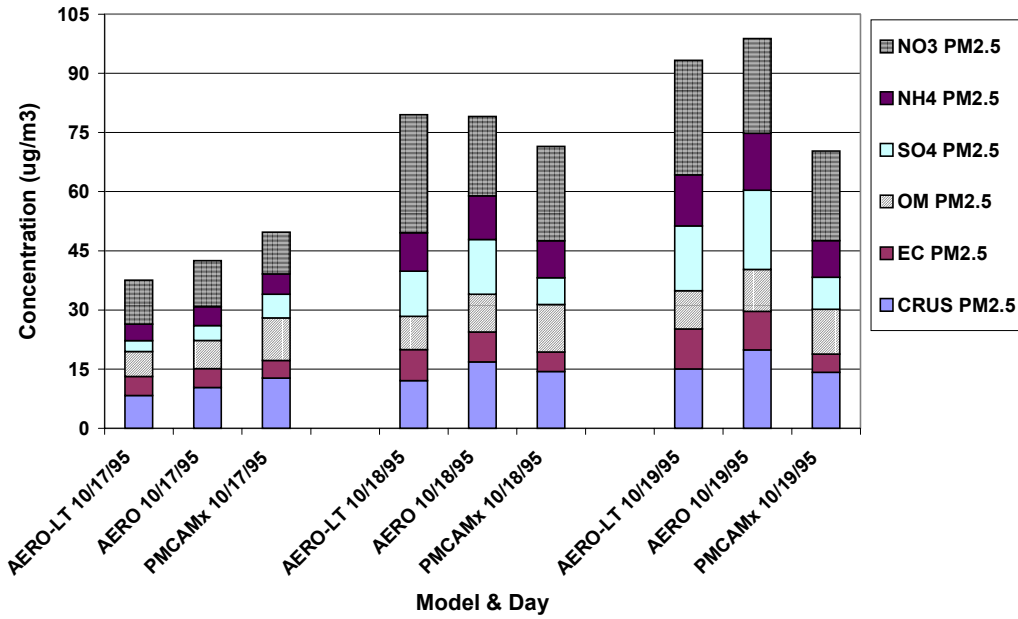


Figure 5-11. Comparison of 24-hr PM_{2.5} at Los Angeles North Main between PMCAMx, UAM-AERO and UAMAERO-LT.

NH4, PM2.5 Riverside

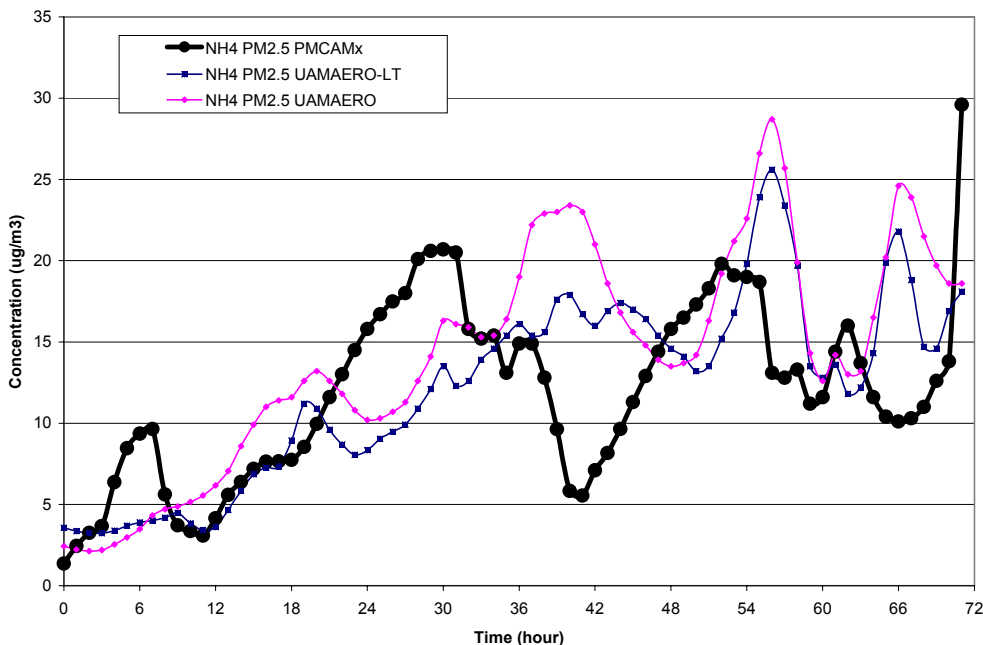


Figure 5-12. Comparison of hourly PM_{2.5} ammonium at Riverside between PMCAMx, UAM-AERO and UAMAERO-LT.

NO3, PM2.5 Riverside

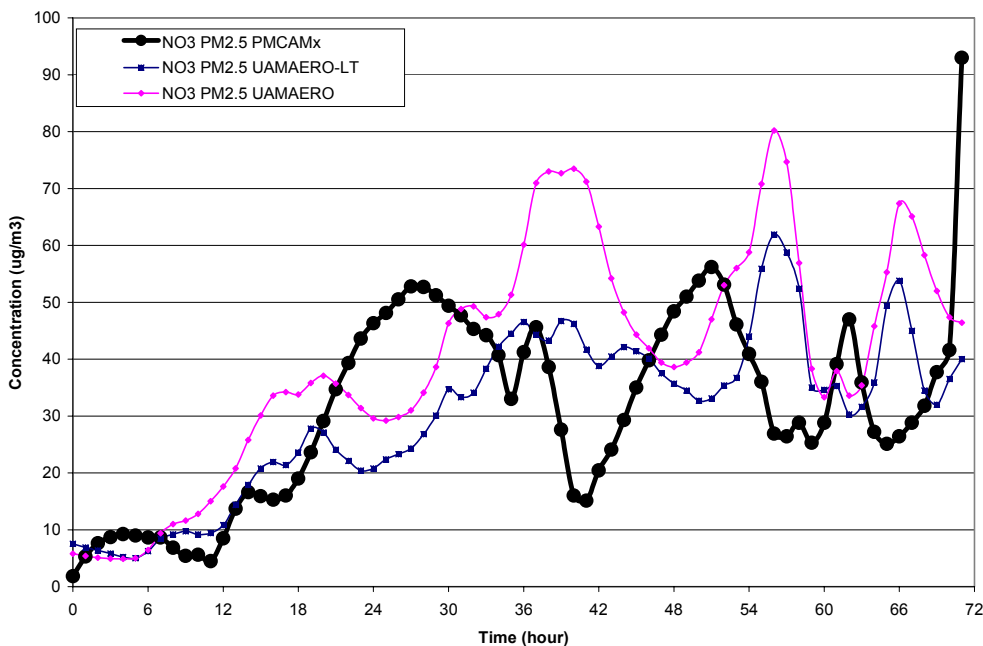


Figure 5-13. Comparison of hourly PM_{2.5} nitrate at Riverside between PMCAMx, UAM-AERO and UAMAERO-LT.

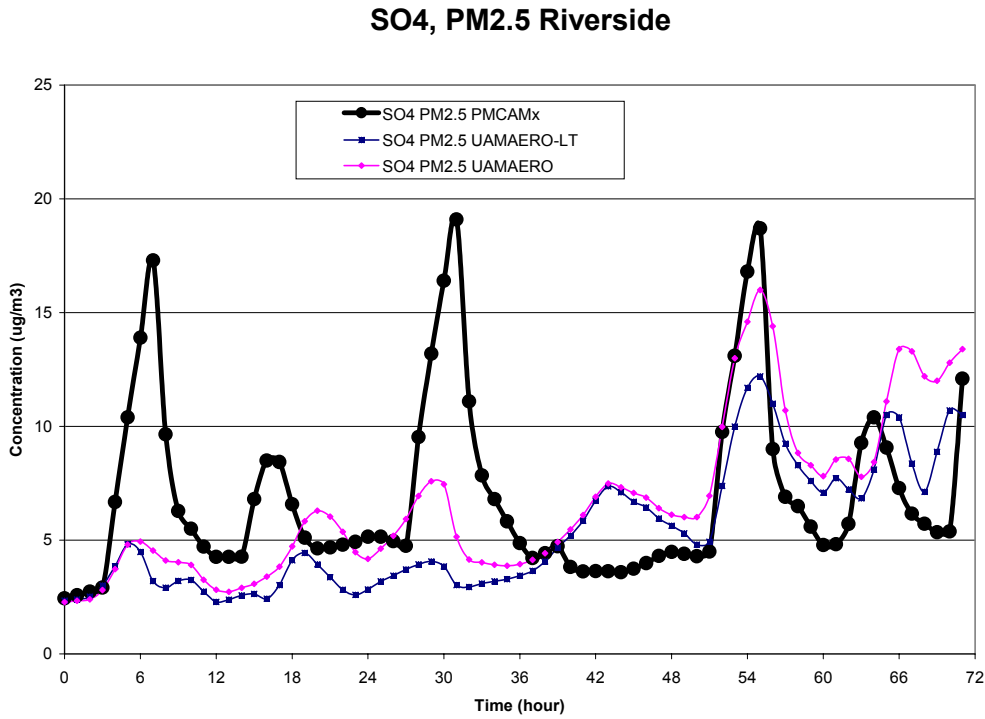


Figure 5-14. Comparison of hourly PM_{2.5} sulfate at Riverside between PMCAMx, UAM-AERO and UAMAERO-LT.

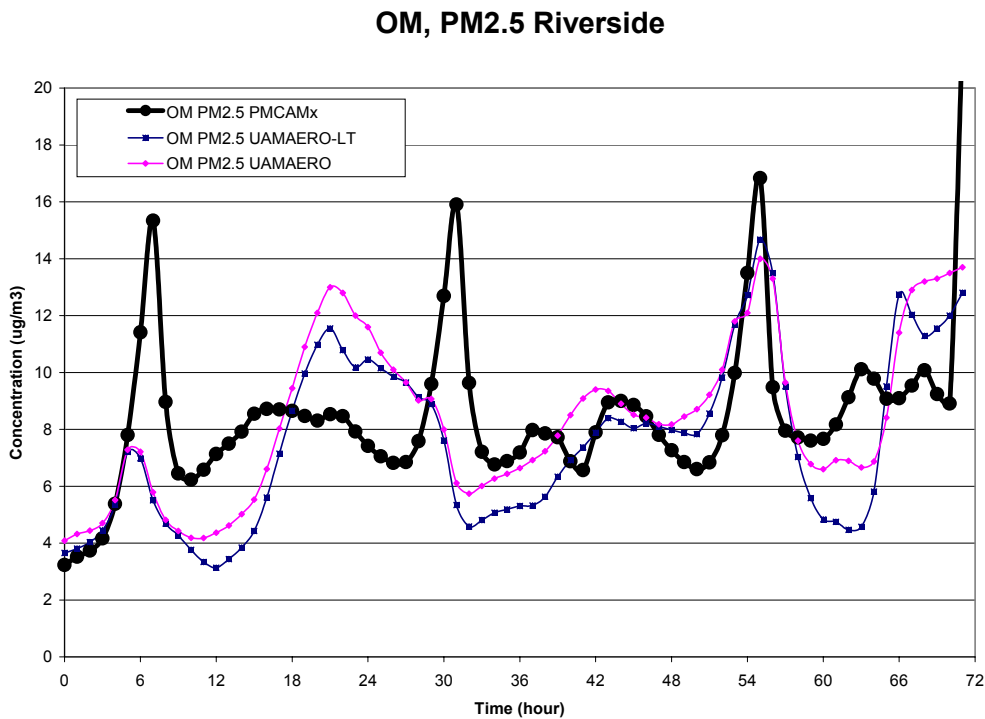


Figure 5-15. Comparison of hourly PM_{2.5} organic matter at Riverside between PMCAMx, UAM-AERO and UAMAERO-LT.

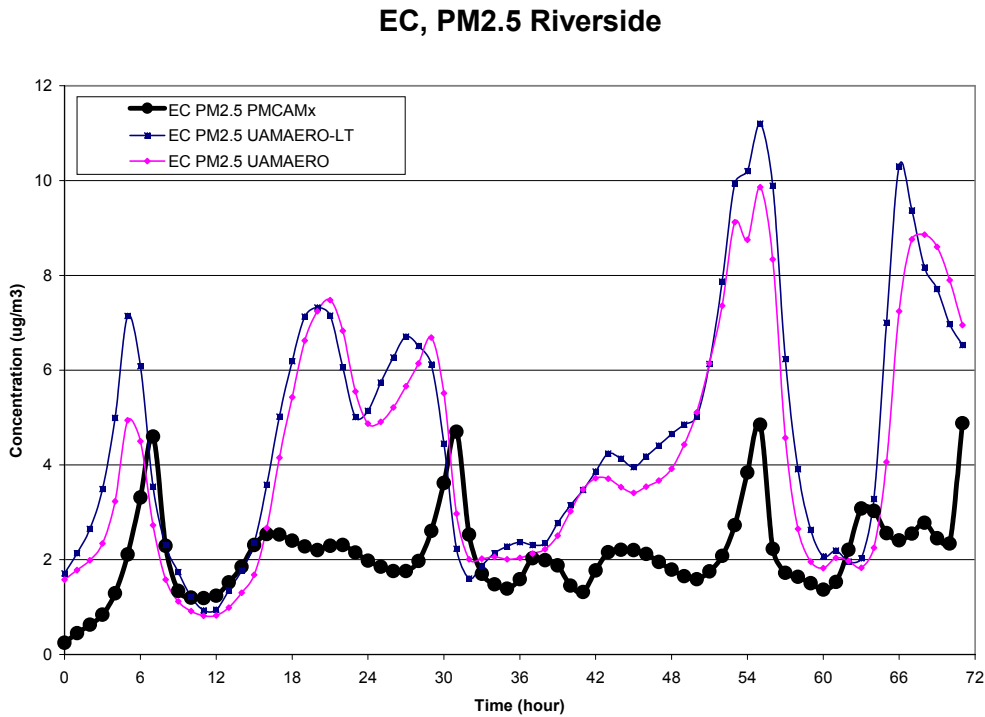


Figure 5-16. Comparison of hourly PM_{2.5} elemental carbon at Riverside between PMCAMx, UAM-AERO and UAMAERO-LT.

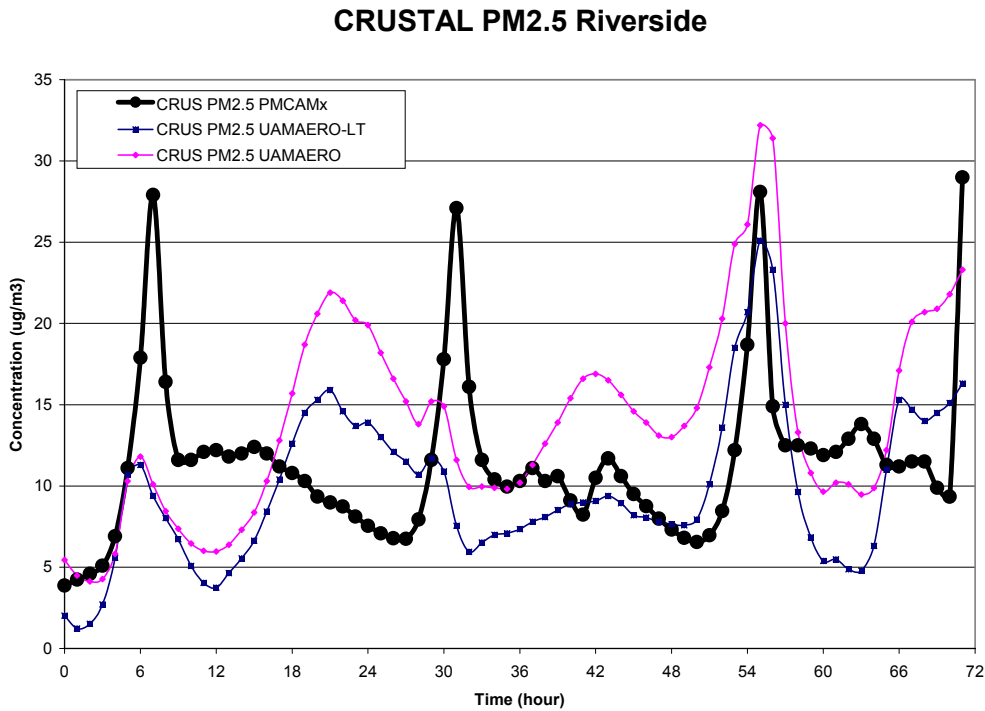


Figure 5-17. Comparison of hourly PM_{2.5} crustal material at Riverside between PMCAMx, UAM-AERO and UAMAERO-LT.

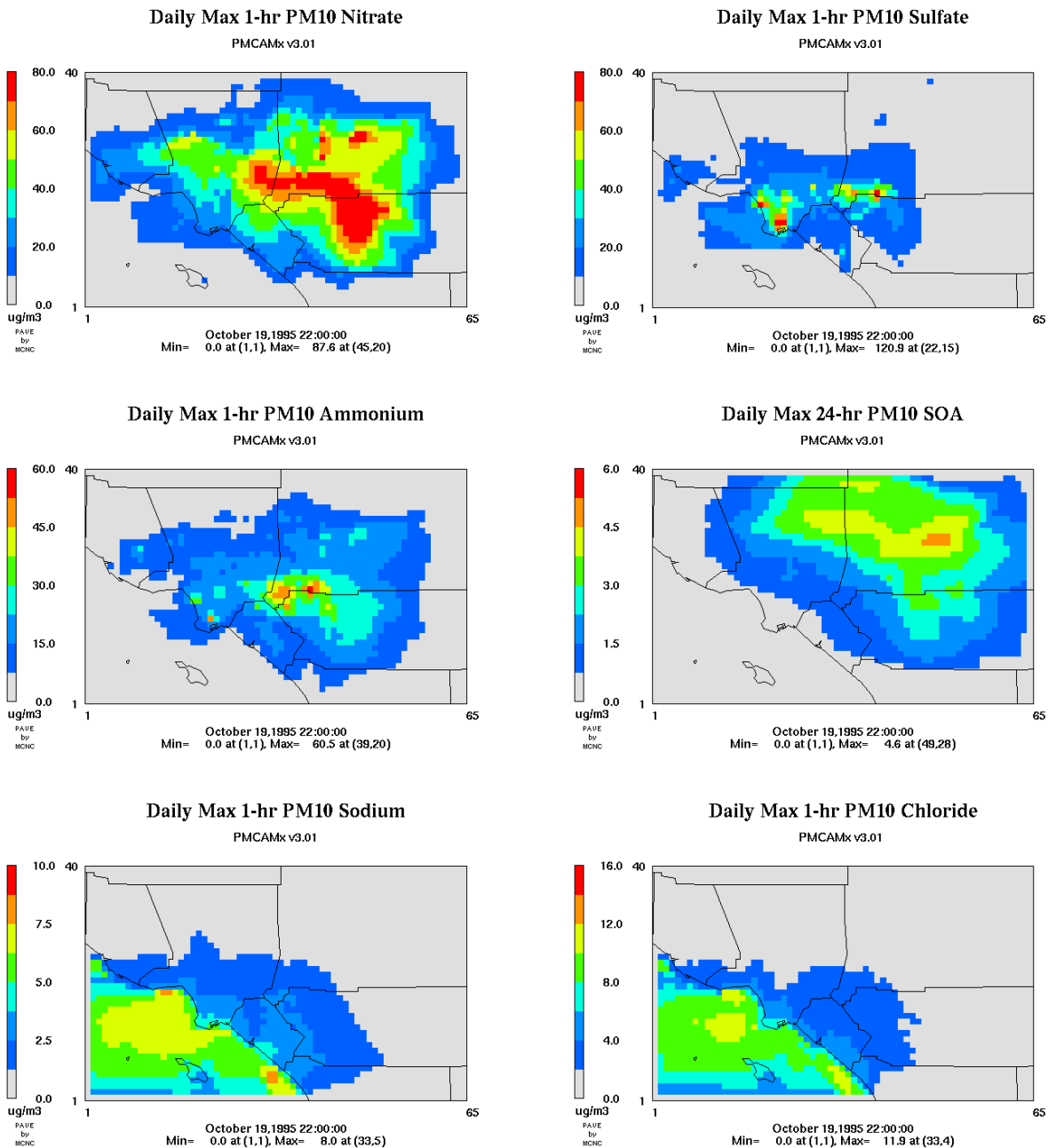
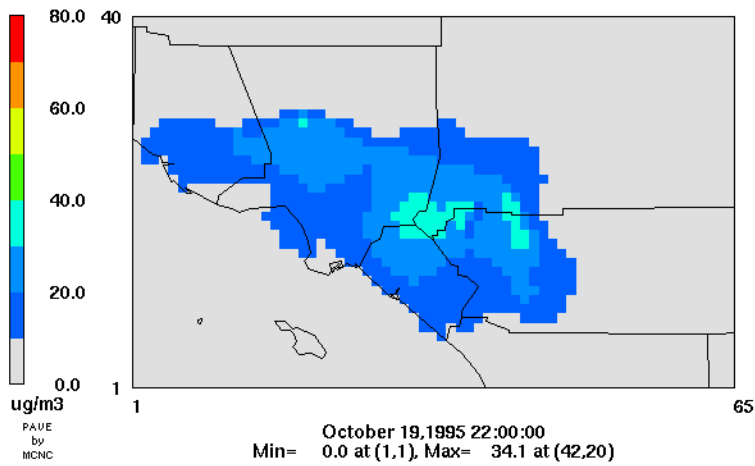


Figure 5-18. Daily maximum 24-hour PM₁₀ concentrations on October 19th, 1995 for nitrate, sulfate, ammonium, secondary organic aerosol, sodium and chloride.

Daily Max 1-hr Coarse Nitrate (PM10 - PM2.5)

PMCAMx v3.01



Daily Max 1-hr PM2.5 Nitrate

PMCAMx v3.01

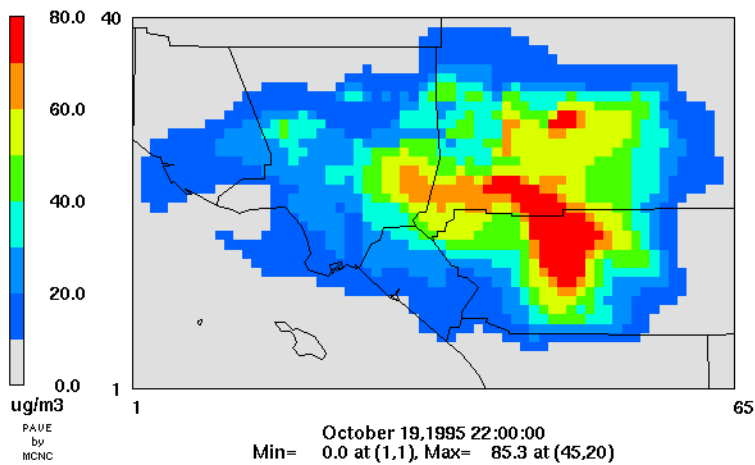


Figure 5-19. Daily maximum 24-hour concentrations on October 19th, 1995 for coarse nitrate (PM₁₀-PM_{2.5}) and fine nitrate (PM_{2.5}).

PLATFORM DEPENDENCY

PMCAMx was tested on three different workstation platforms for the Los Angeles October 17-19, 1995 episode. The ability of a model code to compile and run reliably on multiple computer platforms is referred to as “platform dependency” and is an indicator of code integrity and reliability. The three workstations were:

- Linux PC (Athlon MP2000, 1.67 GHz) running Red Hat 7.2 (2.4.2-2 Kernel) and the Portland Group Workstation Compiler version 3.2-3
- DEC Alpha-station (500 Mz) running DEC OSF/1 V4.0 and the DIGITAL FORTRAN Compiler version 5.2
- Sun Ultra-30 (333 MHz) running SunOS 5.6 and the Sun FORTRAN77 Compiler version 4.0.

CPU Times for PMCAMx

The computer central processing units (CPU) times for the workstations are compared in Table 5-3. The DEC and Sun workstations gave similar performance and the Linux PC was much faster because of the higher CPU clock speed. The DEC workstation halted on the third day (October 19th) because of a floating-point math error (underflow). The DEC was able to complete the third simulation day at lower optimization level suggesting that the compiler may be partly responsible for this problem. The CPU time increased on successive days for all workstations.

Table 5-3. CPU Times (hours) for the LA Test Case (65x40 5-km grids with 10 vertical layers) on different workstations.

| Day | Linux | Sun | DEC |
|---------------------------|--------------|------------|-----------------|
| October, 17 th | 1.4 | 7.4 | 7.3 |
| October, 18 th | 1.9 | 10.5 | 11.9 |
| October, 19 th | 2.4 | 11.7 | 15 ^A |

A. The DEC workstation required a lower optimization level to complete this day.

The breakdown of CPU time between the aerosol modules and the CAMx core model was analyzed for the Linux workstation (Table 5-4) leading to the following conclusions:

- The aerosol modules dominate the CPU-time (55 – 81%) over the host CAMx model. This means that most of the CPU time in PMCAMx is going toward the aerosol science calculations.
- Adding 130 PM species to the CAMx host model adds relatively little CPU-burden relative to the science calculations within the aerosol modules.

- The SOAP module is efficient and contributes a small fraction (7-9%) of the total CPU-time.
- The MADM aerosol chemistry and the aqueous-phase chemistry are the largest contributors to the CPU-time.
- The CPU-time for the MADM and aqueous chemistry modules varies significantly between days in response to differences in chemical/environmental conditions.

Table 5-4. CPU time used by each aerosol module on the Linux workstation.

| Day | CAMx Host Model | MADM Aerosol Chemistry and Size | VSRM Aqueous Phase Chemistry | SOAP Secondary Organic Aerosols | Total |
|----------------------------------|--------------------|--|---------------------------------------|--|-------|
| CPU time (minutes) | | | | | |
| 17 | 38 | 39 | 9 | 8 | 95 |
| 18 | 29 | 78 | 53 | 10 | 169 |
| 19 | 28 | 108 | 86 | 10 | 233 |
| Percent of total CPU time | | | | | |
| 17 | 45% | 35% | 11% | 9% | 100% |
| 18 | 25% | 21% | 45% | 8% | 100% |
| 19 | 19% | 15% | 59% | 7% | 100% |

Concentration Differences Between Platforms

The surface layer concentrations on each day were analyzed to find the average and maximum concentration differences between workstations. The differences between the Linux and Sun workstations are summarized in Table 5-5, and differences between the DEC and Linux workstations are shown in Table 5-6. Concentration differences are shown for a few gases (NO, NO₂, ozone and the SOA precursors CG1-CG4) and for all PM species aggregated over sections 1-6 (PM_{2.5}) and sections 1-8 (PM₁₀). Relative concentration differences (i.e., percentages) are expressed relative to the mean base case concentration so that differences in near-zero values (which are trivial) do not dominate.

The findings from the platform dependency tests are:

- The DEC workstation could not complete the whole simulation because of a floating-point math error.
- There were no average concentration differences exceeding 1 percent.
- There are some maximum concentration differences exceeding 10 percent (shaded gray in the Tables) on all days for both workstation pairs. Species that tend to show maximum differences greater than 10 percent are nitrate, sulfate, ammonium, chloride, SO₂ and the condensable gases CG3 and CG4.
- The differences for PM-related species are much larger than for ozone and NO_x.

Conclusions on Platform Dependency

The conclusions from these tests are that the PM modules should receive additional attention to reduce concentration differences between workstations. We believe these differences are related to the PM science modules rather than the PMCAMx host model because the differences of ozone and NO_x are small, as seen previously for CAMx.

Table 5-5a. Summary of concentration differences between Linux and Sun workstations tests for October 17th, 1995.

| Species | Concentration ^A | | Average Difference ^B | | Max. Difference ^C | |
|--------------|----------------------------|----------|---------------------------------|----------------------|------------------------------|----------------------|
| | Linux | Sun | Value | Percent ^D | Value | Percent ^D |
| NO | 6.73E+00 | 6.73E+00 | 1.97E-05 | 0.00% | 2.08E-03 | 0.03% |
| NO2 | 9.87E+00 | 9.87E+00 | 2.09E-05 | 0.00% | 2.05E-03 | 0.02% |
| O3 | 3.38E+01 | 3.38E+01 | 8.66E-05 | 0.00% | 5.17E-03 | 0.02% |
| CG1 | 5.95E+01 | 5.95E+01 | 5.26E-04 | 0.00% | 3.02E-01 | 0.51% |
| CG2 | 3.30E+02 | 3.30E+02 | 1.14E-03 | 0.00% | 2.54E-01 | 0.08% |
| CG3 | 5.89E+00 | 5.89E+00 | 3.33E-04 | 0.01% | 5.73E-01 | 9.73% |
| CG4 | 1.77E+00 | 1.77E+00 | 9.08E-05 | 0.01% | 3.22E-01 | 18.17% |
| SO2 | 8.87E-01 | 8.87E-01 | 5.86E-05 | 0.01% | 7.35E-02 | 8.28% |
| PNO3 (PM2.5) | 3.30E+00 | 3.30E+00 | 2.61E-02 | 0.79% | 2.33E+00 | 70.61% |
| PNH4 (PM2.5) | 1.96E+00 | 1.96E+00 | 7.85E-03 | 0.40% | 9.18E-01 | 46.84% |
| PSO4 (PM2.5) | 2.84E+00 | 2.84E+00 | 2.78E-04 | 0.01% | 2.97E-01 | 10.46% |
| NA (PM2.5) | 4.63E-01 | 4.63E-01 | 3.92E-07 | 0.00% | 9.54E-05 | 0.02% |
| PCL (PM2.5) | 3.27E-01 | 3.27E-01 | 1.53E-03 | 0.47% | 3.14E-01 | 96.02% |
| PEC (PM2.5) | 8.21E-01 | 8.21E-01 | 4.56E-07 | 0.00% | 2.25E-04 | 0.03% |
| POC (PM2.5) | 3.31E+00 | 3.31E+00 | 1.21E-06 | 0.00% | 1.37E-04 | 0.00% |
| CRST (PM2.5) | 4.93E+00 | 4.93E+00 | 2.14E-06 | 0.00% | 5.91E-04 | 0.01% |
| SOA1 (PM2.5) | 5.07E-02 | 5.07E-02 | 6.11E-07 | 0.00% | 2.88E-04 | 0.57% |
| SOA2 (PM2.5) | 2.12E-02 | 2.12E-02 | 3.46E-07 | 0.00% | 2.44E-04 | 1.15% |
| SOA3 (PM2.5) | 1.16E-01 | 1.16E-01 | 1.23E-06 | 0.00% | 5.16E-04 | 0.44% |
| SOA4 (PM2.5) | 1.42E-02 | 1.42E-02 | 1.66E-07 | 0.00% | 2.75E-04 | 1.94% |
| PNO3 (PM10) | 3.57E+00 | 3.57E+00 | 2.68E-02 | 0.75% | 2.33E+00 | 65.27% |
| PNH4 (PM10) | 2.12E+00 | 2.12E+00 | 7.72E-03 | 0.36% | 9.25E-01 | 43.63% |
| PSO4 (PM10) | 3.46E+00 | 3.46E+00 | 2.80E-04 | 0.01% | 2.96E-01 | 8.55% |
| NA (PM10) | 1.04E+00 | 1.04E+00 | 1.13E-06 | 0.00% | 2.61E-04 | 0.03% |
| PCL (PM10) | 1.02E+00 | 1.02E+00 | 3.22E-03 | 0.32% | 3.74E-01 | 36.67% |
| PEC (PM10) | 9.26E-01 | 9.26E-01 | 5.68E-07 | 0.00% | 2.25E-04 | 0.02% |
| POC (PM10) | 4.50E+00 | 4.50E+00 | 2.28E-06 | 0.00% | 4.62E-04 | 0.01% |
| CRST (PM10) | 9.09E+00 | 9.09E+00 | 6.88E-06 | 0.00% | 2.63E-03 | 0.03% |
| SOA1 (PM10) | 5.08E-02 | 5.08E-02 | 6.01E-07 | 0.00% | 2.89E-04 | 0.57% |
| SOA2 (PM10) | 2.12E-02 | 2.12E-02 | 3.38E-07 | 0.00% | 2.44E-04 | 1.15% |
| SOA3 (PM10) | 1.17E-01 | 1.17E-01 | 1.23E-06 | 0.00% | 5.17E-04 | 0.44% |
| SOA4 (PM10) | 1.42E-02 | 1.42E-02 | 1.57E-07 | 0.00% | 2.77E-04 | 1.95% |

A. Average over all surface grid cells. Gases in ppb, particulate sulfate in ug/m3.

B. Average un-signed difference over all surface grid cells.

C. Maximum un-signed difference over all surface grid cells.

D. Percent difference relative to the base case average concentration.

Table 5-5b. Summary of concentration differences between Linux and Sun workstations tests for October 18th, 1995.

| Species | Concentration ^A | | Average Difference ^B | | Max. Difference ^C | |
|--------------|----------------------------|----------|---------------------------------|----------------------|------------------------------|----------------------|
| | Linux | Sun | Value | Percent ^D | Value | Percent ^D |
| NO | 6.58E+00 | 6.58E+00 | 3.96E-05 | 0.00% | 8.16E-03 | 0.12% |
| NO2 | 1.14E+01 | 1.14E+01 | 4.97E-05 | 0.00% | 5.65E-03 | 0.05% |
| O3 | 3.59E+01 | 3.59E+01 | 1.93E-04 | 0.00% | 9.17E-03 | 0.03% |
| CG1 | 9.02E+01 | 9.02E+01 | 8.02E-04 | 0.00% | 2.45E-01 | 0.27% |
| CG2 | 7.35E+02 | 7.35E+02 | 3.63E-03 | 0.00% | 2.25E-01 | 0.03% |
| CG3 | 5.15E+00 | 5.15E+00 | 1.51E-04 | 0.00% | 6.11E-01 | 11.86% |
| CG4 | 1.08E+00 | 1.08E+00 | 5.05E-05 | 0.00% | 1.00E-01 | 9.29% |
| SO2 | 8.74E-01 | 8.74E-01 | 2.39E-04 | 0.03% | 2.66E-01 | 30.46% |
| PNO3 (PM2.5) | 9.94E+00 | 9.94E+00 | 2.66E-02 | 0.27% | 1.24E+01 | 124.75% |
| PNH4 (PM2.5) | 4.08E+00 | 4.08E+00 | 8.17E-03 | 0.20% | 3.55E+00 | 87.01% |
| PSO4 (PM2.5) | 3.66E+00 | 3.66E+00 | 1.16E-03 | 0.03% | 1.16E+00 | 31.69% |
| NA (PM2.5) | 5.10E-01 | 5.10E-01 | 5.48E-07 | 0.00% | 6.70E-05 | 0.01% |
| PCL (PM2.5) | 4.85E-01 | 4.85E-01 | 2.21E-03 | 0.46% | 5.53E-01 | 114.02% |
| PEC (PM2.5) | 1.09E+00 | 1.09E+00 | 6.20E-07 | 0.00% | 1.51E-04 | 0.01% |
| POC (PM2.5) | 3.23E+00 | 3.23E+00 | 1.51E-06 | 0.00% | 1.96E-04 | 0.01% |
| CRST (PM2.5) | 5.20E+00 | 5.20E+00 | 2.69E-06 | 0.00% | 9.13E-04 | 0.02% |
| SOA1 (PM2.5) | 1.79E-01 | 1.79E-01 | 1.51E-06 | 0.00% | 2.14E-04 | 0.12% |
| SOA2 (PM2.5) | 1.15E-01 | 1.15E-01 | 1.35E-06 | 0.00% | 1.11E-04 | 0.10% |
| SOA3 (PM2.5) | 2.78E-01 | 2.78E-01 | 2.76E-06 | 0.00% | 5.70E-04 | 0.20% |
| SOA4 (PM2.5) | 3.78E-02 | 3.78E-02 | 3.14E-07 | 0.00% | 7.96E-05 | 0.21% |
| PNO3 (PM10) | 1.15E+01 | 1.15E+01 | 2.29E-02 | 0.20% | 1.24E+01 | 107.83% |
| PNH4 (PM10) | 4.38E+00 | 4.38E+00 | 7.65E-03 | 0.17% | 3.55E+00 | 81.05% |
| PSO4 (PM10) | 4.51E+00 | 4.51E+00 | 1.12E-03 | 0.02% | 1.15E+00 | 25.50% |
| NA (PM10) | 1.16E+00 | 1.16E+00 | 1.95E-06 | 0.00% | 2.31E-04 | 0.02% |
| PCL (PM10) | 1.31E+00 | 1.31E+00 | 3.11E-03 | 0.24% | 7.29E-01 | 55.65% |
| PEC (PM10) | 1.22E+00 | 1.22E+00 | 8.00E-07 | 0.00% | 1.65E-04 | 0.01% |
| POC (PM10) | 4.43E+00 | 4.43E+00 | 3.17E-06 | 0.00% | 8.02E-04 | 0.02% |
| CRST (PM10) | 1.02E+01 | 1.02E+01 | 9.93E-06 | 0.00% | 4.11E-03 | 0.04% |
| SOA1 (PM10) | 1.80E-01 | 1.80E-01 | 1.52E-06 | 0.00% | 2.14E-04 | 0.12% |
| SOA2 (PM10) | 1.15E-01 | 1.15E-01 | 1.32E-06 | 0.00% | 1.11E-04 | 0.10% |
| SOA3 (PM10) | 2.79E-01 | 2.79E-01 | 2.82E-06 | 0.00% | 5.71E-04 | 0.20% |
| SOA4 (PM10) | 3.78E-02 | 3.78E-02 | 2.99E-07 | 0.00% | 7.98E-05 | 0.21% |

- A. Average over all surface grid cells. Gases in ppb, particulate sulfate in ug/m3.
 B. Average un-signed difference over all surface grid cells.
 C. Maximum un-signed difference over all surface grid cells.
 D. Percent difference relative to the base case average concentration.

Table 5-5c. Summary of concentration differences between Linux and Sun workstations tests for October 19th, 1995.

| Species | Concentration ^A | | Average Difference ^B | | Max. Difference ^C | |
|--------------|----------------------------|----------|---------------------------------|----------------------|------------------------------|----------------------|
| | Linux | Sun | Value | Percent ^D | Value | Percent ^D |
| NO | 5.31E+00 | 5.31E+00 | 3.70E-05 | 0.00% | 7.71E-03 | 0.15% |
| NO2 | 1.03E+01 | 1.03E+01 | 4.32E-05 | 0.00% | 8.51E-03 | 0.08% |
| O3 | 3.88E+01 | 3.88E+01 | 1.85E-04 | 0.00% | 2.49E-02 | 0.06% |
| CG1 | 9.66E+01 | 9.66E+01 | 8.92E-04 | 0.00% | 9.94E+00 | 10.29% |
| CG2 | 8.41E+02 | 8.41E+02 | 3.82E-03 | 0.00% | 1.35E+00 | 0.16% |
| CG3 | 5.32E+00 | 5.32E+00 | 1.44E-04 | 0.00% | 4.82E-01 | 9.06% |
| CG4 | 9.67E-01 | 9.67E-01 | 1.20E-04 | 0.01% | 7.96E-01 | 82.25% |
| SO2 | 7.41E-01 | 7.41E-01 | 2.04E-04 | 0.03% | 1.12E-01 | 15.15% |
| PNO3 (PM2.5) | 1.05E+01 | 1.05E+01 | 4.29E-02 | 0.41% | 8.41E+00 | 80.10% |
| PNH4 (PM2.5) | 4.84E+00 | 4.83E+00 | 1.30E-02 | 0.27% | 2.47E+00 | 51.03% |
| PSO4 (PM2.5) | 3.87E+00 | 3.87E+00 | 8.53E-04 | 0.02% | 1.03E+00 | 26.61% |
| NA (PM2.5) | 5.33E-01 | 5.33E-01 | 5.50E-07 | 0.00% | 1.30E-04 | 0.02% |
| PCL (PM2.5) | 4.66E-01 | 4.66E-01 | 3.27E-03 | 0.70% | 3.44E-01 | 73.82% |
| PEC (PM2.5) | 1.09E+00 | 1.09E+00 | 6.94E-07 | 0.00% | 1.98E-04 | 0.02% |
| POC (PM2.5) | 3.11E+00 | 3.11E+00 | 1.66E-06 | 0.00% | 1.81E-04 | 0.01% |
| CRST (PM2.5) | 5.10E+00 | 5.10E+00 | 2.92E-06 | 0.00% | 7.18E-04 | 0.01% |
| SOA1 (PM2.5) | 2.41E-01 | 2.41E-01 | 2.02E-06 | 0.00% | 9.97E-03 | 4.14% |
| SOA2 (PM2.5) | 2.00E-01 | 2.00E-01 | 2.26E-06 | 0.00% | 1.35E-03 | 0.67% |
| SOA3 (PM2.5) | 3.54E-01 | 3.54E-01 | 3.11E-06 | 0.00% | 4.40E-04 | 0.12% |
| SOA4 (PM2.5) | 4.43E-02 | 4.43E-02 | 4.56E-07 | 0.00% | 7.06E-04 | 1.59% |
| PNO3 (PM10) | 1.30E+01 | 1.30E+01 | 4.11E-02 | 0.32% | 8.40E+00 | 64.62% |
| PNH4 (PM10) | 5.19E+00 | 5.18E+00 | 1.28E-02 | 0.25% | 2.46E+00 | 47.40% |
| PSO4 (PM10) | 4.83E+00 | 4.83E+00 | 8.48E-04 | 0.02% | 4.67E-01 | 9.67% |
| NA (PM10) | 1.19E+00 | 1.19E+00 | 1.81E-06 | 0.00% | 3.76E-04 | 0.03% |
| PCL (PM10) | 1.28E+00 | 1.28E+00 | 5.35E-03 | 0.42% | 6.42E-01 | 50.16% |
| PEC (PM10) | 1.22E+00 | 1.22E+00 | 8.90E-07 | 0.00% | 1.97E-04 | 0.02% |
| POC (PM10) | 4.28E+00 | 4.28E+00 | 3.44E-06 | 0.00% | 8.04E-04 | 0.02% |
| CRST (PM10) | 1.02E+01 | 1.02E+01 | 1.15E-05 | 0.00% | 4.05E-03 | 0.04% |
| SOA1 (PM10) | 2.41E-01 | 2.41E-01 | 1.90E-06 | 0.00% | 1.01E-02 | 4.20% |
| SOA2 (PM10) | 2.00E-01 | 2.00E-01 | 1.86E-06 | 0.00% | 1.37E-03 | 0.68% |
| SOA3 (PM10) | 3.55E-01 | 3.55E-01 | 3.09E-06 | 0.00% | 4.40E-04 | 0.12% |
| SOA4 (PM10) | 4.45E-02 | 4.45E-02 | 3.99E-07 | 0.00% | 7.07E-04 | 1.59% |

- A. Average over all surface grid cells. Gases in ppb, particulate sulfate in ug/m3.
 B. Average un-signed difference over all surface grid cells.
 C. Maximum un-signed difference over all surface grid cells.
 D. Percent difference relative to the base case average concentration.

Table 5-6a. Summary of concentration differences between Linux and DEC workstations tests for October 17th, 1995.

| Species | Concentration ^A | | Average Difference ^B | | Max. Difference ^C | |
|--------------|----------------------------|----------|---------------------------------|----------------------|------------------------------|----------------------|
| | Linux | DEC | Value | Percent ^D | Value | Percent ^D |
| NO | 6.73E+00 | 6.73E+00 | 2.99E-05 | 0.00% | 3.84E-03 | 0.06% |
| NO2 | 9.87E+00 | 9.87E+00 | 2.61E-05 | 0.00% | 3.93E-03 | 0.04% |
| O3 | 3.38E+01 | 3.38E+01 | 9.40E-05 | 0.00% | 1.13E-02 | 0.03% |
| CG1 | 5.95E+01 | 5.95E+01 | 5.28E-04 | 0.00% | 3.02E-01 | 0.51% |
| CG2 | 3.30E+02 | 3.30E+02 | 1.29E-03 | 0.00% | 2.54E-01 | 0.08% |
| CG3 | 5.89E+00 | 5.89E+00 | 3.49E-04 | 0.01% | 5.74E-01 | 9.74% |
| CG4 | 1.77E+00 | 1.77E+00 | 9.66E-05 | 0.01% | 3.22E-01 | 18.17% |
| SO2 | 8.87E-01 | 8.87E-01 | 7.57E-05 | 0.01% | 5.04E-02 | 5.68% |
| PNO3 (PM2.5) | 3.30E+00 | 3.30E+00 | 2.51E-02 | 0.76% | 2.08E+00 | 63.03% |
| PNH4 (PM2.5) | 1.96E+00 | 1.96E+00 | 7.57E-03 | 0.39% | 8.65E-01 | 44.13% |
| PSO4 (PM2.5) | 2.84E+00 | 2.84E+00 | 3.69E-04 | 0.01% | 3.38E-01 | 11.90% |
| NA (PM2.5) | 4.63E-01 | 4.63E-01 | 3.91E-07 | 0.00% | 9.54E-05 | 0.02% |
| PCL (PM2.5) | 3.27E-01 | 3.27E-01 | 1.57E-03 | 0.48% | 3.17E-01 | 96.94% |
| PEC (PM2.5) | 8.21E-01 | 8.21E-01 | 4.50E-07 | 0.00% | 2.14E-04 | 0.03% |
| POC (PM2.5) | 3.31E+00 | 3.31E+00 | 1.20E-06 | 0.00% | 1.34E-04 | 0.00% |
| CRST (PM2.5) | 4.93E+00 | 4.93E+00 | 2.14E-06 | 0.00% | 5.92E-04 | 0.01% |
| SOA1 (PM2.5) | 5.07E-02 | 5.07E-02 | 6.27E-07 | 0.00% | 2.88E-04 | 0.57% |
| SOA2 (PM2.5) | 2.12E-02 | 2.12E-02 | 3.48E-07 | 0.00% | 2.44E-04 | 1.15% |
| SOA3 (PM2.5) | 1.16E-01 | 1.16E-01 | 1.09E-06 | 0.00% | 5.17E-04 | 0.45% |
| SOA4 (PM2.5) | 1.42E-02 | 1.42E-02 | 1.78E-07 | 0.00% | 2.64E-04 | 1.87% |
| PNO3 (PM10) | 3.57E+00 | 3.57E+00 | 2.58E-02 | 0.72% | 2.09E+00 | 58.54% |
| PNH4 (PM10) | 2.12E+00 | 2.12E+00 | 7.48E-03 | 0.35% | 8.66E-01 | 40.85% |
| PSO4 (PM10) | 3.46E+00 | 3.46E+00 | 3.55E-04 | 0.01% | 2.00E-01 | 5.78% |
| NA (PM10) | 1.04E+00 | 1.04E+00 | 1.13E-06 | 0.00% | 2.61E-04 | 0.03% |
| PCL (PM10) | 1.02E+00 | 1.02E+00 | 3.17E-03 | 0.31% | 4.88E-01 | 47.84% |
| PEC (PM10) | 9.26E-01 | 9.26E-01 | 5.64E-07 | 0.00% | 2.14E-04 | 0.02% |
| POC (PM10) | 4.50E+00 | 4.50E+00 | 2.28E-06 | 0.00% | 4.61E-04 | 0.01% |
| CRST (PM10) | 9.09E+00 | 9.09E+00 | 6.88E-06 | 0.00% | 2.64E-03 | 0.03% |
| SOA1 (PM10) | 5.08E-02 | 5.08E-02 | 6.18E-07 | 0.00% | 2.89E-04 | 0.57% |
| SOA2 (PM10) | 2.12E-02 | 2.12E-02 | 3.40E-07 | 0.00% | 2.44E-04 | 1.15% |
| SOA3 (PM10) | 1.17E-01 | 1.17E-01 | 1.10E-06 | 0.00% | 5.18E-04 | 0.44% |
| SOA4 (PM10) | 1.42E-02 | 1.42E-02 | 1.72E-07 | 0.00% | 2.65E-04 | 1.87% |

- A. Average over all surface grid cells. Gases in ppb, particulate sulfate in ug/m3.
 B. Average un-signed difference over all surface grid cells.
 C. Maximum un-signed difference over all surface grid cells.
 D. Percent difference relative to the base case average concentration.

Table 5-6b. Summary of concentration differences between Linux and DEC workstations tests for October 18th, 1995.

| Species | Concentration ^A | | Average Difference ^B | | Max. Difference ^C | |
|--------------|----------------------------|----------|---------------------------------|----------------------|------------------------------|----------------------|
| | Linux | DEC | Value | Percent ^D | Value | Percent ^D |
| NO | 6.58E+00 | 6.58E+00 | 3.92E-05 | 0.00% | 8.54E-03 | 0.13% |
| NO2 | 1.14E+01 | 1.14E+01 | 5.01E-05 | 0.00% | 5.83E-03 | 0.05% |
| O3 | 3.59E+01 | 3.59E+01 | 1.95E-04 | 0.00% | 9.11E-03 | 0.03% |
| CG1 | 9.02E+01 | 9.02E+01 | 7.84E-04 | 0.00% | 3.46E-01 | 0.38% |
| CG2 | 7.35E+02 | 7.35E+02 | 3.51E-03 | 0.00% | 2.46E-01 | 0.03% |
| CG3 | 5.15E+00 | 5.15E+00 | 1.68E-04 | 0.00% | 1.59E+00 | 30.98% |
| CG4 | 1.08E+00 | 1.08E+00 | 4.75E-05 | 0.00% | 1.28E-01 | 11.84% |
| SO2 | 8.74E-01 | 8.74E-01 | 2.31E-04 | 0.03% | 1.10E-01 | 12.57% |
| PNO3 (PM2.5) | 9.94E+00 | 9.94E+00 | 2.69E-02 | 0.27% | 9.90E+00 | 99.60% |
| PNH4 (PM2.5) | 4.08E+00 | 4.08E+00 | 8.19E-03 | 0.20% | 2.85E+00 | 69.85% |
| PSO4 (PM2.5) | 3.66E+00 | 3.66E+00 | 1.14E-03 | 0.03% | 4.58E-01 | 12.51% |
| NA (PM2.5) | 5.10E-01 | 5.10E-01 | 5.49E-07 | 0.00% | 6.70E-05 | 0.01% |
| PCL (PM2.5) | 4.85E-01 | 4.85E-01 | 2.36E-03 | 0.49% | 5.51E-01 | 113.61% |
| PEC (PM2.5) | 1.09E+00 | 1.09E+00 | 6.15E-07 | 0.00% | 1.55E-04 | 0.01% |
| POC (PM2.5) | 3.23E+00 | 3.23E+00 | 1.50E-06 | 0.00% | 1.96E-04 | 0.01% |
| CRST (PM2.5) | 5.20E+00 | 5.20E+00 | 2.68E-06 | 0.00% | 9.13E-04 | 0.02% |
| SOA1 (PM2.5) | 1.79E-01 | 1.79E-01 | 1.47E-06 | 0.00% | 2.74E-04 | 0.15% |
| SOA2 (PM2.5) | 1.15E-01 | 1.15E-01 | 1.41E-06 | 0.00% | 1.23E-04 | 0.11% |
| SOA3 (PM2.5) | 2.78E-01 | 2.78E-01 | 2.30E-06 | 0.00% | 1.31E-03 | 0.47% |
| SOA4 (PM2.5) | 3.78E-02 | 3.78E-02 | 3.08E-07 | 0.00% | 1.33E-04 | 0.35% |
| PNO3 (PM10) | 1.15E+01 | 1.15E+01 | 2.31E-02 | 0.20% | 9.91E+00 | 86.17% |
| PNH4 (PM10) | 4.38E+00 | 4.38E+00 | 7.62E-03 | 0.17% | 2.85E+00 | 65.07% |
| PSO4 (PM10) | 4.51E+00 | 4.51E+00 | 1.11E-03 | 0.02% | 4.56E-01 | 10.11% |
| NA (PM10) | 1.16E+00 | 1.16E+00 | 1.96E-06 | 0.00% | 2.31E-04 | 0.02% |
| PCL (PM10) | 1.31E+00 | 1.31E+00 | 3.24E-03 | 0.25% | 7.02E-01 | 53.59% |
| PEC (PM10) | 1.22E+00 | 1.22E+00 | 7.96E-07 | 0.00% | 1.65E-04 | 0.01% |
| POC (PM10) | 4.43E+00 | 4.43E+00 | 3.17E-06 | 0.00% | 8.02E-04 | 0.02% |
| CRST (PM10) | 1.02E+01 | 1.02E+01 | 9.94E-06 | 0.00% | 4.11E-03 | 0.04% |
| SOA1 (PM10) | 1.80E-01 | 1.80E-01 | 1.49E-06 | 0.00% | 2.74E-04 | 0.15% |
| SOA2 (PM10) | 1.15E-01 | 1.15E-01 | 1.38E-06 | 0.00% | 1.23E-04 | 0.11% |
| SOA3 (PM10) | 2.79E-01 | 2.79E-01 | 2.44E-06 | 0.00% | 1.31E-03 | 0.47% |
| SOA4 (PM10) | 3.78E-02 | 3.78E-02 | 2.89E-07 | 0.00% | 1.33E-04 | 0.35% |

- A. Average over all surface grid cells. Gases in ppb, particulate sulfate in ug/m3.
 B. Average un-signed difference over all surface grid cells.
 C. Maximum un-signed difference over all surface grid cells.
 D. Percent difference relative to the base case average concentration.

Table 5-6c. Summary of concentration differences between Linux and DEC workstations tests for October 19th, 1995.

| Species | Concentration ^A | | Average Difference ^B | | Max. Difference ^C | |
|--------------|----------------------------|----------|---------------------------------|----------------------|------------------------------|----------------------|
| | Linux | DEC | Value | Percent ^D | Value | Percent ^D |
| NO | 5.31E+00 | 5.31E+00 | 6.97E-04 | 0.01% | 2.03E-05 | 0.00% |
| NO2 | 1.03E+01 | 1.03E+01 | 6.29E-04 | 0.01% | 1.80E-05 | 0.00% |
| O3 | 3.88E+01 | 3.88E+01 | 2.04E-03 | 0.01% | 2.30E-05 | 0.00% |
| CG1 | 9.66E+01 | 9.66E+01 | 2.77E-03 | 0.00% | 9.94E-03 | 0.01% |
| CG2 | 8.41E+02 | 8.41E+02 | 3.80E-02 | 0.00% | 1.35E-03 | 0.00% |
| CG3 | 5.32E+00 | 5.32E+00 | 3.21E-04 | 0.01% | 5.53E-04 | 0.01% |
| CG4 | 9.67E-01 | 9.67E-01 | 1.87E-04 | 0.02% | 8.49E-04 | 0.09% |
| SO2 | 7.41E-01 | 7.42E-01 | 6.60E-04 | 0.09% | 1.11E-04 | 0.02% |
| PNO3 (PM2.5) | 1.05E+01 | 1.05E+01 | 4.33E-02 | 0.41% | 8.36E+00 | 79.62% |
| PNH4 (PM2.5) | 4.84E+00 | 4.83E+00 | 1.32E-02 | 0.27% | 2.44E+00 | 50.41% |
| PSO4 (PM2.5) | 3.87E+00 | 3.86E+00 | 2.87E-03 | 0.07% | 5.47E-01 | 14.13% |
| NA (PM2.5) | 5.33E-01 | 5.33E-01 | 5.53E-07 | 0.00% | 1.30E-04 | 0.02% |
| PCL (PM2.5) | 4.66E-01 | 4.66E-01 | 3.17E-03 | 0.68% | 3.47E-01 | 74.46% |
| PEC (PM2.5) | 1.09E+00 | 1.09E+00 | 6.86E-07 | 0.00% | 1.66E-04 | 0.02% |
| POC (PM2.5) | 3.11E+00 | 3.11E+00 | 1.64E-06 | 0.00% | 1.53E-04 | 0.00% |
| CRST (PM2.5) | 5.10E+00 | 5.10E+00 | 2.89E-06 | 0.00% | 7.16E-04 | 0.01% |
| SOA1 (PM2.5) | 2.41E-01 | 2.41E-01 | 1.70E-05 | 0.01% | 9.97E-03 | 4.14% |
| SOA2 (PM2.5) | 2.00E-01 | 2.00E-01 | 1.57E-05 | 0.01% | 1.35E-03 | 0.67% |
| SOA3 (PM2.5) | 3.54E-01 | 3.54E-01 | 2.68E-05 | 0.01% | 5.16E-04 | 0.15% |
| SOA4 (PM2.5) | 4.43E-02 | 4.43E-02 | 2.02E-06 | 0.00% | 7.90E-04 | 1.78% |
| PNO3 (PM10) | 1.30E+01 | 1.30E+01 | 4.13E-02 | 0.32% | 8.39E+00 | 64.54% |
| PNH4 (PM10) | 5.19E+00 | 5.18E+00 | 1.31E-02 | 0.25% | 2.45E+00 | 47.21% |
| PSO4 (PM10) | 4.83E+00 | 4.82E+00 | 3.17E-03 | 0.07% | 4.14E-01 | 8.57% |
| NA (PM10) | 1.19E+00 | 1.19E+00 | 1.81E-06 | 0.00% | 3.76E-04 | 0.03% |
| PCL (PM10) | 1.28E+00 | 1.28E+00 | 5.19E-03 | 0.41% | 6.49E-01 | 50.70% |
| PEC (PM10) | 1.22E+00 | 1.22E+00 | 9.04E-07 | 0.00% | 1.64E-04 | 0.01% |
| POC (PM10) | 4.28E+00 | 4.28E+00 | 3.44E-06 | 0.00% | 8.04E-04 | 0.02% |
| CRST (PM10) | 1.02E+01 | 1.02E+01 | 1.15E-05 | 0.00% | 4.04E-03 | 0.04% |
| SOA1 (PM10) | 2.41E-01 | 2.41E-01 | 1.67E-05 | 0.01% | 1.01E-02 | 4.20% |
| SOA2 (PM10) | 2.00E-01 | 2.00E-01 | 1.55E-05 | 0.01% | 1.37E-03 | 0.68% |
| SOA3 (PM10) | 3.55E-01 | 3.55E-01 | 2.67E-05 | 0.01% | 5.17E-04 | 0.15% |
| SOA4 (PM10) | 4.45E-02 | 4.45E-02 | 2.01E-06 | 0.00% | 7.91E-04 | 1.78% |

- A. Average over all surface grid cells. Gases in ppb, particulate sulfate in ug/m3.
 B. Average un-signed difference over all surface grid cells.
 C. Maximum un-signed difference over all surface grid cells.
 D. Percent difference relative to the base case average concentration.

VSRM AQUEOUS CHEMISTRY

The VSRM aqueous chemistry model consumed a significant fraction of the PMCAMx CPU time and tests of VSRM prior to implementation in PMCAMx had addressed problems with the numerical integration schemes in VSRM (discussed above). Therefore, a series of sensitivity tests was performed using the Los Angeles episode to evaluate the efficiency and accuracy of the aqueous-phase chemistry. These tests are discussed using the following descriptive names:

Base Case – Standard aqueous-phase chemistry module (VSRM) that automatically selects between size-resolved and bulk methodologies for each grid cell at each time step. Numerical integration performed using VODE but if the sulfur-balance error exceeds 0.1% the integration is replaced using LSODE.

No aqueous – Aqueous-phase chemistry turned off in PMCAMx.

No S-balance check – The S-balance check in the VSRM removed. This means that VODE is used all the time and no calculations are repeated to correct S-balance errors.

LSODE – The numerical integration in the VSRM performed using LSODE every time.

Bulk – The VSRM size-resolved/bulk selection logic over-ridden so that the aqueous-phase chemistry is always performed for a bulk droplet mode.

Revised VSRM – Revised S-balance error control in VSRM so that VODE calculations are replaced by LSODE in the S-balance error exceeds 2%.

The CPU times for these runs are shown in Table 5-7 and the concentration differences between runs are summarized for October 19th, 1995 in Table 5-8. The concentration differences focus on the gases SO₂ and H₂O₂ and particulate sulfate since these are the most important species in the aqueous-phase chemistry. Relative concentration differences (i.e., percentages) are expressed relative to the mean base case concentration (rather than the concentration paired with the difference) to prevent differences in near-zero concentrations (which are trivial) from dominating the results.

The findings from the aqueous-chemistry sensitivity tests are as follows:

- The total CPU time for aqueous chemistry depends upon the fraction of cloudy grid cells, which was 2.4%, 12.3% and 8.9% for October 17-19th respectively. The total CPU time also depends upon the time per grid cell, which varies by more than a factor of two between days for the base case PMCAMx configuration.
- VODE requires about half the CPU time of LSODE for each grid cell. This is seen by comparing the times per cell for the LSODE run and the “No S-balance” run (which always used VODE). However, the overall efficiency of VODE is compromised by the need to go back and correct VODE mass-balance errors using LSODE in some cases.

- Always using LSODE is less efficient overall than the “combined VODE/LSODE strategy” used in the base case PMCAMx configuration. Using LSODE is 93% and 74% slower on the first two days but slightly (13%) faster on the third day. LSODE becomes more efficient than VODE/LSODE when VODE makes a large number of S-balance errors, as happens on the third day.
- VODE makes a large number of S-balance errors. A significant number of S-balance errors occurred in the base case VSRM. On October 18th, correcting S-balance errors incurred a 33% CPU penalty to, and on October 19th correcting S-balance errors incurred a 140% CPU time penalty in the aqueous chemistry. These time penalties are estimated from the difference between the base case and “No S-balance check” runs.
- The impact of the VODE S-balance errors on average concentration levels is small (errors of tenths of a percent) but some errors are large (tens to hundreds of percent), as seen from the difference between the base case and "No S-balance check" runs.
- Based on these findings, the revised VSRM strategy was developed. VODE calculations are only repeated when S-balance errors exceed 2%. This may be viewed as correcting large errors while letting small errors go. This strategy resulted in small errors in average concentration levels (below 0.1 percent) and reduced the errors in maximum concentration levels to a range similar to always using LSODE (about ten percent).
- The bulk aqueous chemistry is faster than the VSRM algorithm which selects between size-resolved and bulk-droplet methodologies. The bulk algorithm required 33% to 64% of the CPU time for VSRM, depending on daily conditions. The differences in average concentration levels between the bulk and size-resolved methodologies are moderate (about 10 percent) but the maximum differences are very large (hundreds to thousands of percent). The bulk algorithm tends to over-estimate sulfate levels, as expected, because it fails to account for the tendency of small droplets to become highly acidic inhibiting the rate of sulfate formation.

Table 5-7. CPU times for aqueous-chemistry module sensitivity tests.

| Day | No Aqueous | Base Case VSRM | No S-balance Check | Bulk Aqueous | LSODE | Revised VSRM |
|---|------------|----------------|--------------------|--------------|-------|--------------|
| CPU time (seconds) | | | | | | |
| October 17 th | 4539 | 5106 | 5086 | 4902 | 5635 | 5088 |
| October 18 th | 3810 | 6990 | 6179 | 5703 | 9348 | 6898 |
| October 19 th | 3631 | 8818 | 5777 | 5333 | 8165 | 7300 |
| CPU Time for Aqueous Chemistry (milliseconds/grid cell)^A | | | | | | |
| October 17 th | | 38 | 37 | 24 | 73 | 37 |
| October 18 th | | 41 | 31 | 25 | 72 | 40 |
| October 19 th | | 93 | 39 | 31 | 81 | 66 |
| Ratio = (CPU time for Aqueous Chemistry) / (CPU time for Base Aqueous Chemistry) | | | | | | |
| October 17 th | | | 0.97 | 0.64 | 1.93 | 0.97 |
| October 18 th | | | 0.75 | 0.60 | 1.74 | 0.97 |
| October 19 th | | | 0.41 | 0.33 | 0.87 | 0.71 |

A. The number of cloudy grid cells per day is 14988, 76668 and 55728 for October 17th, 18th and 19th.

Table 5-8. Summary of concentration differences for aqueous-chemistry module sensitivity tests for October 19th, 1995.

| Species | Concentration ^A | | Average Difference ^B | | Max. Difference ^C | |
|--|----------------------------|-------------|---------------------------------|----------------------|------------------------------|----------------------|
| | Base | Sensitivity | Value | Percent ^D | Value | Percent ^D |
| No S-Balance | | | | | | |
| SO ₂ | 0.74 | 0.75 | 4.38E-03 | 0.59% | 1.78E-03 | 240.7% |
| H ₂ O ₂ | 1.63 | 1.63 | 2.99E-03 | 0.18% | 5.39E-04 | 33.1% |
| PSO4 (PM _{2.5}) | 3.87 | 3.88 | 1.21E-02 | 0.31% | 1.76E+00 | 45.5% |
| PSO4 (PM ₁₀) | 4.83 | 4.84 | 1.43E-02 | 0.30% | 3.11E+00 | 64.4% |
| PSO4 (PM _{CRS}) ^E | 1.39 | 1.39 | 4.58E-03 | 0.33% | 1.69E+00 | 121.6% |
| LSODE | | | | | | |
| SO ₂ | 0.74 | 0.74 | 6.75E-04 | 0.09% | 1.18E-01 | 15.9% |
| H ₂ O ₂ | 1.63 | 1.63 | 2.84E-03 | 0.17% | 1.57E-01 | 9.7% |
| PSO4 (PM _{2.5}) | 3.87 | 3.86 | 3.03E-03 | 0.08% | 5.74E-01 | 14.8% |
| PSO4 (PM ₁₀) | 4.83 | 4.82 | 3.31E-03 | 0.07% | 4.39E-01 | 9.1% |
| PSO4 (PM _{CRS}) | 1.39 | 1.39 | 1.28E-03 | 0.09% | 2.49E-01 | 17.9% |
| Bulk | | | | | | |
| SO ₂ | 0.74 | 0.81 | 7.37E-02 | 9.95% | 4.31E+00 | 581.7% |
| H ₂ O ₂ | 1.63 | 1.66 | 6.05E-02 | 8.43% | 9.95E-01 | 430.6% |
| PSO4 (PM _{2.5}) | 3.87 | 3.34 | 5.79E-01 | 14.96% | 4.44E+01 | 1147.3% |
| PSO4 (PM ₁₀) | 4.83 | 4.45 | 4.07E-01 | 8.43% | 2.08E+01 | 430.6% |
| PSO4 (PM _{CRS}) | 1.39 | 1.44 | 1.55E-01 | 11.15% | 2.38E+01 | 1712.2% |
| Revised VSRM | | | | | | |
| SO ₂ | 0.74 | 0.74 | 2.71E-04 | 0.04% | 1.68E-01 | 22.6% |
| H ₂ O ₂ | 1.63 | 1.63 | 8.92E-04 | 0.05% | 7.59E-02 | 4.7% |
| PSO4 (PM _{2.5}) | 3.87 | 3.87 | 1.01E-03 | 0.03% | 0.433 | 11.2% |
| PSO4 (PM ₁₀) | 4.83 | 4.83 | 1.07E-03 | 0.02% | 0.275 | 5.7% |
| PSO4 (PM _{CRS}) | 1.39 | 1.39 | 4.22E-04 | 0.03% | 0.134 | 9.6% |

A. Average over all surface grid cells. Gases in ppb, particulate sulfate in ug/m³.

B. Average un-signed difference over all surface grid cells.

C. Maximum un-signed difference over all surface grid cells.

D. Percent difference relative to the base case average concentration.

E. PM_{CRS} = (PM₁₀ - PM_{2.5}).

Conclusions for VSRM Aqueous Phase Chemistry

The VSRM aqueous chemistry is expensive in CPU time. VSRM consumed about half of the CPU time in for an episode where only about 10% of the grid cells were cloudy which suggests that the CPU demands of the VSRM may become problematic for simulating cloudy conditions (e.g., winter PM episodes). We recommend continuing efforts to improve the efficiency of the VSRM. Improvements may be possible in the numerical integration scheme (e.g., use of an implicit-explicit hybrid solver), error control, or the logic for selecting between the bulk and size-resolved algorithms. An alternative strategy may be to add a much simpler, reduced-form, aqueous-phase chemistry algorithm to be called in situations where there is very little sulfate production taking place.

The comparison of the VSRM size-resolved droplet model to a bulk droplet model confirms that resolving the size distribution of droplets can alter sulfate production rates, and that neglecting size distribution tends to over-estimate sulfate production rates. Further study is recommended to investigate how this impacts peak sulfate levels, 24-hour average sulfate levels, and sulfate deposition for eastern US conditions.

Care is warranted in using the VODE integration package for atmospheric chemistry problems. VODE has proven to be fast but unreliable in the VSRM (although strategies to manage this problem have been developed and implemented in VSRM). It is unclear whether the problem lies with VODE (e.g., with the internal error control algorithms) or the way VODE interacts with the function supplied to evaluate the chemical rates. VODE is attractive because it is more efficient than LSODE, but this efficiency is compromised by need to repeat calculations using another method in cases where VODE is inaccurate.

SENSITIVITY TESTS

A series of emission sensitivity tests were performed for the Los Angeles October 17-19, 1995 episode to investigate the response of predicted concentrations to emission changes and check that PMCAMx was stable for a range of emission scenarios. The anthropogenic emissions of NO_x, VOC and NH₃ were reduced by 50% separately and in combination to give a matrix of eight emission scenarios, as shown in Table 5-9. The runs were performed on a Linux (Athlon MP2000) workstation. The PMCAMx runs all completed without problems and the run times were all within a 15% range (Table 5-9). There was a small tendency for run times to decrease as the NO_x and VOC emissions were reduced.

The impacts of emission reductions on 24-hour PM₁₀ concentrations at Riverside and Los Angeles North Main are shown in Figures 5-20 through 5-23. Riverside was selected as representing downwind conditions, whereas Los Angeles North Main represents an upwind high anthropogenic emission area. The speciated PM₁₀ concentrations are shown in Figures 5-20 and 5-22, whereas Figures 5-21 and 5-22 show the changes relative to the base case to make clear which PM components are affected by the emissions reductions. The main impacts of changing precursor emissions singly on PM₁₀ concentrations at Riverside and Los Angeles North Main are summarized in Table 5-10.

The emissions/PM relationships at the upwind and downwind sites are summarized as follows:

- Reducing ammonia emissions reduces nitrate, sulfate and ammonium at both upwind and downwind sites. Nitrate is reduced because there is less ammonia to combine with nitric acid so less ammonium nitrate forms. Sulfate is reduced because more acidic water droplets inhibit aqueous sulfate production. Ammonium reductions are associated with both the nitrate and sulfate reductions.
- Reducing VOC emissions reduces organic matter (i.e., secondary organics) at both upwind and downwind sites. At the downwind site, reducing VOC also reduces ammonium nitrate by reducing the production of nitric acid from NO_x.
- Reducing NO_x emissions increases ammonium nitrate at the upwind site and decreases ammonium nitrate at the downwind site. This demonstrates that fundamental differences can exist between the NO_x-nitrate relationships at different sites, similar to well-known differences in ozone-NO_x relationships.

- The upwind increase in ammonium nitrate is explained by more rapid nitric acid production when NOx emissions are reduced, i.e., nitric acid production is NOx-inhibited at the upwind site in the base case.
- The downwind decrease in ammonium nitrate is explained by lower nitric acid production when NOx emissions are reduced, i.e., nitric acid is NOx-limited at the downwind site in the base case.
- Reducing NOx emissions increases organic matter (i.e., secondary organics) at the upwind and downwind sites. This is due to acceleration in the oxidation of VOCs to SOA when NOx emissions are reduced.

The concentrations responses to reductions in combinations of precursor emissions are generally consistent with the points listed above, but do not necessarily reflect linear combinations of effects.

Table 5-9. PMCAMx emission sensitivity runs and run times on a Linux (Athon MP2000) workstation.

| Anthropogenic Emissions Level (%) | | | CPU Time (seconds) | | | Total CPU (hrs) |
|-----------------------------------|-----|-----------------|--------------------|------------|------------|-----------------|
| NOx | VOC | NH ₃ | October 17 | October 18 | October 19 | |
| 100 | 100 | 100 | 5000 | 7811 | 9078 | 6.1 |
| 100 | 100 | 50 | 5103 | 7556 | 8736 | 5.9 |
| 100 | 50 | 100 | 5082 | 7333 | 7792 | 5.6 |
| 100 | 50 | 50 | 5143 | 8036 | 8525 | 6.0 |
| 50 | 100 | 100 | 5048 | 6253 | 8116 | 5.4 |
| 50 | 100 | 50 | 5084 | 6159 | 8787 | 5.6 |
| 50 | 50 | 100 | 5069 | 6219 | 7938 | 5.3 |
| 50 | 50 | 50 | 5079 | 6135 | 9817 | 5.8 |

Table 5-10. Summary of changes in PM concentrations due to changing emissions of a single precursor species.

| 50% Emissions Reduction | Change in PM Concentration | | | |
|---------------------------|----------------------------|---------|----------|----|
| | Nitrate | Sulfate | Ammonium | OM |
| LA North Main | | | | |
| NOx emissions | ++ | ● | + | + |
| VOC emissions | ● | ● | ● | - |
| NH ₃ emissions | -- | -- | -- | ● |
| Riverside | | | | |
| NOx emissions | -- | ● | -- | + |
| VOC emissions | - | ● | -- | - |
| NH ₃ emissions | - | - | -- | ● |

Key:

- ++ > 4% increase
- + 1-4% increase
- less than 1% change
- 1-4% decrease
- > 4% decrease

**24-hr PM 10 for Riverside
for different NOx, VOC, NH3 emission levels
19 October, 1995**

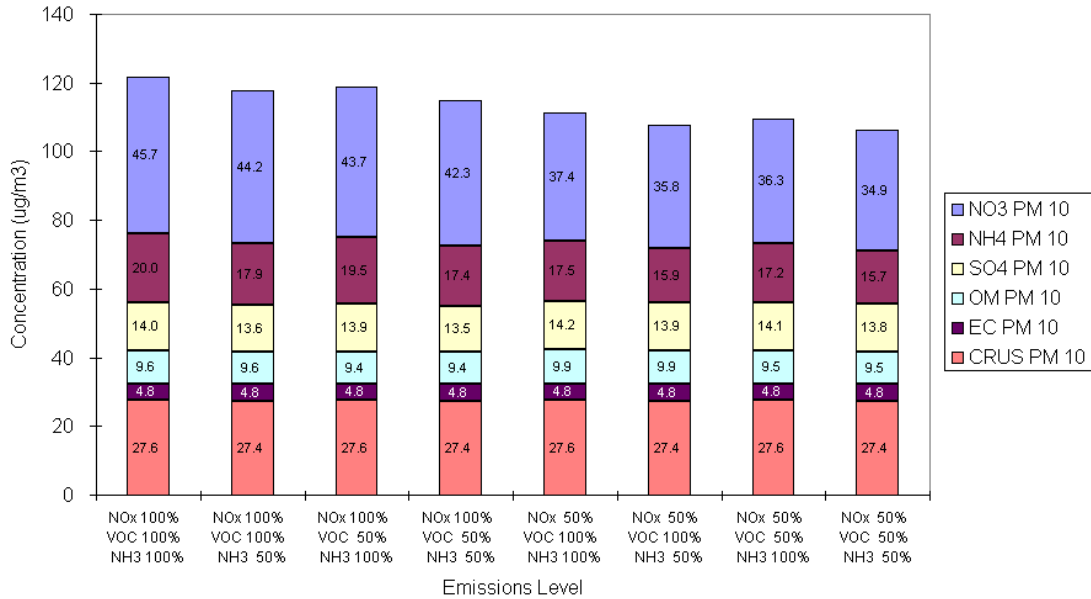


Figure 5-20. Riverside PM₁₀ on October 19th at different emission levels.

**Percent Change in 24-hr PM 10 for Riverside
in response to NOx, VOC, NH3 emission reductions
19 October, 1995**

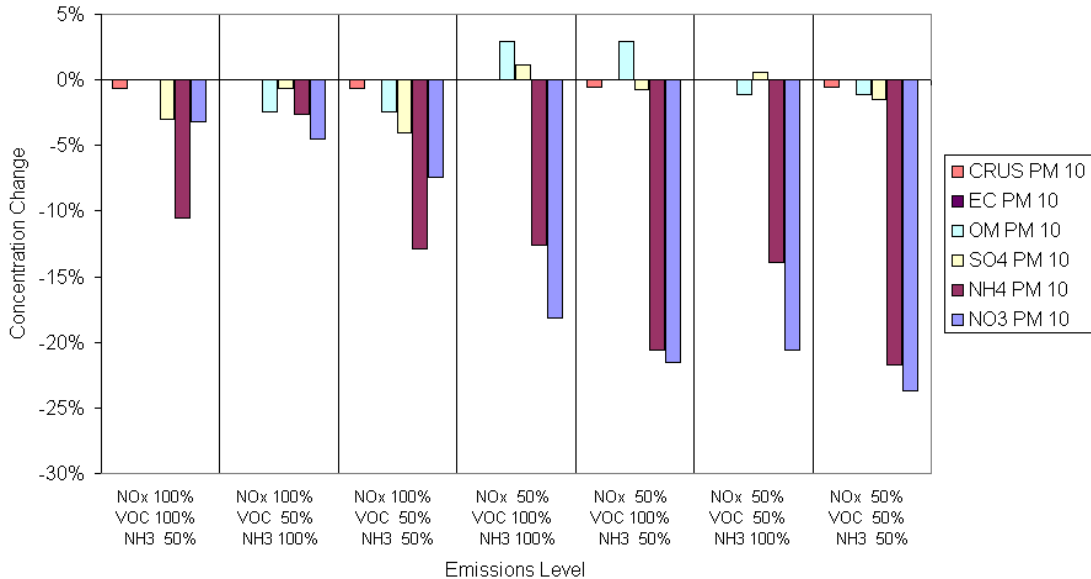


Figure 5-21. Change in Riverside PM₁₀ on October 19th with emission level.

**24-hr PM 10 for Los Angeles North Main
for different NOx, VOC, NH3 emission levels
19 October, 1995**

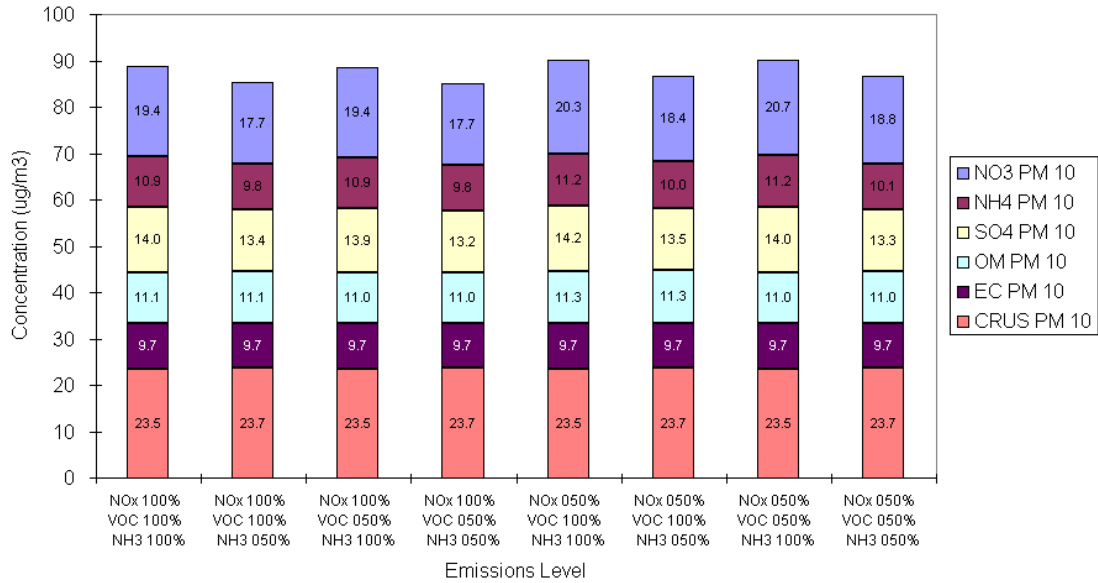


Figure 5-22. LA North Main PM₁₀ on October 19th at different emission levels.

**Percent Change in 24-hr PM 10 for Los Angeles North Main
in response to NOx, VOC, NH3 emission reductions
19 October, 1995**

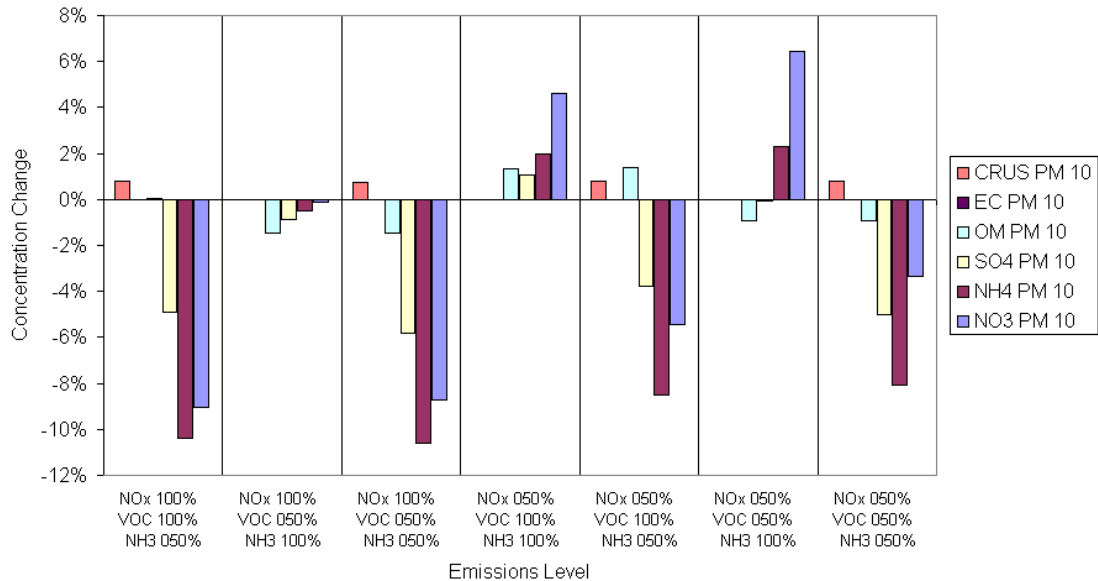


Figure 5-23. Change in LA North Main PM₁₀ on October 19th with emission level.

REFERENCES

- Ansari, A. and S. N. Pandis. 1999. "An Analysis of Four Models Predicting The Partitioning of Semi-volatile Inorganic Aerosol Components." *Aerosol Science and Technology*, 31, 129-153.
- Brown, P.N., G. D. Byrne, and A.C. Hindmarsh. 1989. "VODE: A Variable-Coefficient ODE Solver." *SIAM J. Sci. Stat. Comp.*, 10, 1038-1051.
- Capaldo K., C. Pilinis, and S. N. Pandis. 2000. "A computationally efficient hybrid approach for the simulation of dynamic gas/aerosol transfer in air quality models." *Atmos. Environ.* 34, 3617-3627.
- Capaldo, K. P., C. Pilinis, and S. N. Pandis. 1998. "Dynamic aerosol mass transfer in aerosol models." *J. Aerosol Sci.*, 29, 797-798.
- CARB. 1998. "PM10 Technical Enhancement Program (PTEP)"
<http://www.arb.ca.gov/pm25/tecforum/pmmfmz.ppt>
- Dassios, K. and S. N. Pandis. 1999. "The mass accommodation coefficient of ammonium nitrate." *Atmos. Environ.* 33, 2993-3003.
- Douglas, S. G., R. C. Kessler, and E. Carr. 1990. "User's Guide for the Urban Airshed Model. Volume III: User's Manual for the Diagnostic Wind Model." EPA Publication No. EPA-450/4-90-007C. U. S. Environmental Protection Agency, Research Triangle Park, NC.
- ENVIRON. 2002. User's Guide: Comprehensive Air Quality Model with Extensions (CAMx). Version 3.1. ENVIRON International Corporation, Novato, CA. April.
- EPA. 1995. A User's Guide for the CALPUFF Dispersion Model. U.S. Environmental Protection Agency, Office of Air Quality Planning and Standards, Research Triangle Park, NC. EPA-454/B-95-006.
- Fahey, K.M., and S.N. Pandis. 2001. Optimizing model performance: variable size reduction in cloud chemistry modeling. *Atmos. Environ.* 35, 4471-4478.
- Friedlander, S.K. 1977. "Smoke, dust and Haze. Fundamentals of aerosol behavior." John Wiley & Sons. New York, New York.
- Gurciullo, C.S., Pandis, S.N. 1997. Effect of composition variations in cloud droplet populations on aqueous-phase chemistry. *J. Geophys Res.*, 102, 9375-9385.
- Hindmarsh, A.C. 1983. "ODEPACK, a Systematized Collection of ODE Solvers." In *Numerical Methods for Scientific Computation*, 55, R.S. Stepleman, Ed., North-Holland, New York.

- Jaeger-Voirol, A., and P. Mirabel. 1989. "Heteromolecular nucleation in the sulfuric acid-water system." *Atmos. Environ.* 23, 2053-2057.
- Kim, B. M., J. C. Lester and M. D. Zeldin. 1996. "Characterization of Particulate Matter in the South Coast Air Basin," 89th Annual Meeting & Exhibition, Air & Waste Management Association, June, Nashville, Tennessee, 1996.
- Kumar, N., F.W. Lurmann, A.S. Wexler, S. Pandis, and J.H. Seinfeld. 1996. "Development and Application of a Three Dimensional Aerosol Model." Presented at the A&WMA Specialty Conference on Computing in Environmental Resource Management, Research Triangle Park, NC, December 2-4, 1996.
- Kumar, N. and F. W. Lurmann. 1996. "User's Guide to the UAM-Aero Model." Prepared for the South Coast AQMD by Sonoma Technology Inc., Santa Rosa, CA
- Lurmann F.W., A.S. Wexler, S.N. Pandis, S. Musarra, N. Kumar, and J.H. Seinfeld. 1997. "Modeling urban and regional aerosols: II. application to California's South Coast Air Basin." *Atmos. Environ.* 31, 2695-2715.
- Maul, P.R. 1980. Atmospheric Transport of Sulfur Compound Pollutants. Central Electricity Generating Board, MID/SSD/80/0026/R, Nottingham, England.
- Meng, Z. and J. H. Seinfeld. 1996. "Time scales to achieve atmospheric gas aerosol equilibrium for volatile species." *Atmos. Environ.* 30, 2889-2900.
- Nenes, A, C. Pilinis, and S.N. Pandis. 1999. "Continued Development and Testing of a New Thermodynamic Aerosol Module for Urban and Regional Air Quality Models." *Atmos. Environ.* 33, 1553-1560.
- Nenes, A, C. Pilinis, and S.N. Pandis. 1998. "ISORROPIA: A New Thermodynamic Model for Multiphase Multicomponent Inorganic Aerosols." *Aquatic Geochemistry*, 4, 123-152.
- Pandis, S. N., A. S. Wexler and J. H. Seinfeld. 1993. "Secondary organic aerosol formation and transport." *Atmos. Environ.* 27A, 2403-2416.
- Pandis, S.N., J.H. Seinfeld, and C Pilinis. 1990. "Chemical composition differences in fog and cloud droplets of different sizes." *Atmos. Environ.* 24A, 1954-1969.
- Pandis, S.N. and Seinfeld J.H. 1989. Sensitivity analysis of a chemical mechanism for aqueous-phase atmospheric chemistry. *J. Geophys. Res.* **94**, 1105-1126.
- Pilinis, C., Capaldo, K.P., Nenes, A., Pandis, S.N. 2000. "MADM - A new multicomponent aerosol dynamics model." *Aerosol Sci. Tech.*, 32(5), 482-502
- Pilinis, C. and J. H. Seinfeld. 1987. "Continued Development of a General Equilibrium Model for Inorganic Multicomponent Atmospheric Aerosols", *Atmos. Environ.* 21, 2453.

- Russell, L. M., S. N. Pandis, and J. H. Seinfeld. 1994. "Aerosol production and growth in the marine boundary layer." *J. Geophys. Res.*, 99, 20,989-21,003.
- Sandu, A, J.G. Verwer, M. van Loon, G.R. Carmichael, F.A. Potra, D. Dabdub and J.H. Seinfeld. 1997. "Benchmarking stiff ODE solvers for atmospheric chemistry problems I: implicit versus explicit." *Atmos. Environ.* 31, 3151-3166.
- Seigneur, C. and P. Saxena. 1988. A theoretical investigation of sulfate formation in clouds. *Atmos. Environ.* 22, 101-115.
- Scire, J.S., E.M. Insley, and R. Yamartino. 1990. "Model Formulation And User's Guide For The Calmet Meteorological Model." Prepared for the California Air Resource Board.
- Seinfeld, J.H. and S.N. Pandis. 1998. *Atmospheric Chemistry and Physics: From Air Pollution to Global Change*. Wiley, New York.
- Seinfeld, J. H. 1986. "Atmospheric Chemistry and Physics of Air Pollution." John Wiley & Sons, Inc. New York, New York.
- Slinn, S.A. and W.G.N. Slinn. 1980. Predictions for particle deposition in natural waters. *Atmos. Environ.* 14, 1013-1016.
- Strader, R., C. Gurciullo, S.N. Pandis, N. Kumar, and F.W. Lurmann. 1998. Development of gas-phase chemistry, secondary organic aerosol, and aqueous-phase chemistry modules for PM modeling. Final report for CRC Project A21-1 prepared for the Coordinating Research Council, Atlanta, GA by Sonoma Technology, Inc., Petaluma, CA, STI-97510-1822-FR, October.
- Strader, R., F. W. Lurmann and S.N. Pandis. 1999. "Evaluation of secondary organic aerosol formation in winter." *Atmos. Environ.* 33, 4849-4864.
- Wexler, A. S. and J. H. Seinfeld. 1990. "The distribution of ammonium salts among a size and composition dispersed aerosol." *Atmos. Environ.* 24A, 1231-1246.
- Wesely, M.L. 1989. "Parameterization of Surface Resistances to Gaseous Dry Deposition in Regional-Scale Numerical Models." *Atmos. Environ.* 23, 1293-1304.

Appendix A

**Gas Phase Chemistry for PMCAMx
Based on the Carbon Bond 4 (CB4)
Chemical Mechanism**

Table A-1. Listing of the CB4 mechanism for aerosol modeling in PMCAMx.

| Rxn | Reactants | | | = | Products | | |
|-----|-----------|------|-----|---|----------|--------|---------|
| 1 | NO2 | | | = | 1 NO | 1 O | |
| 2 | O | | | = | 1 O3 | | |
| 3 | O3 | NO | | = | 1 NO2 | | |
| 4 | O | NO2 | | = | 1 NO | | |
| 5 | O | NO2 | | = | 1 NO3 | | |
| 6 | O | NO | | = | 1 NO2 | | |
| 7 | NO2 | O3 | | = | 1 NO3 | | |
| 8 | O3 | | | = | 1 O | | |
| 9 | O3 | | | = | 1 O1D | | |
| 10 | O1D | | | = | 1 O | | |
| 11 | O1D | H2O | | = | 2 OH | | |
| 12 | O3 | OH | | = | 1 HO2 | | |
| 13 | O3 | HO2 | | = | 1 OH | | |
| 14 | NO3 | | | = | 0.89 NO2 | 0.89 O | 0.11 NO |
| 15 | NO3 | NO | | = | 2 NO2 | | |
| 16 | NO3 | NO2 | | = | 1 NO | 1 NO2 | |
| 17 | NO3 | NO2 | | = | 1 N2O5 | | |
| 18 | N2O5 | H2O | | = | 2 HNO3 | | |
| 19 | N2O5 | | | = | 1 NO3 | 1 NO2 | |
| 20 | NO | NO | | = | 2 NO2 | | |
| 21 | NO | NO2 | H2O | = | 2 HNO2 | | |
| 22 | NO | OH | | = | 1 HNO2 | | |
| 23 | HNO2 | | | = | 1 NO | 1 OH | |
| 24 | OH | HNO2 | | = | 1 NO2 | | |
| 25 | HNO2 | HNO2 | | = | 1 NO | 1 NO2 | |
| 26 | NO2 | OH | | = | 1 HNO3 | | |
| 27 | OH | HNO3 | | = | 1 NO3 | | |
| 28 | HO2 | NO | | = | 1 OH | 1 NO2 | |
| 29 | HO2 | NO2 | | = | 1 PNA | | |
| 30 | PNA | | | = | 1 HO2 | 1 NO2 | |
| 31 | OH | PNA | | = | 1 NO2 | | |
| 32 | HO2 | HO2 | | = | 1 H2O2 | | |
| 33 | HO2 | HO2 | H2O | = | 1 H2O2 | | |
| 34 | H2O2 | | | = | 2 OH | | |
| 35 | OH | H2O2 | | = | 1 HO2 | | |
| 36 | OH | CO | | = | 1 HO2 | | |
| 37 | FORM | OH | | = | 1 HO2 | 1 CO | |
| 38 | FORM | | | = | 2 HO2 | 1 CO | |
| 39 | FORM | | | = | 1 CO | | |
| 40 | FORM | O | | = | 1 OH | 1 HO2 | 1 CO |
| 41 | FORM | NO3 | | = | 1 HNO3 | 1 HO2 | 1 CO |
| 42 | ALD2 | O | | = | 1 C2O3 | 1 OH | |
| 43 | ALD2 | OH | | = | 1 C2O3 | | |
| 44 | ALD2 | NO3 | | = | 1 C2O3 | 1 HNO3 | |
| 45 | ALD2 | | | = | 1 FORM | 2 HO2 | 1 CO |
| | | | | | 1 XO2 | | |
| 46 | C2O3 | NO | | = | 1 FORM | 1 NO2 | 1 HO2 |
| | | | | | 1 XO2 | | |
| 47 | C2O3 | NO2 | | = | 1 PAN | | |
| 48 | PAN | | | = | 1 C2O3 | 1 NO2 | |

Table A-1. Listing of the CB4 mechanism for aerosol modeling in PMCAMx (continued).

| Rxn | Reactants | | | Products | | |
|-----|-----------|------|---|-----------------------------------|----------------------------------|-----------------------------------|
| 49 | C2O3 | C2O3 | = | 2 FORM | 2 XO2 | 2 HO2 |
| 50 | C2O3 | HO2 | = | 0.79 FORM 0.79 OH | 0.79 XO2 | 0.79 HO2 |
| 50 | C2O3 | HO2 | = | 0.79 FORM 0.79 OH | 0.79 XO2 | 0.79 HO2 |
| 51 | OH | | = | 1 FORM | 1 XO2 | 1 HO2 |
| 52 | PAR | OH | = | 0.87 XO2 0.11 ALD2 53.4 CG3 | 0.13 XO2N -0.11 PAR | 0.11 HO2 0.76 ROR |
| 53 | ROR | | = | 0.96 XO2 -2.1 PAR | 1.1 ALD2 0.04 XO2N | 0.94 HO2 |
| 54 | ROR | | = | 1 HO2 | | |
| 55 | ROR | NO2 | = | 1 NTR | | |
| 56 | O | OLE | = | 0.63 ALD2 0.3 CO 0.22 PAR | 0.38 HO2 0.2 FORM 0.2 OH | 0.28 XO2 0.02 XO2N 14.6 CG3 |
| 57 | OH | OLE | = | 1 FORM 1 XO2 | 1 ALD2 1 HO2 | -1 PAR 14.6 CG3 |
| 58 | O3 | OLE | = | 0.5 ALD2 0.1 OH -1 PAR | 0.74 FORM 0.33 CO 14.6 CG3 | 0.22 XO2 0.44 HO2 |
| 59 | NO3 | OLE | = | 0.91 XO2 1 ALD2 14.6 CG3 | 1 FORM 1 NO2 | 0.09 XO2N -1 PAR |
| 60 | O | ETH | = | 1 FORM 0.7 XO2 | 1.7 HO2 0.3 OH | 1 CO |
| 61 | OH | ETH | = | 1 XO2 1 HO2 | 1.56 FORM | 0.22 ALD2 |
| 62 | O3 | ETH | = | 1 FORM | 0.42 CO | 0.12 HO2 |
| 63 | TOL | OH | = | 0.44 HO2 0.56 TO2 | 0.08 XO2 430 CG1 | 0.36 CRES 836 CG2 |
| 64 | TO2 | NO | = | 0.9 NO2 0.1 NTR | 0.9 HO2 | 0.9 OPEN |
| 65 | TO2 | | = | 1 CRES | 1 HO2 | |
| 66 | OH | CRES | = | 0.4 CRO 0.3 OPEN | 0.6 XO2 221 CG3 | 0.6 HO2 |
| 67 | CRES | NO3 | = | 1 CRO | 1 HNO3 | 221 CG3 |
| 68 | CRO | NO2 | = | 1 NTR | | |
| 69 | OPEN | | = | 1 C2O3 | 1 HO2 | 1 CO |
| 70 | OPEN | OH | = | 1 XO2 1 C2O3 | 2 CO 1 FORM | 2 HO2 |
| 71 | OPEN | O3 | = | 0.03 ALD2 0.03 XO2 0.76 HO2 | 0.62 C2O3 0.69 CO 0.2 MGLY | 0.7 FORM 0.08 OH |
| 72 | OH | XYL | = | 0.7 HO2 0.8 MGLY 268 CG1 | 0.5 XO2 1.1 PAR 1178 CG2 | 0.2 CRES 0.3 TO2 |
| 73 | OH | MGLY | = | 1 XO2 | 1 C2O3 | |
| 74 | MGLY | | = | 1 C2O3 | 1 HO2 | 1 CO |

Table A-1. Listing of the CB4 mechanism for aerosol modeling in PMCAMx (concluded).

| Rxn | Reactants | | = | Products | | | |
|-----|-----------|------|---|------------|------------|------------|--|
| 75 | O | ISOP | = | 0.75 ISPD | 0.5 FORM | 0.25 XO2 | |
| | | | | 0.25 HO2 | 0.25 C2O3 | 0.25 PAR | |
| 76 | OH | ISOP | = | 0.912 ISPD | 0.629 FORM | 0.991 XO2 | |
| | | | | 0.912 HO2 | 0.088 XO2N | | |
| 77 | O3 | ISOP | = | 0.65 ISPD | 0.6 FORM | 0.2 XO2 | |
| | | | | 0.066 HO2 | 0.266 OH | 0.2 C2O3 | |
| | | | | 0.15 ALD2 | 0.35 PAR | 0.066 CO | |
| 78 | NO3 | ISOP | = | 0.2 ISPD | 0.8 NTR | 1 XO2 | |
| | | | | 0.8 HO2 | 0.2 NO2 | 0.8 ALD2 | |
| | | | | 2.4 PAR | | | |
| 79 | XO2 | NO | = | 1 NO2 | | | |
| 80 | XO2 | XO2 | = | | | | |
| 81 | XO2N | NO | = | 1 NTR | | | |
| 82 | SO2 | OH | = | 1 SULF | 1 HO2 | | |
| 83 | SO2 | | = | 1 SULF | | | |
| 84 | MEOH | OH | = | 1 FORM | 1 HO2 | | |
| 85 | ETOH | OH | = | 1 HO2 | 1 ALD2 | | |
| 86 | XO2 | HO2 | = | | | | |
| 87 | XO2N | HO2 | = | | | | |
| 88 | XO2N | XO2N | = | | | | |
| 89 | XO2 | XO2N | = | | | | |
| 90 | OH | HO2 | = | | | | |
| 91 | CRO | | = | | | | |
| 92 | OH | ISPD | = | 1.565 PAR | 0.167 FORM | 0.713 XO2 | |
| | | | | 0.503 HO2 | 0.334 CO | 0.168 MGLY | |
| | | | | 0.273 ALD2 | 0.498 C2O3 | | |
| 93 | O3 | ISPD | = | 0.114 C2O3 | 0.15 FORM | 0.85 MGLY | |
| | | | | 0.154 HO2 | 0.268 OH | 0.064 XO2 | |
| | | | | 0.02 ALD2 | 0.36 PAR | 0.225 CO | |
| 94 | NO3 | ISPD | = | 0.357 ALD2 | 0.282 FORM | 1.282 PAR | |
| | | | | 0.925 HO2 | 0.643 CO | 0.85 NTR | |
| | | | | 0.075 C2O3 | 0.075 XO2 | 0.15 HNO3 | |
| 95 | ISPD | | = | 0.333 CO | 0.067 ALD2 | 0.9 FORM | |
| | | | | 0.832 PAR | 1.033 HO2 | 0.7 XO2 | |
| | | | | 0.967 C2O3 | | | |
| 96 | NO2 | ISOP | = | 0.2 ISPD | 0.8 NTR | 1 XO2 | |
| | | | | 0.8 HO2 | 0.2 NO | 0.8 ALD2 | |
| | | | | 2.4 PAR | | | |
| 97 | O | OLE2 | = | 0.63 ALD2 | 0.38 HO2 | 0.28 XO2 | |
| | | | | 0.3 CO | 0.2 FORM | 0.02 XO2N | |
| | | | | 0.22 PAR | 0.2 OH | 999 CG4 | |
| 98 | OH | OLE2 | = | 1 FORM | 1 ALD2 | -1 PAR | |
| | | | | 1 XO2 | 1 HO2 | 999 CG4 | |
| 99 | O3 | OLE2 | = | 0.5 ALD2 | 0.74 FORM | 0.22 XO2 | |
| | | | | 0.1 OH | 0.33 CO | 0.44 HO2 | |
| | | | | -1 PAR | 999 CG4 | | |
| 100 | NO3 | OLE2 | = | 0.91 XO2 | 1 FORM | 0.09 XO2N | |
| | | | | 1 ALD2 | 1 NO2 | -1 PAR | |
| | | | | 999 CG4 | | | |

Table A-2. CB4 chemistry parameters file for PMCAMx.

| | | | | | | |
|---------------------|-------------------------------|----------|--------|---------|-----------|--|
| CAMx Version | PMCAMx3.01 | | | | | |
| Mechanism ID | 8 | | | | | |
| Description | CBM-IV (mech 3) plus aerosols | | | | | |
| No of gas species | 34 | | | | | |
| No of aero species | 13 10 0.0390625 40.0 15.0 | | | | | |
| No of reactions | 100 | | | | | |
| Prim photo rxns | 6 1 38 39 9 45 95 | | | | | |
| No of sec photo rxn | 6 | | | | | |
| ID, prim ID, scale | 8 1 0.053 | | | | | |
| | 14 1 33.9 | | | | | |
| | 23 1 0.1975 | | | | | |
| | 34 39 0.189 | | | | | |
| | 69 38 9.04 | | | | | |
| | 74 38 9.64 | | | | | |
| Species Records | | | | | | |
| Gas Spec | lower bnd | H-law | T-fact | Diffrat | Reactivty | |
| 1 NO | 1.00E-15 | 1.90e-03 | -1480. | 1.29 | 0.0 | |
| 2 NO2 | 1.00E-09 | 1.00e-02 | -2516. | 1.60 | 0.1 | |
| 3 O3 | 1.00E-09 | 1.10e-02 | -2415. | 1.63 | 1.0 | |
| 4 PAN | 1.00E-09 | 3.60e+00 | -5910. | 2.59 | 0.1 | |
| 5 NXOY | 1.00E-12 | 3.20e+04 | -8706. | 2.45 | 0.1 | |
| 6 OLE | 1.00E-09 | 5.00e-03 | 0. | 1.80 | 0.0 | |
| 7 PAR | 1.00E-04 | 1.00e-03 | 0. | 2.00 | 0.0 | |
| 8 TOL | 1.00E-09 | 1.20e+00 | 0. | 2.26 | 0.0 | |
| 9 XYL | 1.00E-09 | 1.40e+00 | 0. | 2.43 | 0.0 | |
| 10 FORM | 1.00E-09 | 6.30e+03 | -6492. | 1.29 | 0.0 | |
| 11 ALD2 | 1.00E-09 | 6.30e+03 | -6492. | 1.56 | 0.0 | |
| 12 ETH | 1.00E-09 | 1.00e-02 | 0. | 1.25 | 0.0 | |
| 13 CRES | 1.00E-09 | 2.70e+03 | -6492. | 2.45 | 0.0 | |
| 14 MGLY | 1.00E-09 | 2.70e+03 | -6492. | 2.00 | 0.0 | |
| 15 OPEN | 1.00E-12 | 2.70e+03 | -6492. | 2.47 | 0.0 | |
| 16 PNA | 1.00E-09 | 2.00e+04 | -5910. | 2.09 | 0.0 | |
| 17 CO | 1.00E-04 | 1.00e-10 | 0. | 1.25 | 0.0 | |
| 18 HONO | 1.00E-09 | 5.90e+01 | -4781. | 1.62 | 0.1 | |
| 19 H2O2 | 1.00E-09 | 7.40e+04 | -6643. | 1.37 | 1.0 | |
| 20 HNO3 | 1.00E-09 | 2.00e+05 | -8707. | 1.87 | 0.0 | |
| 21 ISOP | 1.00E-09 | 1.00e-02 | 0. | 1.94 | 0.0 | |
| 22 MEOH | 1.00E-09 | 2.20e+02 | -4932. | 1.33 | 0.0 | |
| 23 ETOH | 1.00E-09 | 2.20e+02 | -4932. | 1.60 | 0.0 | |
| 24 ISPD | 1.00E-09 | 6.30e+03 | -6492. | 1.97 | 0.0 | |
| 25 NTR | 1.00E-09 | 9.40e+03 | -8706. | 2.72 | 0.0 | |
| 26 OLE2 | 1.00E-09 | 5.00e-03 | 0. | 1.80 | 0.0 | |
| 27 CG1 | 1.00E-09 | 2.70e+03 | -6492. | 2.50 | 0.0 | |
| 28 CG2 | 1.00E-09 | 2.70e+03 | -6492. | 2.50 | 0.0 | |
| 29 CG3 | 1.00E-09 | 2.70e+03 | -6492. | 2.50 | 0.0 | |
| 30 CG4 | 1.00E-09 | 2.70e+03 | -6492. | 2.50 | 0.0 | |
| 31 NH3 | 1.00E-09 | 2.00e+04 | -3400. | 0.97 | 0.0 | |
| 32 HCL | 1.00E-12 | 1.00e+05 | 0. | 1.42 | 0.0 | |
| 33 SO2 | 1.00E-09 | 1.00e+05 | -3156. | 1.89 | 0.0 | |
| 34 SULF | 1.00E-12 | 1.00e-10 | 0. | 1.00 | 0.0 | |
| Aero Spec | lower bnd | mol wt | | | | |
| 1 SOA1 | 1.00E-09 | 150. | | | | |
| 2 SOA2 | 1.00E-09 | 150. | | | | |
| 3 SOA3 | 1.00E-09 | 150. | | | | |
| 4 SOA4 | 1.00E-09 | 180. | | | | |
| 5 POC | 1.00E-09 | 100. | | | | |
| 6 PEC | 1.00E-09 | 100. | | | | |
| 7 CRST | 1.00E-09 | 100. | | | | |
| 8 PH2O | 1.00E-09 | 18. | | | | |
| 9 PCL | 1.00E-09 | 36.5 | | | | |
| 10 NA | 1.00E-09 | 23. | | | | |
| 11 PNH4 | 1.00E-09 | 18. | | | | |
| 12 PNO3 | 1.00E-09 | 62. | | | | |
| 13 PSO4 | 1.00E-09 | 96. | | | | |

Table A-2. CB4 chemistry parameters file for PMCAMx (continued).

| Reaction Records | | | |
|------------------|-----|--|-------------|
| Rxn | Typ | Parameters (1 to 10, depending upon Typ) | |
| 1 | 1 | 0.0000E+00 | |
| 2 | 2 | 4.3233E+06 | -1.1750E+03 |
| 3 | 2 | 2.6640E+01 | 1.3700E+03 |
| 4 | 1 | 1.3750E+04 | |
| 5 | 2 | 2.3090E+03 | -6.8700E+02 |
| 6 | 2 | 2.4380E+03 | -6.0200E+02 |
| 7 | 2 | 4.7310E-02 | 2.4500E+03 |
| 8 | 1 | 0.0000E+00 | |
| 9 | 1 | 0.0000E+00 | |
| 10 | 2 | 4.2500E+10 | -3.9000E+02 |
| 11 | 1 | 3.2600E+05 | |
| 12 | 2 | 1.0000E+02 | 9.4000E+02 |
| 13 | 2 | 2.9990E+00 | 5.8000E+02 |
| 14 | 1 | 0.0000E+00 | |
| 15 | 2 | 4.4167E+04 | -2.5000E+02 |
| 16 | 2 | 5.9010E-01 | 1.2300E+03 |
| 17 | 2 | 1.8530E+03 | -2.5600E+02 |
| 18 | 1 | 1.9000E-06 | |
| 19 | 2 | 2.7760E+00 | 1.0897E+04 |
| 20 | 2 | 1.5390E-04 | -5.3000E+02 |
| 21 | 1 | 1.6000E-11 | |
| 22 | 2 | 9.7990E+03 | -8.0600E+02 |
| 23 | 1 | 0.0000E+00 | |
| 24 | 1 | 9.7700E+03 | |
| 25 | 1 | 1.5000E-05 | |
| 26 | 2 | 1.6817E+04 | -7.1300E+02 |
| 27 | 2 | 2.1790E+02 | -1.0000E+03 |
| 28 | 2 | 1.2270E+04 | -2.4000E+02 |
| 29 | 1 | 0.0000E+00 | |
| 30 | 1 | 0.0000E+00 | |
| 31 | 1 | 0.0000E+00 | |
| 32 | 2 | 4.1440E+03 | -1.1500E+03 |
| 33 | 2 | 2.1810E-01 | -5.8000E+03 |
| 34 | 1 | 0.0000E+00 | |
| 35 | 2 | 2.5200E+03 | 1.8700E+02 |
| 36 | 1 | 3.2200E+02 | |
| 37 | 1 | 1.5000E+04 | |
| 38 | 1 | 0.0000E+00 | |
| 39 | 1 | 0.0000E+00 | |
| 40 | 2 | 2.3700E+02 | 1.5500E+03 |
| 41 | 1 | 9.3000E-01 | |
| 42 | 2 | 6.3600E+02 | 9.8600E+02 |
| 43 | 2 | 2.4000E+04 | -2.5000E+02 |
| 44 | 1 | 3.7000E+00 | |
| 45 | 1 | 0.0000E+00 | |
| 46 | 2 | 2.8200E+04 | 1.8000E+02 |
| 47 | 2 | 1.3700E+04 | -3.8000E+02 |
| 48 | 2 | 2.5400E-02 | 1.3500E+04 |
| 49 | 1 | 3.7000E+03 | |
| 50 | 1 | 9.6000E+03 | |
| 51 | 2 | 2.1000E+01 | 1.7100E+03 |
| 52 | 1 | 1.2030E+03 | |
| 53 | 2 | 1.3710E+05 | 8.0000E+03 |
| 54 | 1 | 9.5450E+04 | |
| 55 | 1 | 2.2000E+04 | |
| 56 | 2 | 5.9200E+03 | 3.2400E+02 |
| 57 | 2 | 4.2000E+04 | -5.0400E+02 |
| 58 | 2 | 1.8000E-02 | 2.1050E+03 |
| 59 | 1 | 1.1350E+01 | |
| 60 | 2 | 1.0800E+03 | 7.9200E+02 |
| 61 | 2 | 1.1920E+04 | -4.1100E+02 |
| 62 | 2 | 2.7000E-03 | 2.6330E+03 |

Table A-2. CB4 chemistry parameters file for PMCAMx (concluded).

| | | | |
|-----|---|------------|-------------|
| 63 | 2 | 9.1500E+03 | -3.2200E+02 |
| 64 | 1 | 1.2000E+04 | |
| 65 | 1 | 2.5000E+02 | |
| 66 | 1 | 6.1000E+04 | |
| 67 | 1 | 3.2500E+04 | |
| 68 | 1 | 2.0000E+04 | |
| 69 | 1 | 0.0000E+00 | |
| 70 | 1 | 4.4000E+04 | |
| 71 | 2 | 1.5000E-02 | 5.0000E+02 |
| 72 | 2 | 3.6200E+04 | -1.1600E+02 |
| 73 | 1 | 2.6000E+04 | |
| 74 | 1 | 0.0000E+00 | |
| 75 | 1 | 5.3200E+04 | |
| 76 | 1 | 1.4760E+05 | |
| 77 | 1 | 1.9000E-02 | |
| 78 | 1 | 9.9600E+02 | |
| 79 | 1 | 1.2000E+04 | |
| 80 | 2 | 2.0000E+03 | -1.3000E+03 |
| 81 | 1 | 1.2000E+04 | |
| 82 | 2 | 1.1100E+03 | -1.6000E+02 |
| 83 | 1 | 8.1667E-05 | |
| 84 | 1 | 1.6000E+03 | |
| 85 | 2 | 4.3000E+03 | -1.7600E+02 |
| 86 | 2 | 8.9000E+03 | -1.3000E+03 |
| 87 | 2 | 8.9000E+03 | -1.3000E+03 |
| 88 | 2 | 2.0000E+03 | -1.3000E+03 |
| 89 | 2 | 4.0000E+03 | -1.3000E+03 |
| 90 | 2 | 1.6260E+05 | -2.5000E+02 |
| 91 | 1 | 2.7778E-04 | |
| 92 | 1 | 4.9667E+04 | |
| 93 | 1 | 1.0500E-02 | |
| 94 | 1 | 1.4780E+00 | |
| 95 | 1 | 0.0000E+00 | |
| 96 | 1 | 2.2000E-04 | |
| 97 | 2 | 5.9200E+03 | 3.2400E+02 |
| 98 | 2 | 4.2000E+04 | -5.0400E+02 |
| 99 | 2 | 1.8000E-02 | 2.1050E+03 |
| 100 | 1 | 1.1350E+01 | |

See the CAMx User's Guide (available from <http://www.camx.com>) for an explanation of the chemistry parameter file format how the reaction rate constants are calculated from the parameters listed in the chemistry parameters file. For convenience, Table A-3 lists the rate constant values calculated for standard conditions (298 K and 1 atmosphere).

Table A-3. Rate constants at 298 K and 1 atmosphere for the CB4 mechanism for aerosol modeling in PMCAMx.

| Reaction | Type | k ₂₉₈ (ppm ⁻ⁿ min ⁻¹) | Reaction | Type | k ₂₉₈ (ppm ⁻ⁿ min ⁻¹) |
|----------|------------|---|----------|------------|---|
| 1 | Photolysis | N/A | 51 | Arrhenius | 21 |
| 2 | Arrhenius | 4323300 | 52 | Constant | 1203 |
| 3 | Arrhenius | 26.64 | 53 | Arrhenius | 137100 |
| 4 | Constant | 13750 | 54 | Constant | 95450 |
| 5 | Arrhenius | 2309 | 55 | Constant | 22000 |
| 6 | Arrhenius | 2438 | 56 | Arrhenius | 5920 |
| 7 | Arrhenius | 0.04731 | 57 | Arrhenius | 42000 |
| 8 | Photolysis | N/A | 58 | Arrhenius | 0.018 |
| 9 | Photolysis | N/A | 59 | Constant | 11.35 |
| 10 | Arrhenius | 42500000000 | 60 | Arrhenius | 1080 |
| 11 | Constant | 326000 | 61 | Arrhenius | 11920 |
| 12 | Arrhenius | 100 | 62 | Arrhenius | 0.0027 |
| 13 | Arrhenius | 2.999 | 63 | Arrhenius | 9150 |
| 14 | Photolysis | N/A | 64 | Constant | 12000 |
| 15 | Arrhenius | 44167 | 65 | Constant | 250 |
| 16 | Arrhenius | 0.5901 | 66 | Constant | 61000 |
| 17 | Arrhenius | 1853 | 67 | Constant | 32500 |
| 18 | Constant | 0.0000019 | 68 | Constant | 20000 |
| 19 | Arrhenius | 2.776 | 69 | Photolysis | N/A |
| 20 | Arrhenius | 0.0001539 | 70 | Constant | 44000 |
| 21 | Constant | 1.6E-11 | 71 | Arrhenius | 0.015 |
| 22 | Arrhenius | 9799 | 72 | Arrhenius | 36200 |
| 23 | Photolysis | N/A | 73 | Constant | 26000 |
| 24 | Constant | 9770 | 74 | Photolysis | N/A |
| 25 | Constant | 0.000015 | 75 | Constant | 53200 |
| 26 | Arrhenius | 16817 | 76 | Constant | 147600 |
| 27 | Arrhenius | 217.9 | 77 | Constant | 0.019 |
| 28 | Arrhenius | 12270 | 78 | Constant | 996 |
| 29 | Constant | 0 | 79 | Constant | 12000 |
| 30 | Constant | 0 | 80 | Arrhenius | 2000 |
| 31 | Constant | 0 | 81 | Constant | 12000 |
| 32 | Arrhenius | 4144 | 82 | Arrhenius | 1110 |
| 33 | Arrhenius | 0.2181 | 83 | Constant | 0.000081667 |
| 34 | Photolysis | N/A | 84 | Constant | 1600 |
| 35 | Arrhenius | 2520 | 85 | Arrhenius | 4300 |
| 36 | Constant | 322 | 86 | Arrhenius | 8900 |
| 37 | Constant | 15000 | 87 | Arrhenius | 8900 |
| 38 | Photolysis | N/A | 88 | Arrhenius | 2000 |
| 39 | Photolysis | N/A | 89 | Arrhenius | 4000 |
| 40 | Arrhenius | 237 | 90 | Arrhenius | 162600 |
| 41 | Constant | 0.93 | 91 | Constant | 0.00027778 |
| 42 | Arrhenius | 636 | 92 | Constant | 49667 |
| 43 | Arrhenius | 24000 | 93 | Constant | 0.0105 |
| 44 | Constant | 3.7 | 94 | Constant | 1.478 |
| 45 | Photolysis | N/A | 95 | Constant | 0 |
| 46 | Arrhenius | 28200 | 96 | Constant | 0.00022 |
| 47 | Arrhenius | 13700 | 97 | Arrhenius | 5920 |
| 48 | Arrhenius | 0.0254 | 98 | Arrhenius | 42000 |
| 49 | Constant | 3700 | 99 | Arrhenius | 0.018 |
| 50 | Constant | 9600 | 100 | Constant | 11.35 |

Appendix B

List of Chemical Equilibria
In the ISORROPIA Aerosol
Thermodynamics Module

Table B-1. Equilibrium relations and constants (Nenes et al., 1998, *Aquatic Geochemistry* 4, 123-152)

| Reaction | Constant expression | K^0 (298.15 K) | $\frac{\Delta H^0(T_0)}{RT_0}$ | $\frac{\Delta C_p^0}{R}$ | Units |
|--|---|-------------------------|--------------------------------|--------------------------|---|
| $\text{HSO}_4^- \leftarrow^{K_1} \text{H}^+ + \text{SO}_4^{2-}$ | $\frac{[\text{H}^+][\text{SO}_4^{2-}]}{[\text{HSO}_4^-]} \frac{\gamma_{\text{H}^+} \gamma_{\text{SO}_4^{2-}}}{\gamma_{\text{HSO}_4^-}}$ | 1.015×10^{-2} | 8.85 | 25.14 | mol kg^{-1} |
| $\text{NH}_3(\text{g}) \leftarrow^{K_{21}} \text{NH}_3(\text{aq})$ | $\frac{[\text{NH}_3(\text{aq})]}{P_{\text{NH}_3}} \gamma_{\text{NH}_3}$ | 5.764×10^1 | 13.79 | -5.39 | $\text{mol kg}^{-1} \text{ atm}^{-1}$ |
| $\text{NH}_3(\text{aq}) + \text{H}_2\text{O}(\text{aq}) \leftarrow^{K_{22}} \text{NH}_4^+(\text{aq}) + \text{OH}^-(\text{aq})$ | $\frac{[\text{NH}_4^+][\text{OH}^-]}{[\text{NH}_3(\text{aq})]a_w} \frac{\gamma_{\text{NH}_4^+} \gamma_{\text{OH}^-}}{\gamma_{\text{NH}_3}}$ | 1.805×10^{-5} | -1.50 | 26.92 | mol kg^{-1} |
| $\text{HNO}_3(\text{g}) \leftarrow^{K_4} \text{H}^+(\text{aq}) + \text{NO}_3^-(\text{aq})$ | $\frac{[\text{H}^+][\text{NO}_3^-]}{P_{\text{HNO}_3}} \gamma_{\text{H}^+} \gamma_{\text{NO}_3^-}$ | 2.511×10^6 | 29.17 | 16.83 | $\text{mol}^2 \text{ kg}^{-2} \text{ atm}^{-1}$ |
| $\text{HCl}(\text{g}) \leftarrow^{K_3} \text{H}^+(\text{aq}) + \text{Cl}^-(\text{aq})$ | $\frac{[\text{H}^+][\text{Cl}^-]}{P_{\text{HCl}}} \gamma_{\text{H}^+} \gamma_{\text{Cl}^-}$ | 1.971×10^6 | 30.20 | 19.91 | $\text{mol}^2 \text{ kg}^{-2} \text{ atm}^{-1}$ |
| $\text{H}_2\text{O}(\text{aq}) \leftarrow^{K_w} \text{H}^+(\text{aq}) + \text{OH}^-(\text{aq})$ | $\frac{[\text{H}^+][\text{OH}^-]}{a_w} \gamma_{\text{H}^+} \gamma_{\text{OH}^-}$ | 1.010×10^{-14} | -22.52 | 26.92 | $\text{mol}^2 \text{ kg}^{-2}$ |
| $\text{Na}_2\text{SO}_4(\text{s}) \leftarrow^{K_5} 2\text{Na}^+(\text{aq}) + \text{SO}_4^{2-}(\text{aq})$ | $[\text{Na}^+]^2[\text{SO}_4^{2-}] \gamma_{\text{Na}^+}^2 \gamma_{\text{SO}_4^{2-}}$ | 4.799×10^{-1} | 0.98 | 39.75 | $\text{mol}^3 \text{ kg}^{-3}$ |
| $(\text{NH}_4)_2\text{SO}_4(\text{s}) \leftarrow^{K_7} 2\text{NH}_4^+(\text{aq}) + \text{SO}_4^{2-}(\text{aq})$ | $[\text{NH}_4^+]^2[\text{SO}_4^{2-}] \gamma_{\text{NH}_4^+}^2 \gamma_{\text{SO}_4^{2-}}$ | 1.817×10^0 | -2.65 | 38.57 | $\text{mol}^3 \text{ kg}^{-3}$ |
| $\text{NH}_4\text{Cl}(\text{s}) \leftarrow^{K_6} \text{NH}_3(\text{g}) + \text{HCl}(\text{g})$ | $P_{\text{NH}_3} P_{\text{HCl}}$ | 1.086×10^{-16} | -71.00 | 2.40 | atm^2 |
| $\text{NaNO}_3(\text{s}) \leftarrow^{K_9} \text{Na}^+(\text{aq}) + \text{NO}_3^-(\text{aq})$ | $[\text{Na}^+][\text{NO}_3^-] \gamma_{\text{Na}^+} \gamma_{\text{NO}_3^-}$ | 1.197×10^1 | -8.22 | 16.01 | $\text{mol}^2 \text{ kg}^{-2}$ |
| $\text{NaCl}(\text{s}) \leftarrow^{K_8} \text{Na}^+(\text{aq}) + \text{Cl}^-(\text{aq})$ | $[\text{Na}^+][\text{Cl}^-] \gamma_{\text{Na}^+} \gamma_{\text{Cl}^-}$ | 3.766×10^1 | -1.56 | 16.90 | $\text{mol}^2 \text{ kg}^{-2}$ |
| $\text{NaHSO}_4(\text{s}) \leftarrow^{K_{11}} \text{Na}^+(\text{aq}) + \text{HSO}_4^-(\text{aq})$ | $[\text{Na}^+][\text{HSO}_4^-] \gamma_{\text{Na}^+} \gamma_{\text{HSO}_4^-}$ | 2.413×10^4 | 0.79 | 14.75 | $\text{mol}^2 \text{ kg}^{-2}$ |
| $\text{NH}_4\text{NO}_3(\text{s}) \leftarrow^{K_{10}} \text{NH}_3(\text{g}) + \text{HNO}_3(\text{g})$ | $P_{\text{NH}_3} P_{\text{HNO}_3}$ | 5.746×10^{-17} | -74.38 | 6.12 | atm^2 |
| $\text{NH}_4\text{HSO}_4(\text{s}) \leftarrow^{K_{12}} \text{NH}_4^+(\text{aq}) + \text{HSO}_4^-(\text{aq})$ | $[\text{NH}_4^+][\text{HSO}_4^-] \gamma_{\text{NH}_4^+} \gamma_{\text{HSO}_4^-}$ | 1.383×10^0 | -2.87 | 15.83 | $\text{mol}^2 \text{ kg}^{-2}$ |
| $(\text{NH}_4)_3\text{H}(\text{SO}_4)_2(\text{s}) \leftarrow^{K_{13}} 3\text{NH}_4^+(\text{aq}) + \text{HSO}_4^-(\text{aq}) + \text{SO}_4^{2-}(\text{aq})$ | $[\text{NH}_4^+]^3[\text{SO}_4^{2-}][\text{HSO}_4^-] \gamma_{\text{NH}_4^+}^3 \gamma_{\text{SO}_4^{2-}} \gamma_{\text{HSO}_4^-}$ | 2.972×10^1 | -5.19 | 54.40 | $\text{mol}^5 \text{ kg}^{-5}$ |

Appendix C

List of Chemical Reactions
And Equilibria in the
AQCHEM Aqueous Phase
Chemistry Module

Aqueous Phase Chemical Mechanism

| Rxn No. | Reaction | k_{298} ($M^n s^{-1}$) | -E/R | Reference |
|---------|--|-----------------------------------|-------|------------------------------|
| 1 | $H_2O_2 \xrightarrow{h\nu} 2 OH$ | | | Graedel and Weschler (1981) |
| 2 | $O_3 \xrightarrow{h\nu, H_2O} H_2O_2 + O_2$ | | | Graedel and Weschler (1981) |
| 3 | $OH + HO_2 \longrightarrow H_2O + O_2$ | 7.0×10^9 | -1500 | Sehested et al. (1968) |
| 4 | $OH + O_2^- \longrightarrow OH^-$ | 1.0×10^{10} | -1500 | Sehested et al. (1968) |
| 5 | $OH + H_2O_2 \longrightarrow H_2O + HO_2$ | 2.7×10^7 | -1700 | Christensen et al. (1982) |
| 6 | $HO_2 + HO_2 \longrightarrow H_2O_2 + O_2$ | 8.6×10^5 | -2365 | Bielski (1978) |
| 7 | $HO_2 + O_2^- \xrightarrow{H_2O} H_2O_2 + O_2 + OH^-$ | 1.0×10^8 | -1500 | Bielski (1978) |
| 8 | $O_2^- + O_2^- \xrightarrow{2H_2O} H_2O_2 + O_2 + OH^-$ | < 0.3 | | Bielski (1978) |
| 9 | $HO_2 + H_2O_2 \longrightarrow OH + O_2 + H_2O$ | 0.5 | | Weinstein and Bielski (1979) |
| 10 | $O_2^- + H_2O_2 \longrightarrow OH + O_2 + OH^-$ | 0.13 | | Weinstein and Bielski (1979) |
| 11 | $OH + O_3 \longrightarrow HO_2 + O_2$ | 2×10^9 | | Stahelin et al. (1984) |
| 12 | $HO_2 + O_3 \longrightarrow OH + 2O_2$ | $< 1 \times 10^4$ | | Sehested et al. (1984) |
| 13 | $O_2^- + O_3 \xrightarrow{H_2O} OH + 2O_2 + OH^-$ | 1.5×10^9 | -1500 | Sehested et al. (1983) |
| 14 | $OH^- + O_3 \xrightarrow{H_2O} H_2O_2 + O_2 + OH^-$ | 70 | | Stahelin and Hoigne (1982) |
| 15 | $HO_2^- + O_3 \longrightarrow OH + O_2^- + O_2$ | 2.8×10^6 | -2500 | Stahelin and Hoigne (1982) |
| 16 | $H_2O_2 + O_3 \longrightarrow H_2O + 2O_2$ | $7.8 \times 10^{-3} [O_3]^{-0.5}$ | | Martin et al. (1981) |
| 17 | $HCO_3^- + OH \longrightarrow H_2O + CO_3^-$ | 1.5×10^7 | -1910 | Weeks and Rabani (1966) |
| 18 | $HCO_3^- + O_2^- \longrightarrow HO_2^- + CO_3^-$ | 1.5×10^6 | 0 | Schmidt (1972) |
| 19 | $CO_3^- + O_2^- \xrightarrow{H_2O} HCO_3^- + O_2 + OH^-$ | 4.0×10^8 | -1500 | Behar et al. (1970) |
| 20 | $CO_3^- + H_2O_2 \longrightarrow HO_2 + HCO_3^-$ | 8.0×10^5 | -2820 | Behar et al. (1970) |
| 21 | $Cl^- + OH \longrightarrow ClOH^-$ | 4.3×10^9 | -1500 | Jayson et al. (1973) |
| 22 | $ClOH^- \longrightarrow Cl^- + OH$ | 6.1×10^9 | 0 | Jayson et al. (1973) |
| 23 | $ClOH^- \xrightarrow{H^+} Cl + H_2O$ | $2.1 \times 10^{10} [H^+]$ | 0 | Jayson et al. (1973) |
| 24 | $Cl \xrightarrow{H_2O} ClOH^- + H^+$ | 1.3×10^3 | 0 | Jayson et al. (1973) |
| 25 | $HO_2 + Cl_2^- \longrightarrow 2Cl^- + O_2 + H^+$ | 4.5×10^9 | -1500 | Ross and Neta (1979) |
| 26 | $O_2^- + Cl_2^- \longrightarrow 2Cl^- + O_2$ | 1.0×10^9 | -1500 | Ross and Neta (1979) |
| 27 | $HO_2 + Cl \longrightarrow Cl^- + O_2 + H^+$ | 3.1×10^9 | -1500 | Graedel and Goldberg (1983) |
| 28 | $H_2O_2 + Cl_2^- \longrightarrow 2Cl^- + HO_2 + H^+$ | 1.4×10^5 | -3370 | Hagesawa and Neta (1978) |
| 29 | $H_2O_2 + Cl \longrightarrow Cl^- + HO_2 + H^+$ | 4.5×10^7 | 0 | Graedel and Goldberg (1983) |
| 30 | $OH^- + Cl_2^- \longrightarrow 2Cl^- + OH$ | 7.3×10^6 | -2160 | Hagesawa and Neta (1978) |
| 31 | $NO + NO_2 \xrightarrow{H_2O} 2NO_2^- + 2H^+$ | 2.1×10^8 | -1500 | Lee (1984a) |
| 32 | $NO_2 + NO_2 \xrightarrow{H_2O} NO_2^- + NO_3^- + 2H^+$ | 1.0×10^8 | -1500 | Lee (1984a) |
| 33 | $NO + OH \longrightarrow NO_2^- + H^+$ | 2.0×10^{10} | -1500 | Strehlow and Wagner (1982) |

| | | | | |
|----|--|--------------------------------|-------|------------------------------------|
| | | | | Wagner (1982) |
| 34 | $\text{NO}_2 + \text{OH} \longrightarrow \text{NO}_3^- + \text{H}^+$ | 1.3×10^9 | -1500 | Gratzel et al. (1970) |
| 35 | $\text{HNO}_2 \xrightarrow{h\nu} \text{NO} + \text{OH}$ | | | Rettich (1978) |
| 36 | $\text{NO}_2^- \xrightarrow{h\nu, \text{H}_2\text{O}} \text{NO} + \text{OH} + \text{OH}^-$ | | | Graedel and Weschler (1981) |
| 37 | $\text{HNO}_2 + \text{OH} \longrightarrow \text{NO}_2 + \text{H}_2\text{O}$ | 1.0×10^9 | -1500 | Rettich (1978) |
| 38 | $\text{NO}_2^- + \text{OH} \longrightarrow \text{NO}_2 + \text{OH}^-$ | 1.0×10^{10} | -1500 | Treinin and Hayon (1978) |
| 39 | $\text{HNO}_2 + \text{H}_2\text{O}_2 \xrightarrow{\text{H}^+} \text{NO}_3^- + 2\text{H}^+ + \text{H}_2\text{O}$ | $6.3 \times 10^3 [\text{H}^+]$ | -6693 | Lee and Lind (1986) |
| 40 | $\text{NO}_2^- + \text{O}_3 \longrightarrow \text{NO}_3^- + \text{O}_2$ | 5.0×10^5 | -6950 | Damschen and Martin (1983) |
| 41 | $\text{NO}_2^- + \text{CO}_3^{2-} \longrightarrow \text{NO}_2 + \text{CO}_3^{2-}$ | 4.0×10^5 | 0 | Lilie et al. (1978) |
| 42 | $\text{NO}_2^- + \text{Cl}_2^- \longrightarrow \text{NO}_2 + 2\text{Cl}^-$ | 2.5×10^8 | -1500 | Hagesawa and Neta (1978) |
| 43 | $\text{NO}_2^- + \text{NO}_3 \longrightarrow \text{NO}_2 + \text{NO}_3^-$ | 1.2×10^9 | -1500 | Ross and Neta (1979) |
| 44 | $\text{NO}_3^- \xrightarrow{h\nu, \text{H}_2\text{O}} \text{NO}_2 + \text{OH} + \text{OH}^-$ | | | Graedel and Weschler (1981) |
| 45 | $\text{NO}_3 \xrightarrow{h\nu} \text{NO} + \text{O}_2$ | | | Graedel and Weschler (1981) |
| 46 | $\text{NO}_3 + \text{HO}_2 \longrightarrow \text{NO}_3^- + \text{H}^+ + \text{O}_2$ | 4.5×10^9 | -1500 | Jacob (1986) |
| 47 | $\text{NO}_3 + \text{O}_2^- \longrightarrow \text{NO}_3^- + \text{O}_2$ | 1.0×10^9 | -1500 | Jacob (1986) |
| 48 | $\text{NO}_3 + \text{H}_2\text{O}_2 \longrightarrow \text{NO}_3^- + \text{H}^+ + \text{HO}_2$ | 1.0×10^6 | -2800 | Chameides (1984) |
| 49 | $\text{NO}_3 + \text{Cl}^- \longrightarrow \text{NO}_3^- + \text{Cl}$ | 1.0×10^8 | -1500 | Ross and Neta (1979) |
| 50 | $\text{H}_2\text{C}(\text{OH})_2 + \text{OH} \xrightarrow{\text{O}_2} \text{HCOOH} + \text{HO}_2 + \text{H}_2\text{O}$ | 2.0×10^9 | -1500 | Bothe and Schulte-Frohlinde (1980) |
| 51 | $\text{H}_2\text{C}(\text{OH})_2 + \text{O}_3 \longrightarrow \text{Products}$ | 0.1 | 0 | Hoigne and Bader (1983a) |
| 52 | $\text{HCOOH} + \text{OH} \xrightarrow{\text{O}_2} \text{CO}_2 + \text{HO}_2 + \text{H}_2\text{O}$ | 2.0×10^8 | -1500 | Scholes and Willson (1967) |
| 53 | $\text{HCOOH} + \text{H}_2\text{O}_2 \longrightarrow \text{Product} + \text{H}_2\text{O}$ | 4.6×10^{-6} | -5180 | Shapilov et al. (1974) |
| 54 | $\text{HCOOH} + \text{NO}_3 \xrightarrow{\text{O}_2} \text{NO}_3^- + \text{H}^+ + \text{CO}_2 + \text{HO}_2$ | 2.1×10^5 | -3200 | Dogliotti and Hayon (1967) |
| 55 | $\text{HCOOH} + \text{O}_3 \longrightarrow \text{CO}_2 + \text{HO}_2 + \text{OH}$ | 5.0 | 0 | Hoigne and Bader (1983b) |
| 56 | $\text{HCOOH} + \text{Cl}_2^- \xrightarrow{\text{O}_2} \text{CO}_2 + \text{HO}_2 + 2\text{Cl}^- + \text{H}^+$ | 6.7×10^3 | -4300 | Hagesawa and Neta (1978) |
| 57 | $\text{HCOO}^- + \text{OH} \xrightarrow{\text{O}_2} \text{CO}_2 + \text{HO}_2 + \text{OH}^-$ | 2.5×10^9 | -1500 | Anbar and Neta (1967) |
| 58 | $\text{HCOO}^- + \text{O}_3 \longrightarrow \text{CO}_2 + \text{OH} + \text{O}_2^-$ | 100.0 | 0 | Hoigne and Bader (1983b) |
| 59 | $\text{HCOO}^- + \text{NO}_3 \xrightarrow{\text{O}_2} \text{NO}_3^- + \text{CO}_2 + \text{HO}_2$ | 6.0×10^7 | -1500 | Jacob (1986) |
| 60 | $\text{HCOO}^- + \text{CO}_3^{2-} \xrightarrow{\text{O}_2, \text{H}_2\text{O}} \text{CO}_2 + \text{HCO}_3^- + \text{HO}_2 + \text{OH}^-$ | 1.1×10^5 | -3400 | Chen et al. (1973) |
| 61 | $\text{HCOO}^- + \text{Cl}_2^- \xrightarrow{\text{O}_2} \text{CO}_2 + \text{HO}_2 + 2\text{Cl}^-$ | 1.9×10^6 | -2600 | Hagesawa and Neta (1978) |
| 62 | $\text{CH}_3\text{C}(\text{O})\text{O}_2\text{NO}_2 \longrightarrow \text{NO}_3^- + \text{Products}$ | 4.0×10^{-4} | 0 | Lee (1984b) |
| 63 | $\text{CH}_3\text{O}_2 + \text{HO}_2 \longrightarrow \text{CH}_3\text{OOH} + \text{O}_2$ | 4.3×10^5 | -3000 | Jacob (1986) |
| 64 | $\text{CH}_3\text{O}_2 + \text{O}_2^- \xrightarrow{\text{H}_2\text{O}} \text{CH}_3\text{OOH} + \text{O}_2 + \text{OH}^-$ | 5.0×10^7 | -1600 | Jacob (1986) |
| 65 | $\text{CH}_3\text{OOH} + h\nu \xrightarrow{\text{O}_2} \text{HCHO} + \text{OH} + \text{HO}_2$ | | | Graedel and Weschler (1981) |
| 66 | $\text{CH}_3\text{OOH} + \text{OH} \longrightarrow \text{CH}_3\text{O}_2 + \text{H}_2\text{O}$ | 2.7×10^7 | -1700 | Jacob (1986) |
| 67 | $\text{CH}_3\text{OH} + \text{OH} \longrightarrow \text{HCHO} + \text{HO}_2 + \text{H}_2\text{O}$ | 4.5×10^8 | -1500 | Anbar and Neta (1967) |
| 68 | $\text{CH}_3\text{OH} + \text{CO}_3^{2-} \xrightarrow{\text{O}_2} \text{HCHO} + \text{HO}_2 + \text{HCO}_3^-$ | 2.6×10^3 | -4500 | Chen et al. (1973) |

| | | | | |
|------------------|--|---|----------------|-------------------------------|
| 69 | $\text{CH}_3\text{OH} + \text{Cl}_2^- \xrightarrow{\text{O}_2} \text{HCHO} + \text{HO}_2 + \text{H}^+ + 2\text{Cl}^-$ | 3.5×10^3 | -4400 | Hagesawa and Neta (1978) |
| 70 | $\text{CH}_3\text{OOH} + \text{OH}^- \longrightarrow \text{HCHO} + \text{OH}^- + \text{H}_2\text{O}$ | 1.9×10^7 | -1800 | Jacob (1986) |
| 71 | $\text{CH}_3\text{OH} + \text{NO}_3^- \xrightarrow{\text{O}_2} \text{NO}_3^- + \text{H}^+ + \text{HCHO} + \text{HO}_2$ | 1.0×10^6 | -2800 | Dogliotti and Hayon (1967) |
| 72 ^a | $\text{S(IV)} + \text{O}_3 \longrightarrow \text{S(VI)} + \text{O}_2$ | 2.4×10^4 3.7×10^5 1.5×10^9 | -5530 -5280 | Hoffmann and Calvert (1985) |
| 73 ^a | $\text{S(IV)} + \text{H}_2\text{O}_2 \longrightarrow \text{S(VI)} + \text{H}_2\text{O}$ | 7.5×10^7 | -4430 | McArdle and Hoffmann (1983) |
| 74 ^a | $\text{S(IV)} + 0.5\text{O}_2 \xrightarrow{\text{Fe}^{3+}, \text{Mn}^{2+}} \text{S(VI)}$ | See Below | | Martin et al. (1991) |
| 75 | $\text{SO}_3^{2-} + \text{OH}^- \xrightarrow{\text{O}_2} \text{SO}_5^- + \text{OH}^-$ | 5.2×10^9 | -1500 | Huie and Neta (1987) |
| 76 | $\text{HSO}_3^- + \text{OH}^- \xrightarrow{\text{O}_2} \text{SO}_5^- + \text{H}_2\text{O}$ | 4.5×10^9 | -1500 | Huie and Neta (1987) |
| 77 | $\text{SO}_5^- + \text{HSO}_3^- \xrightarrow{\text{O}_2, \text{H}_2\text{O}} \text{HSO}_5^- + \text{SO}_5^-$ $\text{SO}_5^- + \text{SO}_3^{2-} \xrightarrow{\text{O}_2} \text{HSO}_5^- + \text{SO}_5^- + \text{OH}^-$ | 2.5×10^4 2.5×10^4 | -3100 -2000 | Huie and Neta (1987) |
| 78 | $\text{SO}_5^- + \text{O}_2^- \xrightarrow{\text{H}_2\text{O}} \text{HSO}_5^- + \text{OH}^- + \text{O}_2$ | 1.0×10^8 | -1500 | Jacob (1986) |
| 79 | $\text{SO}_5^- + \text{HCOOH} \xrightarrow{\text{O}_2} \text{HSO}_5^- + \text{CO}_2 + \text{HO}_2$ | 200 | -5300 | Jacob (1986) |
| 80 | $\text{SO}_5^- + \text{HCOO}^- \xrightarrow{\text{O}_2} \text{HSO}_5^- + \text{CO}_2 + \text{O}_2^-$ | 1.4×10^4 | -4000 | Jacob (1986) |
| 81 | $\text{SO}_5^- + \text{SO}_5^- \longrightarrow 2\text{SO}_4^- + \text{O}_2$ | 6.0×10^8 | -1500 | Huie and Neta (1987) |
| 82 | $\text{HSO}_5^- + \text{HSO}_3^- + \text{H}^+ \longrightarrow 2\text{SO}_4^{2-} + 3\text{H}^+$ | 7.1×10^6 | -3100 | Betterton and Hoffmann (1988) |
| 83 | $\text{HSO}_5^- + \text{OH}^- \longrightarrow \text{SO}_5^- + \text{H}_2\text{O}$ | 1.7×10^7 | -1900 | Jacob (1986) |
| 84 | $\text{HSO}_5^- + \text{SO}_4^- \longrightarrow \text{SO}_5^- + \text{SO}_4^{2-} + \text{H}^+$ | $< 1.0 \times 10^5$ | 0 | Jacob (1986) |
| 85 | $\text{HSO}_5^- + \text{NO}_2^- \longrightarrow \text{HSO}_4^- + \text{NO}_3^-$ | 0.31 | -6650 | Jacob (1986) |
| 86 | $\text{HSO}_5^- + \text{Cl}^- \longrightarrow \text{SO}_4^{2-} + \text{Product}$ | 1.8×10^{-3} | -7050 | Jacob (1986) |
| 87 | $\text{SO}_4^- + \text{HSO}_3^- \xrightarrow{\text{O}_2} \text{SO}_4^{2-} + \text{H}^+ + \text{SO}_5^-$ | 1.3×10^9 | -1500 | Jacob (1986) |
| 88 | $\text{SO}_4^- + \text{SO}_3^{2-} \xrightarrow{\text{O}_2} \text{SO}_4^{2-} + \text{SO}_5^-$ | 5.3×10^8 | -1500 | Jacob (1986) |
| 89 | $\text{SO}_4^- + \text{HO}_2 \longrightarrow \text{SO}_4^{2-} + \text{H}^+ + \text{O}_2$ | 5.0×10^9 | -1500 | Jacob (1986) |
| 90 | $\text{SO}_4^- + \text{O}_2^- \longrightarrow \text{SO}_4^{2-} + \text{O}_2$ | 5.0×10^9 | -1500 | Jacob (1986) |
| 91 | $\text{SO}_4^- + \text{OH}^- \longrightarrow \text{SO}_4^{2-} + \text{OH}^-$ | 8.0×10^7 | -1500 | Jacob (1986) |
| 92 | $\text{SO}_4^- + \text{H}_2\text{O}_2 \longrightarrow \text{SO}_4^{2-} + \text{H}^+ + \text{HO}_2$ | 1.2×10^7 | -2000 | Ross and Neta (1979) |
| 93 | $\text{SO}_4^- + \text{NO}_2^- \longrightarrow \text{SO}_4^{2-} + \text{NO}_2$ | 8.8×10^8 | -1500 | Jacob (1986) |
| 94 | $\text{SO}_4^- + \text{HCO}_3^- \longrightarrow \text{SO}_4^{2-} + \text{H}^+ + \text{CO}_3^-$ | 9.1×10^6 | -2100 | Ross and Neta (1979) |
| 95 | $\text{SO}_4^- + \text{HCOO}^- \xrightarrow{\text{O}_2} \text{SO}_4^{2-} + \text{CO}_2 + \text{HO}_2$ | 1.7×10^8 | -1500 | Jacob (1986) |
| 96 | $\text{SO}_4^- + \text{Cl}^- \longrightarrow \text{SO}_4^{2-} + \text{Cl}^-$ | 2.0×10^8 | -1500 | Ross and Neta (1979) |
| 97 | $\text{SO}_4^- + \text{HCOOH} \xrightarrow{\text{O}_2} \text{SO}_4^{2-} + \text{H}^+ + \text{CO}_2 + \text{HO}_2$ | 1.4×10^6 | -2700 | Jacob (1986) |
| 98 ^a | $\text{S(IV)} + \text{CH}_3\text{C(O)O}_2\text{NO}_2 \longrightarrow \text{S(VI)}$ | 6.7×10^{-3} | 0 | Lee (1984a) |
| 99 | $\text{HSO}_3^- + \text{CH}_3\text{OOH} \xrightarrow{\text{H}^+} \text{SO}_4^{2-} + 2\text{H}^+ + \text{CH}_3\text{OH}$ | 2.3×10^7 | -3800 | Lind et al. (1987) |
| 100 ^a | $\text{HSO}_3^- + \text{CH}_3\text{C(O)OOH} \longrightarrow \text{SO}_4^{2-} + \text{H}^+ + \text{CH}_3\text{COOH}$ | 5.0×10^7 6.0×10^2 | -4000 | Lind et al. (1987) |
| 101 | $\text{S(IV)} + \text{HO}_2 \longrightarrow \text{S(VI)} + \text{OH}^-$ $\text{S(IV)} + \text{O}_2^- \xrightarrow{\text{H}_2\text{O}} \text{S(VI)} + \text{OH}^- + \text{OH}^-$ | 1.0×10^6 1.0×10^5 | 0 0 | Hoffmann and Calvert (1985) |
| 102 | $\text{SO}_4^- + \text{CH}_3\text{OH} \xrightarrow{\text{O}_2} \text{SO}_4^{2-} + \text{HCHO} + \text{H}^+ + \text{HO}_2$ | 2.5×10^7 | -1800 | Dogliotti and Hayon (1967) |
| 103 | $\text{HSO}_3^- + \text{NO}_3^- \longrightarrow \text{NO}_3^- + \text{H}^+ + \text{SO}_3^- + \text{SO}_3^-$ | 1.0×10^8 | 0 | Chameides (1984) |
| 104 | $2\text{NO}_2 + \text{HSO}_3^- \xrightarrow{\text{H}_2\text{O}} \text{SO}_4^{2-} + 3\text{H}^+ + 2\text{NO}_2^-$ | 2.0×10^6 | 0 | Lee and Schwartz (1983) |

| | | | | |
|------|--|--|----------------|----------------------------|
| 105a | $S(IV) + N(III) \longrightarrow S(VI) + \text{Product}$ (for pH ≤ 3) | 1.4×10^2 | 0 | Martin (1984) |
| 105b | $2HSO_3^- + NO_2^- \longrightarrow OH^- + \text{Product}$ (for pH > 3) | 4.8×10^3 | -6100 | Oblath et al. (1981) |
| 106 | $HCHO + HSO_3^- \longrightarrow HOCH_2SO_3^-$ $HCHO + SO_3^{2-} \xrightarrow{H_2O} HOCH_2SO_3^- + OH^-$ | 7.9×10^2 2.5×10^7 | -4900 -1800 | Boyce and Hoffmann (1984) |
| 107 | $HOCH_2SO_3^- + OH^- \longrightarrow SO_3^{2-} + HCHO + H_2O$ | 3.6×10^3 | -4500 | Munger et al. (1986) |
| 108 | $HOCH_2SO_3^- + OH^- \xrightarrow{O_2} SO_5^- + HCHO + H_2O$ | 2.6×10^8 | -1500 | Olson and Fessenden (1992) |
| 109 | $HSO_3^- + Cl_2 \xrightarrow{O_2} SO_5^- + 2Cl^- + H^+$ $SO_3^{2-} + Cl_2 \xrightarrow{O_2} SO_5^- + 2Cl^-$ | 3.4×10^8 3.4×10^8 | -1500 -1500 | Huie and Neta (1987) |

^a Reaction with "nonelementary" rate expression

Nonelementary Rate Expressions

| Reaction Number | Rate Expression, $-d[S(IV)]/dt$ |
|-----------------|---|
| 72 | $(k_0[SO_2 \cdot H_2O] + k_1[HSO_3^-] + k_2[SO_3^{2-}])[O_3(aq)]$ |
| 73 | $k_0[H^+][HSO_3^-][H_2O_2(aq)]/(1+K[H^+])$ where $K = 13 M^{-1}$ |
| 74 | For pH ≤ 3 $6[Fe^{3+}][S(IV)]/[H^+]$ For pH > 3 and ≤ 4.5 $1.0 \times 10^9[S(IV)][Fe^{3+}]^2$ For pH > 4.5 and ≤ 6.5 $1.0 \times 10^{-3}[S(IV)]$ For pH > 6.5 $1.0 \times 10^{-4}[S(IV)]$ |
| 98 | $k[CH_3C(O)O_2NO_2][HSO_3^-]/[H^+]$ |
| 100 | $k_0[H^+] + k_1[HSO_3^-][CH_3C(O)OOH]$ |

Equilibrium Reactions

| Equilibrium Reaction | K_{298} (M or M atm ⁻¹) | $-\Delta H/R$ (K) | Reference: |
|---|---------------------------------------|-------------------|---------------------------|
| $SO_2 \cdot H_2O \leftrightarrow HSO_3^- + H^+$ | 1.3×10^{-2} | 1960 | Smith and Martell (1976) |
| $HSO_3^- \leftrightarrow SO_3^{2-} + H^+$ | 6.6×10^{-8} | 1500 | Smith and Martell (1976) |
| $H_2SO_4(aq) \leftrightarrow HSO_4^- + H^+$ | 1000 | | Perrin (1982) |
| $HSO_4^- \leftrightarrow SO_4^{2-} + H^+$ | 1.02×10^{-2} | 2720 | Smith and Martell (1976) |
| $H_2O_2(aq) \leftrightarrow HO_2^- + H^+$ | 2.2×10^{-12} | -3730 | Smith and Martell (1976) |
| $HNO_3(aq) \leftrightarrow NO_3^- + H^+$ | 15.4 | 8700 | Schwartz (1984) |
| $HNO_2(aq) \leftrightarrow NO_2^- + H^+$ | 5.1×10^{-4} | -1260 | Schwartz and White (1981) |
| $CO_2 \cdot H_2O \leftrightarrow HCO_3^- + H^+$ | 4.3×10^{-7} | -1000 | Smith and Martell (1976) |
| $HCO_3^- \leftrightarrow CO_3^{2-} + H^+$ | 4.68×10^{-11} | -1760 | Smith and Martell (1976) |
| $NH_4OH \leftrightarrow NH_4^+ + OH^-$ | 1.7×10^{-5} | -450 | Smith and Martell (1976) |
| $H_2O \leftrightarrow H^+ + OH^-$ | 1.0×10^{-14} | -6710 | Smith and Martell (1976) |
| $HCHO(aq) \leftrightarrow H_2C(OH)_2(aq)$ | 2.53×10^3 | 4020 | Le Hanaff (1968) |
| $HCOOH(aq) \leftrightarrow HCOO^- + H^+$ | 1.8×10^{-4} | -20 | Martell and Smith (1977) |
| $HCl(aq) \leftrightarrow H^+ + Cl^-$ | 1.74×10^6 | 6900 | Marsh and McElroy (1985) |
| $Cl_2 \leftrightarrow Cl + Cl^-$ | 5.26×10^{-6} | | Jayson et al. (1973) |
| $NO_3(g) \leftrightarrow NO_3(aq)$ | 2.1×10^5 | 8700 | Jacob (1986) |

| | | | |
|--|------------------------|------|---------------------------------|
| $\text{HO}_2(\text{aq}) \leftrightarrow \text{H}^+ + \text{O}_2^-$ | 3.5×10^{-5} | | Perrin (1982) |
| $\text{HOCH}_2\text{SO}_3^- \leftrightarrow -\text{OCH}_2\text{SO}_3^- + \text{H}^+$ | 2.00×10^{-12} | | Sorensen and Anderson (1970) |
| $\text{SO}_2(\text{g}) \leftrightarrow \text{SO}_2 \text{H}_2\text{O}$ | 1.23 | 3120 | Smith and Martell (1976) |
| $\text{H}_2\text{O}_2(\text{g}) \leftrightarrow \text{H}_2\text{O}_2(\text{aq})$ | 7.45×10^4 | 6620 | Lind and Kok (1986) |
| $\text{HNO}_3(\text{g}) \leftrightarrow \text{HNO}_3(\text{aq})$ | 2.1×10^5 | | Schwartz (1984) |
| $\text{HNO}_2(\text{g}) \leftrightarrow \text{HNO}_2(\text{aq})$ | 49 | 4780 | Schwartz and White (1981) |
| $\text{O}_3(\text{g}) \leftrightarrow \text{O}_3(\text{aq})$ | 1.13×10^{-2} | 2300 | Kozac-Channing and Heltz (1983) |
| $\text{NO}_2(\text{g}) \leftrightarrow \text{NO}_2(\text{aq})$ | 1.0×10^{-2} | 2500 | Schwartz (1984) |
| $\text{NO}(\text{g}) \leftrightarrow \text{NO}(\text{aq})$ | 1.9×10^{-3} | 1480 | Schwartz and White (1981) |
| $\text{CH}_3\text{O}_2(\text{g}) \leftrightarrow \text{CH}_3\text{O}_2(\text{aq})$ | 6 | 5600 | Jacob (1986) |
| $\text{CH}_3\text{OH}(\text{g}) \leftrightarrow \text{CH}_3\text{OH}(\text{aq})$ | 220 | 4900 | Snider and Dawson (1985) |
| $\text{CO}_2(\text{g}) \leftrightarrow \text{CO}_2 \text{H}_2\text{O}$ | 3.4×10^{-2} | 2420 | Smith and Martell (1976) |
| $\text{NH}_3(\text{g}) \leftrightarrow \text{NH}_4\text{OH}$ | 75 | 3400 | Hales and Drewes (1979) |
| $\text{HCHO}(\text{g}) \leftrightarrow \text{HCHO}(\text{aq})$ | 6.3×10^3 | 6460 | Ledbury and Blair (1925) |
| $\text{HCOOH}(\text{g}) \leftrightarrow \text{HCOOH}(\text{aq})$ | 3.5×10^3 | 5740 | Latimer (1952) |
| $\text{HCl}(\text{g}) \leftrightarrow \text{HCl}(\text{aq})$ | 727 | 2020 | Marsh and McElroy (1985) |
| $\text{CH}_3\text{OOH}(\text{g}) \leftrightarrow \text{CH}_3\text{OOH}(\text{aq})$ | 227 | 5610 | Lind and Kok (1986) |
| $\text{CH}_3\text{C}(\text{O})\text{OOH}(\text{g}) \leftrightarrow \text{CH}_3\text{C}(\text{O})\text{OOH}(\text{aq})$ | 473 | 6170 | Lind and Kok (1986) |
| $\text{OH}(\text{g}) \leftrightarrow \text{OH}(\text{aq})$ | 25 | 5280 | Jacob (1986) |
| $\text{HO}_2(\text{g}) \leftrightarrow \text{HO}_2(\text{aq})$ | 2.0×10^3 | | Jacob (1986) |

Temperature Dependence of Equilibrium Constants

$$K(T_2) = K_{298} \exp\left(\frac{-\Delta H_A}{R} \left(\frac{1}{T_2} - \frac{1}{298}\right)\right)$$

References

- Anbar, M. and Neta, P. (1967) A compilation of specific bimolecular rate constants for the reactions of hydrated electrons, hydrogen atoms, and hydroxyl radicals with inorganic and organic compounds in aqueous solutions. *Int. J. Appl. Radiat. Isotopes*, 18, 493-523.
- Behar, D., Czapski, G., and Duchovny, I. (1970) Carbonate radical in flash photolysis and pulse radiolysis of aqueous carbonate solutions. *J. Phys. Chem.*, 74, 2206-2210.
- Betterton, E. A., and Hoffmann, M. R. (1988) Oxidation of aqueous SO_2 by peroxymonosulfate, *J. Phys. Chem.*, 92, 5962-5965.
- Bielski, B.H.J. (1978) Reevaluation of the spectral and kinetic properties of HO_2 and O_2 free radicals. *Photochem. Photobiol.*, 28, 645-649.
- Bothe, E. and Schulte-Frohlinde, D. (1980) Reaction of the dihydroxymethyl radical with molecular oxygen in aqueous solution. *Anorg. Chem. Org. Chem.*, 35, 1035-1039.

- Boyce, S. D. and Hoffmann, M. R. (1984) Kinetics and mechanism of the formation of hydroxymethanesulfonic acid at low pH. *J. Phys. Chem.*, 88, 4740-4746.
- Chameides, W.L. (1984) The photochemistry of a marine stratiform cloud. *J. Geophys. Res.* 89, 4739-4755.
- Chen, S., Cope, V.W., and Hoffmann, M.Z. (1973) Behavior of CO₃ radicals generated in the flash photolysis of carbonatomine complexes of cobalt(III) in aqueous solutions. *J. Phys. Chem.*, 77, 1111-1116.
- Christensen, H. Sehested, K. and Corfitzen, H. (1982) Reactions of hydroxyl radicals with hydrogen peroxide at ambient and elevated temperatures. *J. Phys. Chem.*, 86, 1588-1590.
- Damschen, D.E. and Martin, L. R. (1983) Aqueous aerosol oxidation of nitrous acid by O₂, O₃, and H₂O₂. *Atmos. Env.*, 17, 2005-2011.
- Dogliotti, L. and Hayon, E. (1967) Flash photolysis of persulfate ions in aqueous solutions. Study of sulfate and ozonide radical ions. *J. Phys. Chem.*, 71, 2511-2516.
- Graedel, T. E. and Goldberg, K. I. (1983) Kinetic studies of raindrop chemistry. 1. Inorganic and organic processes, *J. Geophys. Res.*, 88, 10865-10882.
- Graedel, T.E. and Weschler, C. J. (1981) Chemistry within aqueous atmospheric aerosols and raindrops. *Rev. Geophys.* 19, 505-539.
- Gratzel, M. Henglein, A., and Taniguchi, S. (1970) Pulsradiolytische beobachtungen uber die reduction des NO₃- ions un tuber bildungund zerfall des persalpetrigen saure in wassriger losung. *Ber. Bundsenges. Phys. Chem.* 74, 292-298.
- Hagesawa, K. and Neta, P. (1978) Rate constants and mechanisms of reaction Cl₂⁻ radicals. *J. Phys. Chem.*, 82, 854-857.
- Hales, J.M. and Drewes, D.R. (1979) Solubility of ammonia in water at low concentrations. *Atmos. Environ.* 13, 1133-1147.
- Hoigne, J. and Bader, H. (1983a) Rate constants of reactions of ozone with organic and inorganic compounds in water. 1. Non-dissociating organic compounds. *Water Res.* 17, 173-183.
- Hoigne, J. and Bader, H. (1983b) Rate constants of reactions of ozone with organic and inorganic compounds in water. 2. Dissociating organic compounds.. *Water Res.* 17, 185-194.
- Hoffmann, M.R. and Calvert, J.G. (1985) *Chemical Formation Modules for Eulerian Acid Deposition Models, Volume 2, The Aqueous-Phase Chemistry.* EPA/600/3-85/017. U.S. Environmental Protection Agency, Research Triangle Park, NC.
- Huie, R.E. and Neta, P. (1987) Rate constants for some oxidations of S(IV) by radicals in aqueous solutions, *Atmos. Environ.*, 21, 1743-1747.
- Jacob, D. J. (1986) Chemistry of OH in remote clouds and its role in the production of formic acid and peroxymonosulfate. *J. Geophys. Res.* 91, 9807-9826.
- Jayson, G.G., Parsons, B. J., and Swallow, A.J. (1973) Some simple, highly reactive, inorganic chlorine derivatives in aqueous-solution, *Trans. Faraday Soc.* 69, 1597-1607.

- Kozac-Channing, L.F. and Heltz, G. R. (1983) Solubility of ozone in aqueous solutions of 0-0.6 M ionic strength at 5-30 °C. *Environ. Sci. Technol.* 17, 145-149.
- Latimer, W.M. (1952) *The Oxidation States of the Elements and Their Potentials in Aqueous Solutions*. Prentice-Hall, New York, pp. 70-89.
- Le Hanaff, P. (1968) Methodes d'étude et proprietes des hydrates, hemiacetals et hemiacetals derives des aldehydes et des cetones. *Bull. Soc. Chim. Fr.*, 4687-4700.
- Ledbury, W. and Blair, E.W. (1925) The partial formaldehyde vapour pressure of aqueous solutions of formaldehyde, part II. *J. Chem. Soc.* 127, 2832-2839.
- Lee, Y. N. (1984a) Atmospheric aqueous-phase reactions of nitrogen species, in *Gas-Liquid Chemistry of Natural Waters*, Vol. 1, BNL 51757. Brookhaven National Laboratory, Brookhaven, NY, pp. 20/1-20/10.
- Lee, Y. N. (1984b) Kinetics of some aqueous phase reactions of peroxyacetyl nitrate, in *Gas-Liquid Chemistry of Natural Waters*, Vol. 1, BNL 51757. Brookhaven National Laboratory, Brookhaven, NY, pp. 21/1-21/7.
- Lee, Y. N. and Lind, J. A. (1986) Kinetics of aqueous-phase oxidation of nitrogen(III) by hydrogen peroxide. *J. Geophys. Res.* 91, 2793-2800.
- Lee, Y. N. and Schwartz, S.E. (1983) Kinetics of oxidation of aqueous sulfur(IV) by nitrogen dioxide, in *Precipitation Scavenging, Dry Deposition, and Resuspension*, Vol. 1, edited by H. R. Pruppacher, R. G. Semonin, and W. G. N. Slinn. Elsevier, New York.
- Lilie, J., Henglein, A. and Hanrahan, R. J. (1978) Reactions of the carbonate radical anion with organic and inorganic solutes in aqueous solution, presented at the 176th meeting of the American Chemical Society, Miami Beach, Florida.
- Lind, J.A. and Kok, G.L. (1986) Henry's law determinations for aqueous solutions of hydrogen peroxide, methylhydroperoxide, and peroxyacetic acid. *J. Geophys. Res.* 91, 7889-7895.
- Lind, J. A., Lazrus, A. L. and Kok, G. L. (1987) Aqueous phase oxidation of sulfur(IV) by hydrogen peroxide, methylhydroperoxide, and peroxyacetic acid. *J. Geophys. Res.* 92, 4171-4177.
- Marsh, A.R.W. and McElroy, W.J. (1985) The dissociation constant and Henry's law constant of HCl in aqueous solution, *Atmos. Environ.* 19, 1075-1080.
- Martell, A.E. and Smith, R. M. (1977) *Critical Stability Constants*, vol. 3, *Other Organic Ligands*, Plenum, New York.
- Martin, L. R. (1984) Kinetic studies of sulfite oxidation in aqueous solution in *SO₂, NO, and NO₂ Oxidation Mechanisms: Atmospheric Considerations*, edited by J. G. Calvert. Butterworth, Stoneham, MA. 63-100.
- Martin, L.R., Damschen, D.E., and Judeikis, H.S. (1981) Sulfur dioxide oxidation reactions in aqueous solution, EPA 600/7-81-085. U.S. Environmental Protection Agency, Research Triangle Park, NC.
- Martin, L.R., Hill, M.W., Tai, A.F., and Good, T.W. (1991). The iron-catalyzed oxidation of sulfur(IV) in aqueous solution: differing effects of organics at high and low pH. *J. Geophys. Res.* 96, 3085-3097.

- McArdle, J. V. and Hoffmann, M. R. (1983) Kinetics and mechanism of the oxidation of aquated sulfur dioxide by hydrogen peroxide at low pH. *J. Phys. Chem.*, 87, 5425-5429.
- Munger, J. W., Tiller, C., and Hoffmann, M. R. (1986) Identification of hydroxymethanesulfonate in fog water. *Science*, 231, 247-249.
- Oblath, S.B., Markowitz, S.S., Novakov, T., and Chang, S. G. (1981) Kinetics of the formation of hydroxylamine disulfonate by reaction of nitrite with sulfites. *J. Phys. Chem.*, 85, 1017-1021.
- Olson, T.M. and Fessenden, R.W. (1992) Pulse radiolysis study of the reaction of OH radicals with methanesulfonate and hydroxymethanesulfonate. *J. Phys. Chem.*, 96, 3317-3320.
- Perrin, D.D. (1982) *Ionization Constants of Inorganic Acids and Bases in Aqueous Solution*, 2nd ed., Pergamon Press, New York.
- Rettich, T. R. (1978) Some photochemical reactions of aqueous nitric acid. *Diss. Abstr. Int. B.*, 38, 5968.
- Ross, A. B. and Neta, P. (1979) *Rate Constants for Reactions of Inorganic Radicals in Aqueous Solution*, NSRDS-NBS 65. National Bureau of Standards, U.S. Department of Commerce, Washington, D.C.
- Schmidt, K. H. (1972) Electrical conductivity techniques for studying the kinetics of radiation induced chemical reactions in aqueous solutions. *Int. J. Radiat. Phys. Chem.* 4, 439-468.
- Scholes, G. and Willson, R.L. (1967) γ -radiolysis of aqueous thymine solutions. Determination of relative reaction rates of OH radicals. *Trans. Faraday Soc.* 63, 2892-2993.
- Schwartz, S. E. (1984) Gas- and aqueous-phase chemistry of HO₂ in liquid water clouds. *J. Geophys. Res.* 89, 11589-11598.
- Schwartz, S.E. and White, W.H. (1981) Solubility equilibrium of the nitrogen oxides and oxyacids in dilute aqueous solution, *Adv. Environ. Sci. Eng.*, 4, 1-45.
- Sehested, K, Holcman, J., and Hart, E.J. (1983) Rate constants and products of the reactions of e⁻_{aq}, O₂⁻, and H with ozone in aqueous solutions. *J. Phys. Chem.*, 87, 1951-1954.
- Sehested, K, Holcman, J., and Bjergbakke, E., and Hart, E.J. (1984) A pulse radiolytic study of the reaction of OH+O₃ in aqueous medium. *J. Phys. Chem.*, 88, 4144-4147.
- Sehested, K, Rasmussen, O.L. and Fricke, H. (1968) Rate constants for OH with HO₂, O₂⁻, and H₂O₂⁺ from hydrogen peroxide formation in pulse-irradiated oxygenated water.. *J. Phys. Chem.*, 72, 626-631.
- Shapilov, O.D. and Kostyukovskii, Y. L. (1974) Reaction kinetics of hydrogen peroxide with formic acid in aqueous solutions, *Kinet. Katal.* 15, 1065-1067.
- Smith, R. M. and Martell, A. E. (1976) *Critical Stability Constants, Volume 4: Inorganic Complexes*. Plenum Press, New York.
- Snider, J.R. and Dawson, G.A. (1985) Tropospheric light alcohols, carbonyls, and acetonitrile: concentrations in the southwestern United States and Henry's law data. *J. Geophys. Res.* 90, 3797-3805.

- Sorensen, P. E. and Andersen, V. S. (1970) The formaldehyde-hydrogen sulphite system in alkaline aqueous solution: kinetics, mechanism, and equilibria, *Acta Chem. Scand.* 24, 1301-1306.
- Stahelin, J. and Hoigne, J. (1982) Decomposition of ozone in water: Rate of initiation by hydroxide ions and hydrogen peroxide. *Environ. Sci. Technol.* 16, 676-681.
- Stahelin, J., Buhler, R.E., and Hoigne, J. (1984) Ozone decomposition in water studied by pulse radiolysis. 2. OH and HO₄ as chain intermediates. *J. Phys. Chem.*, 88, 5999-6004/
- Strehlow, H. and Wagner, I. (1982) Flash photolysis in aqueous nitrite solutions, *Z. Phys. Chem. Wiesbaden*, 132, 151-160.
- Treinin, A. and Hayon, E. (1970) Absorption spectra and reaction kinetics of NO₂, N₂O₃, and N₂O₄ in aqueous solutions. *J. Am. Chem. Soc.*, 92, 5821-5828.
- Weeks, J. L. and Rabani, J. (1966) The pulse radiolysis of deaerated aqueous carbonate solutions. *J. Phys. Chem.* 70, 2100-2106.
- Weinstein, J. and Bielski, B.H.J. (1979) Kinetics of the interaction of HO₂ and O₂⁻ radicals with hydrogen peroxide; the Haber-Weiss reaction. *J. Am. Chem. Soc.*, 101, 58-62.